Toxic Winds: Mainstream Inertia, Voter Discontent, and Challenger success*

Davide Cipullo † Massimiliano Onorato ‡ Gianmario Pelleschi §

This version: February 15, 2026

Abstract

This paper investigates how voters react to persistent inaction of mainstream parties in government. We study the illegal burial, dumping, and burning of toxic industrial waste perpetrated by criminal organizations in Southern Italy since the late 1980s. We combine plausibly exogenous geographical variation in exposure to pollutants stemming from historical wind trajectories with the sudden release of information about the exact geo-location of contaminated sites. Difference-in-differences estimates show that, after the information shock, municipalities exposed to toxic winds experienced a persistent decline in turnout of 5.8 percentage points relative to non-exposed municipalities. Using individual-level survey data, we also find that exposure to pollutants reduce trust in parties and in national parliament. Finally, we show that exposure to toxic winds increases the vote share of the challenger Five Star Movement (FSM) in national elections, who actively contrasted mainstream parties' inaction on the issue.

Keywords: Electoral accountability; Organized Crime; Turnout; Challenger parties.
JEL classification: D72, K42, P0.

*We benefitted from discussions with Elias Papaioannou, Jakob Svensson, Claudio Ferraz, Sandra Sequeira, Lorenzo Cappellari, Amanda Dahlstrand, Marco Le Moglie, Tommaso Colussi, Matteo Sandi, Giulia Caprini, Federico Trombetta, Marco Ovidi, Emiliano Santoro, Gianluca Femminis, Federico Franzoni, Alessio Romarri, Felipe Carozzi, Flaviana Palmisano, Davide Furceri, Alberto Bisin, Eugenio Polese, Roberto Dellisanti, Augustìn Casas as well as seminar participants at Cattolica University of Milan WIP Political Economy Seminar Series, the 2025 Sustainability Environmental Economics and Dynamics Studies (SEEDS) Annual Conference, the "Inequalities and Opportunities (insights into wealth, income and education disparities" Conference at the University of Bari, and the 37^{th} Annual Congress of the Italian Society of Public Economics (SIEP) held in Naples. We gratefully acknowledge the Regional Agency for the Protection of the Environment Campania (ARPAC) for granting access to the environmental data. All remaining errors are our own.

†Department of Economics and Finance, Università Cattolica del Sacro Cuore, Milan, Italy; Cesifo, Munich, Germany; Uppsala Centre for Fiscal Studies, Uppsala University, Sweden; CIFREL, Milan, Italy. Email: davide.cipullo@unicatt.it

‡Department of Economics, University of Bologna, Bologna, Italy. Email: massimiliano.onorato@unibo.it

§Department of Economics and Finance, Università Cattolica del Sacro Cuore, Milan, Italy. Email: gianmario.pelleschi@unicatt.it

1 INTRODUCTION

Liberal democracies increasingly face pressure from anti-establishment parties that challenge traditional behaviour of party competition. These parties often adopt bold positions and put pressure on existing institutions, raising concerns about the erosion of constitutional norms. Yet, they repeatedly enter government and, in many cases, continue to receive electoral support even when their governing performance appears poor. This pattern raises questions about how the principal–agent relationship between voters (principals) and politicians (agents) works in practice. In the standard electoral accountability framework, voters evaluate incumbents' performance and use their votes to reward or punish them (Besley, 2006; Fearon, 1999; Barro, 1973). This mechanism relies on some basic conditions, and when these are not met electoral accountability can be weakened. For example, changes in institutional rules shape how effectively voters can discipline and select politicians (Cantoni et al., 2025; Kim, 2023; Jones et al., 2023). Policy shocks tied to government action can alter perceptions of incumbent performance and foster the rise of challenger parties: austerity programs (Fetzer, 2019), trade liberalization (Colantone and Stanig, 2018; Rodrik, 2021), migration waves (Dal Bò et al., 2023), or macroeconomic crises (Algan et al., 2017; Funke et al., 2016). Perceived non-representation and political disillusionment can lead to disengagement and lower turnout, causing disenfranchisement.

Most empirical studies have examined short or medium-run responses to policy shocks that are related to past incumbent decisions. In these settings, shocks are typically observable to both citizens and politicians, and their effects are studied over relatively short periods. Much less is known about long-run failures to address pre-existing issues that are not directly caused by incumbents' policy choices but are already known within public institutions. Voters, by contrast, remain unaware of these risks until an information shock occurs and brings the underlying problem to light. Second, prior work typically focuses on frameworks in which a challenger is already available on the ballot, so dissatisfied voters can immediately reallocate support across political parties. Existing research has not considered settings in which voters' baseline choice is among mainstream political parties that follow similar strategies over many electoral cycles and an information shock makes salient a decades-old problem that voters had been unable to observe. When the entire pool of political parties is viewed as unresponsive, voters may feel unrepresented and choose not to participate rather than reallocating support within the party system, effectively exiting the accountability relationship.

This paper studies how voters respond to long-run inaction of mainstream political parties when a challenger alternative is not feasible and when it becomes suddenly available. We examine the intense burial, dumping, and open-air burning of illegal toxic waste performed by criminal organizations in Southern Italy since the late 1980s. Although the government was aware of this issue from the early nineties, the reaction has been slow and ineffective. We combine plausibly exogenous geographical variation in exposure to pollutants stemming from historical wind trajectories with temporal variation in voters' awareness about the issue. Using a difference-in-differences design, we document a sharp, immediate, and persistent reduction in voter turnout of 5.8 percentage points in municipalities exposed to toxic winds stemming from illegal disposal sites relative to equally proximate non-exposed municipalities, following the public release of the exact geo-location of contaminated sites. This effect pairs with a reduction in trust in parties and in the national parliament according to individual-level survey data. We also study mainstream political parties behaviour before and after the news shock. To this end, we exploit a corpus of over 460,000 lower-house parliamentary speeches over 1996–2022 (Cova, 2025), analyzing changes in how exposed municipalities are mentioned relative to those in the control group. We also implement a sentiment analysis to study subjectivity and polarity of these speeches. We document a persistent inertia among mainstream political parties in addressing this issue before the news shock. In the second part of the paper, we focus on a challenger populist party, the Five Star Movement (henceforth, FSM), that put pressure at national level on mainstream political parties on environmental issues leveraging this scandal. Relying on the plausible exogeneity of wind patterns, we show that exposure to pollutants caused an increase in the national vote share of FSM (2018 and 2022 elections) as well as in FSM probability of participating at local elections. Our effects are stronger in municipalities at higher risk of criminal capture, as measured by mafia dissolutions of municipal councils (see Fenizia and Saggio, 2024; Acconcia et al., 2014; Buonanno et al., 2024; Di Cataldo and Mastrorocco, 2022; Daniele and Geys, 2015).

Our focus is on a setting with two distinct shocks: a long-run environmental shock generated by illegal toxic-waste disposal, and a later news shock that makes this risk salient to voters. We study a large-scale system run by criminal organizations in the "*Terra dei Fuochi*" ("Land of the Fires"), a densely populated area in Southern Italy. Since the late 1980s, criminal networks have handled hazardous industrial waste (often transported from other regions and abroad) through illicit practices including clandestine burial, dumping, and open air burning, causing the environmental shock. In 2005, the first official mapping of contaminated sites was made public, sharply increasing the salience of contamination risk. Local residents remained largely unaware of the environmental, economic, and health risks until this news shock, as these activities were neither tracked nor documented.[1] Although the underlying environmental shock did not stem from mainstream policy choices but from criminal activity, there is evidence that detailed information about the problem was available within public institutions well before it became public.[2]

[1]The existing literature reports descriptive evidence between pollution exposure in the Land of Fires and malignant cancer incidence.

[2]There is evidence that detailed information circulated within national institutions well before the 2005

In this paper, we are able to trace a long-run chain linking an environmental shock, a news shock, and later support for a challenger party. For more than a decade, illegal toxic-waste disposal created substantial environmental and health risks, but these threats were not visible to voters. Information circulated within national institutions, while mainstream political parties alternated in government and did not address the issue. Then, the 2005 information shock changed public awareness. When the map of contaminated sites was released, voters learnt both about the magnitude of the environmental damage and about the prolonged failure of all mainstream political parties to act. In principal–agent terms, the news shock revealed a long history of unfulfilled delegation. The result is a break in the accountability relationship with the political class as a whole, rather than with a single incumbent. We interpret the persistent fall in turnout, together with the drop in trust in parties and in the national parliament, as evidence of this break. Consistently with increased salience, we also document a post-shock decline in tourism in municipalities more exposed to toxic winds. At the same time, although mainstream political parties increase their rhetorical attention to the issue in parliamentary speeches in the years immediately following the news shock, environmentally exposed municipalities do not receive higher EU cohesion funds for remediation, and turnout does not recover. FSM entry marks a second step in this chain. FSM makes the Land of Fires a key topic of its platform: one of its five "stars" is environmental protection, and the party campaigns under the slogan "*In Movimento verso Terra dei Fuochi*" ("In movement toward the Land of Fires"), using bus tours and local protests to highlight the scandal. In this context, exposed voters who have withdrawn from the mainstream pool now face a credible challenger. In subsequent elections, municipalities more exposed to toxic winds exhibit higher FSM vote shares at national elections and a higher probability that FSM runs at local elections. All mainstream parties lose national vote share in exposed areas, proving that FSM draws support broadly from across the traditional party spectrum rather than displacing only a specific incumbent.

Taken together, our results suggest that challenger entry has mixed implications. Turnout remains lower in exposed areas, but the composition of active voters shifts: conditional on voting, residents of more polluted municipalities are more likely to choose FSM and less likely to support any mainstream party. In this sense, the challenger channels discontent among some of the most affected and vulnerable voters away from the mainstream party pool and toward a party that explicitly campaigns on this issue. At the same time, trust in parties and in parliament is lower in exposed areas, and the underlying environmental crisis is largely unresolved, so the legacy of an initial breakdown in accountability

disclosure. In 1993, Carmine Schiavone, a former leader of the criminal organization who began cooperating with judicial authorities, provided information on the illegal waste disposal process during auditions in front of the Italian Chamber of Deputies (declassified in 2013). His testimony describes organized disposal operations since at least 1988 and reports that his group handled several million tons of waste over 1988–1992.

persists. From a policy perspective, FSM's emphasis on the Land of Fires and its national slogan help keep the issue on the political agenda and expand awareness beyond directly affected municipalities. Yet, this representational gain has not restored the accountability relationship: environmental remediation remains incomplete and confidence in core democratic institutions has not been rebuilt.

This paper helps bridge the gap between the literature on electoral accountability under shocks and research on populism. On one hand, much of the work on populism is grounded on a principal–agent framework, where voters evaluate how incumbents manage adverse shocks. When incumbents respond effectively, the relationship between voters and politicians is preserved, as in settings where effective legislators mitigate the China shock (Cipullo and Lee, 2025), or governments compensate workers for COVID-related insecurity (Bordignon et al., 2024). When they do not, voters replace mainstream political parties and turn to challengers, as documented for financial crises (Guiso et al., 2019). On the other hand, a related literature on electoral accountability under shocks studies how policy interventions and exogenous shocks shape electoral punishment, reward, and selection, encompassing government transfer programs that raise support for incumbents (Manacorda et al., 2011), natural disasters that affect climate policy and voting (Gagliarducci et al., forthcoming) or temporarily divert media attention and increase legislators' alignment with special-interest donors (Kaplan et al., 2025), and disclosure of misconduct via corruption audits (Cavalcanti et al., 2018; Ferraz and Finan, 2008). These contributions typically analyse shocks that are either directly related to incumbent policies or contemporaneously observed by voters. In fact, little is known about how environmental shocks that are observable to politicians but not to voters shape electoral accountability, institutional trust, mainstream parties' programmatic responses, and the emergence of challenger parties.

Our work also offers a different perspective on populist parties. Prior research links support for populism to distributional conflict between the "elite" and the "people" (Guriev and Papaioannou, 2022), immigration (Dal Bò et al., 2023), globalization (Colantone and Stanig, 2018; Rodrik, 2021), financial crises (Algan et al., 2017; Funke et al., 2016), austerity (Fetzer, 2019), and electoral systems (Bordignon and Colussi, 2020), and documents negative economic performance of populist leaders once in office (Funke et al., 2023; Bellodi et al., 2024). Anti-establishment parties are often portrayed as threats to liberal democracy, global stability, civil liberties, and minority rights, with an emphasis on their tendency to fuel polarization, misinformation, and hostility toward immigrants (Guriev and Papaioannou, 2022). In contrast, our evidence complements the theoretical contribution of De Vries and Hobolt (2020) by showing that, under some conditions, populist challengers can behave as issue entrepreneurs, politicizing long-standing problems that mainstream political parties have persistently failed to address.[3]

We also contribute to a growing literature connecting environmental shocks, policies, and natural disasters to political outcomes. For example, exposure to climate extremes influences green voting and Californian wildfires increase support for costly climate-related measures in Democratic voting areas (Hoffmann et al., 2022; Hazlett and Mildenberger, 2020). Colantone et al. (2023) examine the electoral consequences of green policies and show that a ban on polluting cars in Milan increased support for the populist right party Lega among owners of restricted vehicles. Mehic (2023) exploits between municipality variation in radioactive fallout over Sweden due to Chernobyl disaster to measure its causal impact on Green voting. Related works study how other environmental shocks affect electoral outcomes, including the Xylella plant disease epidemic (Cremaschi et al., 2025), earthquakes (Masiero and Santarossa, 2021), and hurricanes (Gagliarducci et al., forthcoming). In particular, we extend recent studies that use wind-based exposure designs, common in environmental and health economics (Deryugina et al., 2019; Graff Zivin et al., 2023; Qiu et al., 2024; Borgschulte et al., 2024).

This paper is organized as follows. The next sections present the institutional background and the data. Section 4 discusses the empirical strategy whereas Section 5 presents the main results. Section 6 and 7 explore potential mechanisms and robustness checks. Finally, Section 8 concludes the paper with implications on electoral accountability and environmental challengers.

2 Background

2.1 Historical origins and institutional context

Our setting is a major environmental disaster arising from the illegal disposal of toxic waste in the *Terra dei Fuochi* ("Land of the Fires"), a densely populated area of Southern Italy. Criminal organizations, primarily Camorra clans and in particular the *Casalesi*, operate a large-scale illicit network for trafficking and dumping hazardous materials across the region. Despite persistent rumors and sporadic investigations, the issue did not attract broad public attention until 2005, when authorities released the first official map of contaminated sites. This disclosure provided the first official acknowledgment of a problem that had previously circulated only as an unconfirmed rumor.

Figure 1 presents the institutional and political evolution from 1988 to 2025, with green boxes marking the environmental shock, red boxes the 2005 information shock that makes the issue salient to voters, and yellow boxes the subsequent entry and rise of the challenger

[3] An article in The Economist, titled "Can Potholes Fuel Populism?", similarly argues that the rise of the anti-establishment Reform Party in the UK was fuelled by local neglect of potholes, noting that all four of its gained seats had a "missing road".

FIGURE 1: Timing (1988-2025)

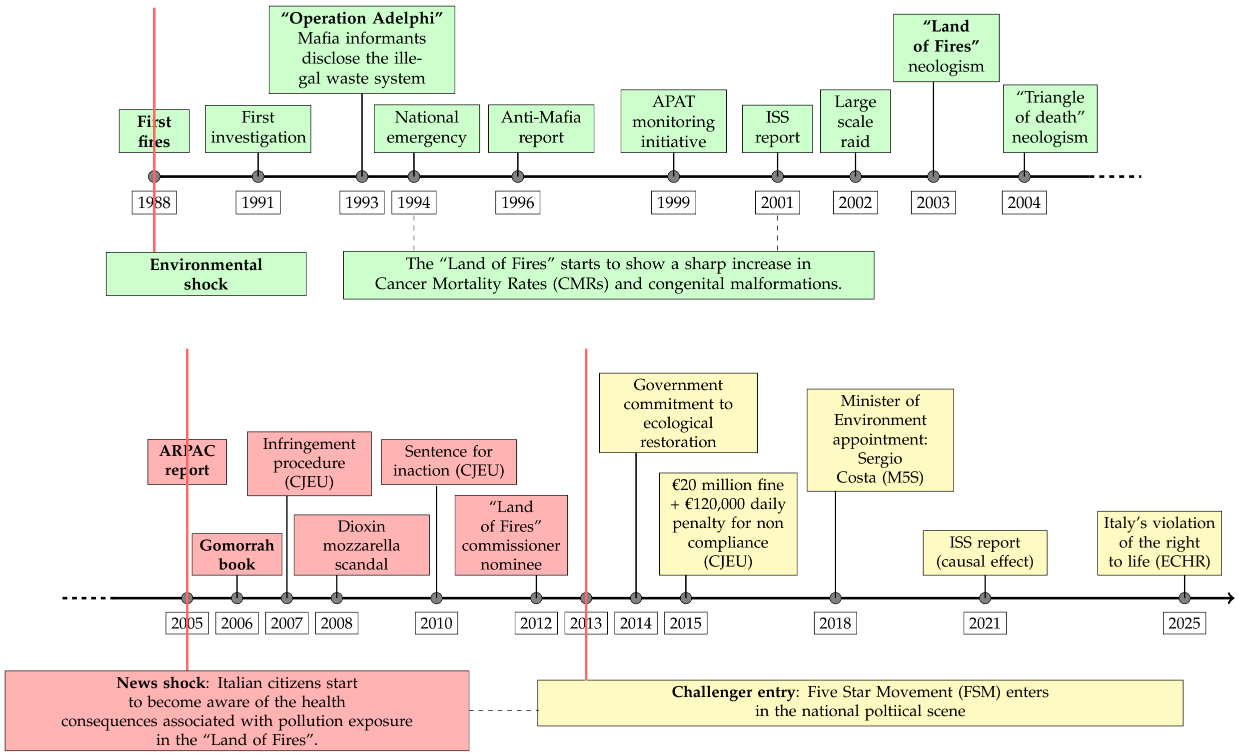

Notes: The chronicle summarizes the Campanian waste emergency. *Anti-mafia report*: the Anti-Mafia Investigation Division unveils that approximately 80% of toxic waste is disposed illegally. *APAT monitoring initiative*: the Italian Agency for Environmental Protection and Technical Services (APAT) starts to inspect Castel Volturno Lakes area using infrared ray instrumentation. *ISS report*: the National Institute of Health (ISS) finds a correlation between childhood mortality distribution and dumping sites in the province of Caserta.

FSM into national politics. Yet, despite increased public attention, toxic waste is still displaced and burnt in the area. In 2025, the European Court of Human Rights ruled that Italy had violated the right to life of residents exposed to toxic dumping.

First fires date back to the 1980s. On February 4, 1991, a truck driver in the Naples area reported a sudden decline in eyesight after transporting toxic waste. This event triggered the first investigation. Two years later, "Operation Adelphi" led to 116 arrest warrants and the Camorra seemed to be behind most of these activities (D'Alisa et al., 2015).

This scandal involves firms, business intermediaries, and public officials, revealing a vertically integrated system whose adverse effects spanned the urban, environmental, health, economic, and political domains. The scheme is profitable because legal disposal is expensive. Hazardous waste regulation imposes high costs on firms, particularly for waste containing toxic or non-degradable substances. Legal disposal requires proper treatment, secure transport, and extensive documentation for traceability. These requirements create rents for intermediaries able to circumvent them. In Campania, criminal organizations supply such an alternative channel: firms can offload waste at a fraction of the legal cost by avoiding compliance protocols. In turn, criminal organizations can exploit territorial control and corruption to operate disposal sites without interference. Criminal networks handle waste for firms across Italy and, in some cases, from abroad.

The illicit disposal activity is concentrated in a cluster of municipalities in the Campania region, primarily in the provinces of Naples and Caserta. This area features a highly concentrated population and fragmented land uses, where housing, agriculture, and industrial activity are closely integrated. Illegal sites are typically small, numerous, and geographically dispersed, often embedded within inhabited areas rather than confined to a few centralized facilities.

Disposal practices include dumping on agricultural land, along roads, near construction sites, and in disused quarries, as well as burial under fill material associated with building activity. A common method for reducing volume is open-air burning, which generate toxic emissions that can travel far from the disposal sites. The recurrent use of such fires is also the origin of the label "*Terra dei Fuochi*" ("Land of the Fires") in public discourse.[4]

Pinning down the exact onset of illegal waste disposal is challenging. Anecdotal evidence suggests that the first unauthorized episode began in the mid-1980s. According to repentant mafioso Carmine Schiavone, a senior member of the *Casalesi* clan and cousin of the boss, the group began systematically managing toxic waste operations in 1988, though some activity had occurred earlier. His declarations remains one of the most detailed sources on the disposal network, including the volume of waste handled and the specific locations, and have been used to identify and map contaminated sites. Subsequent investigations by judicial authorities confirmed contamination at the sites he named, supporting the credibility of his statements.

Fires are neither regulated nor controlled, releasing hazardous pollutants directly into the atmosphere. These airborne emissions spread based on wind direction, reaching areas far from the original site. A key feature of the Land of Fires is the systematic concealment of illicit activity, concentrated around the *Casalesi* headquarter in Casal di Principe. Authorities lacked comprehensive site registries across the years and emissions were not routinely measured. Until the 2005 news shock, local residents had limited information about the existence, timing, and composition of dumped waste.

This lack of information had two major implications. First, people were unable to respond through avoidance or relocation, limiting sorting based on pollution exposure. Second, institutional responses were delayed and partial. Even after official acknowledgment, remediation efforts covered only a fraction of affected sites, and many locations remain classified as "potentially contaminated" due to the absence of formal verification.

[4] The name Terra dei Fuochi appeared for the first time in 2003 in a report of a non-profit proenvironment organization. Nowadays, this name is used to denote the area also in official government reports. The Italian Government recognizes 90 municipalities as being a part of the *Terra dei Fuochi* due to the intensity of contaminated sites in their territory.

The pollutants included substances known to persist in the environment and accumulate in the body, such as dioxins and heavy metals. Medical research links these to cancer types that may take decades to appear. Since soil and groundwater contamination lasts long after dumping stops, exposure continues even today.

2.2 Health risks in the Land of Fires

In September 2001, the National Institute of Health (ISS) reported a correlation between childhood mortality and proximity to dumping sites in the province of Caserta. Three years later, Senior and Mazza (2004) documented malignant cancer rates and congenital malformations markedly above national averages around the towns of Acerra, Nola and Marigliano ("triangle of death"). These descriptive patterns are consistent with toxic profiles of the waste involved. Clinical and epidemiological studies associate exposure to these substances with cancers that typically appear only after long latency periods, often spanning several decades. In this context, Cipullo et al. (2026) provide causal evidence on the long-run health effects of the Land of Fires. Exploiting quasi-random variation in historical wind directions around contaminated sites within a difference-in-differences framework, the study finds that municipalities exposed to toxic winds suffer significantly higher cancer mortality than comparable control municipalities. From the late 2000s onward, the estimates imply roughly two additional cancer deaths per municipality per year, corresponding to several hundred excess deaths annually in the region.

3 Data

To create our municipality-level dataset, we draw from multiple data sources.

Illegal Disposal Sites (IDS). We retrieve data on Potentially Contaminated Sites (henceforth, PCS) from the Campania Regional Agency for the Protection of the Environment (ARPAC). The first inventory was published in 2005 and subsequently expanded in later years. It was updated in 2010, 2013, and annually from 2016 onward. However, only a small number of additional PCSs were added after 2005 (Figure A1 shows the number of sites by year of first registration). Sites are labelled as "potentially" contaminated because no systematic environmental assessment has been carried out at each location.

Updates to the PCS inventory may reflect either new episodes of illegal disposal or the later discovery of older dumping activity. For this reason, in our empirical analysis we do not use the year in which a site first appears in the inventory as a source of variation. The PCS inventory records, for each site, the type of pollutant, a brief description of the activity at the location, and its exact geographic coordinates.

Since the inventory includes sites contaminated for reasons unrelated to the illegal toxic-waste network (e.g., mismanagement of regular municipal waste), we exploit specific descriptions to identify Illegal Disposal Sites (henceforth, IDS) within the full set of PCSs. IDS are those sites directly associated with the Land of Fires pattern of illegal disposal. Hence, we classify as IDS all sites whose descriptions include terms such as "abandoned", "uncontrolled", "dioxin", "toxic", "dismissed", or "quarry".[5] Conversely, we exclude sites explicitly categorized as "business", "industrial", "gas station", or "hotel".

The final dataset used in our analysis comprises 1,674 Illegal Disposal Sites. Figure A2 maps their geographic distribution: most IDS are located in municipalities officially recognized by the Italian government as part of the Land of Fires, though additional sites are found elsewhere in the region.

Weather variables. We obtain daily data for 2001–2009 from the regional agrometeorological archive of the Campania Department of Agriculture.[6] The dataset covers 47 weather stations located in 45 municipalities.[7] For each station–day, it records wind direction, average wind speed, temperature, humidity, and precipitation.

Electoral outcomes. We use administrative data from *Eligendo*, the official election archive of the Italian Ministry of the Interior. For national parliamentary elections, we build a municipality-level panel covering all general elections from 1972 to 2022. For each municipality–election observation, our dataset reports the number of registered voters, number of voters, invalid and blank ballots, and votes by party, from which we compute turnout and party vote shares. For each election, we consider the ten most voted parties. We also use *Eligendo* to obtain information on all local elections held in Campania between 2010 and 2024. From these records, we create an indicator equal to one if FSM presents a list in a given municipality–election, and zero otherwise.

Parliamentary speeches and EU cohesion funds. We exploit data on parliamentary speeches in the Italian lower house from the *ItaParlCorpus* dataset (Cova, 2025). We exploit all plenary debates in the Chamber of Deputies from 1996 to 2022. For each intervention, we have information on the speaker's name, party affiliation, legislature, date of the speech, a unique speech identifier, and the full transcript text.

We also use project-level information on EU cohesion funds from *OpenCoesione*, a transparency portal of the Department for Cohesion Policies and the South, part of the Italian government. For each project, this dataset reports title, thematic area, sector, total public funding, beneficiary municipality, and project start date. In our empirical analysis, we ag-

[5] Anecdotal evidence suggests that abandoned quarries were frequently used for illegal waste disposal once nearby open-air burning locations were no longer available.

[6] See https://agricoltura.regione.campania.it/meteo/archivio_meteo.html.

[7] The database is available from 2001 onward, so earlier years cannot be used.

gregate projects at the municipality–year level to build annual measures of EU cohesion funds received by each municipality.

ITANES. We use individual-level data from the Italian National Election Study (ITANES), a repeated cross-sectional survey carried out immediately before and after all national elections since 1972. Each wave interviews a new, nationally representative sample of about 2,000–3,000 individuals. Our analysis focuses on waves from 2006 to 2022. These surveys include the same questions on trust in political parties and in the national parliament. They also provide detailed information on respondents' self-reported voting behaviour, political participation, and socio-demographic characteristics such as age, gender, education, and employment status. We restrict our attention to the ten parties with the largest national vote shares in each election.

Municipal characteristics. We collect municipal-level controls from several administrative and data sources. We obtain demographic and socio-economic variables from the 2001 population census by ISTAT (Italian National Institute of Statistics), including the shares of men, residents with tertiary education, employment in the health sector, daily commuters, and foreign residents, as well as geographic covariates such as municipality surface and altitude. Information on municipal taxable income over 2000–2004 comes from the Ministry of Economy and Finance. Data on radon concentrations are taken from A2C, a professional consortium specializing in radon measurement and remediation of contaminated sites. Finally, information on civilian victims of mafia-related violence over 1967–2004 is drawn from *Libera*, a civil-society organization that curates the main national database of innocent victims of organized crime.

4 IDENTIFICATION

Figure 2 plots changes in turnout at national elections against exposure to IDS. Panel (a) reports the difference in average turnout between pre- and post-shock elections, defined as $\Delta Turnout = \overline{Turnout_{1972-2001}} - \overline{Turnout_{2006-2022}}$, so darker shades correspond to municipalities where turnout fell more after the news shock. Panel (b) shows the number of IDS per square kilometer, with darker tones denoting higher IDS density. Municipalities with the largest turnout declines cluster in the same north-western area where IDS density is highest, suggesting a strong negative association between pollution exposure and electoral participation. However, IDS density is potentially endogenous: illegal dumping locations may reflect geographical characteristics (such as abandoned areas, lakes, quarries), or the local activity of organized crime (for instance, strategic dumping or corruption). To identify the causal impact of IDS on turnout, we therefore use historical wind trajectories to obtain plausibly exogenous variation in exposure. Conditional on

FIGURE 2: Turnout and pollution exposure

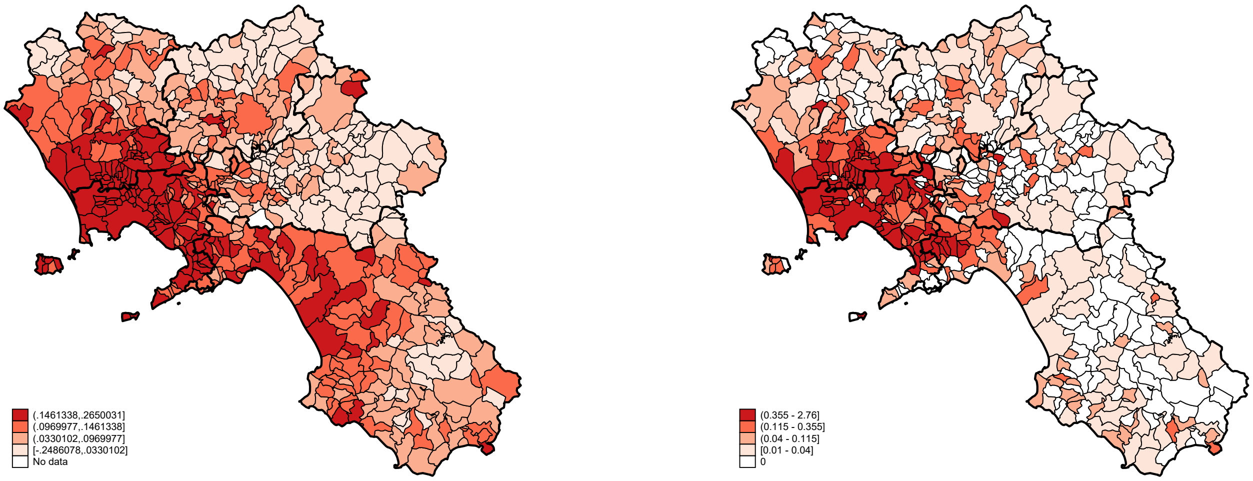

(a) Change in average turnout (1972–2001 vs 2006–2022)

(b) Number of Illegal Disposal Sites (IDS) per square kilometer

proximity to IDS, prevailing winds determine whether a municipality lies predominantly downwind or upwind relative to contaminated sites, which in turn affects its exposure to airborne pollution. Importantly, there is no institutional evidence that wind patterns were considered when selecting dumping sites.[8]

Following this historical evidence, we isolate exogenous variation in the exposure of each municipality to PCS by exploiting wind direction to identify upwind sites and to build our measure of wind exposure, while controlling for surface and the exact number of PCS. In this way, we try to replicate the ideal experiment. Consider two municipalities, each with the same number of PCS (e.g. one PCS): one municipality has an upwind PCS, while the other one does not. If wind direction is exogenous, comparing these municipalities eliminates endogenous variation in PCS intensity, isolating the impact of upwind exposure. The underlying idea is the following: a PCS only affects health and economic outcomes in a municipality if it is upwind exposed relative to the municipality demographic centroid, carrying pollutants (e.g. dioxins) into the municipality. For this reason, we determine the demographic centroid for each municipality by computing the population weighted average of (x, y) coordinates at district level:

$$x_m = \sum_{s=1}^{n} \left(\frac{Pop_{s,m}}{Pop_m^{Tot}} \times x_{s,m} \right) \quad ; \quad y_m = \sum_{s=1}^{n} \left(\frac{Pop_{s,m}}{Pop_m^{Tot}} \times y_{s,m} \right)$$

where m is the municipality, s is the district and Pop refers to the population from 2001

[8]Parliamentary auditions of Carmine Schiavone and his subsequent public statements suggest that sites were chosen according to proximity to highways, distance from urban centers, and availability of flat land, rather than prevailing winds.

census data. Figure 3 provides an example. On top of that, we assume that a PCS is upwind relative to the municipality centroid if the angle θ between the connection vector (linking the municipality demographic centroid and the Potentially Contaminated Site) and the historical wind direction vector in each PCS ($\overline{WINDDIR_{PCS}}$) falls within 0 and 90 degrees. $WindExposed_m$ is a binary indicator equal to 1 if municipality m has a number of upwind exposed PCS greater than zero, capturing whether the municipality is exposed to at least one upwind PCS (extensive margin). We consider all PCS identified between 2005 and 2022, as the timing of a site's official registration by ARPAC does not necessarily correspond to the onset of contamination. Both anecdotal and institutional evidence suggest that many PCS were already active by the 1980s, although formal registration procedures began in the late 1990s and were only officially released from 2005 onward.

FIGURE 3: Demographic centroid

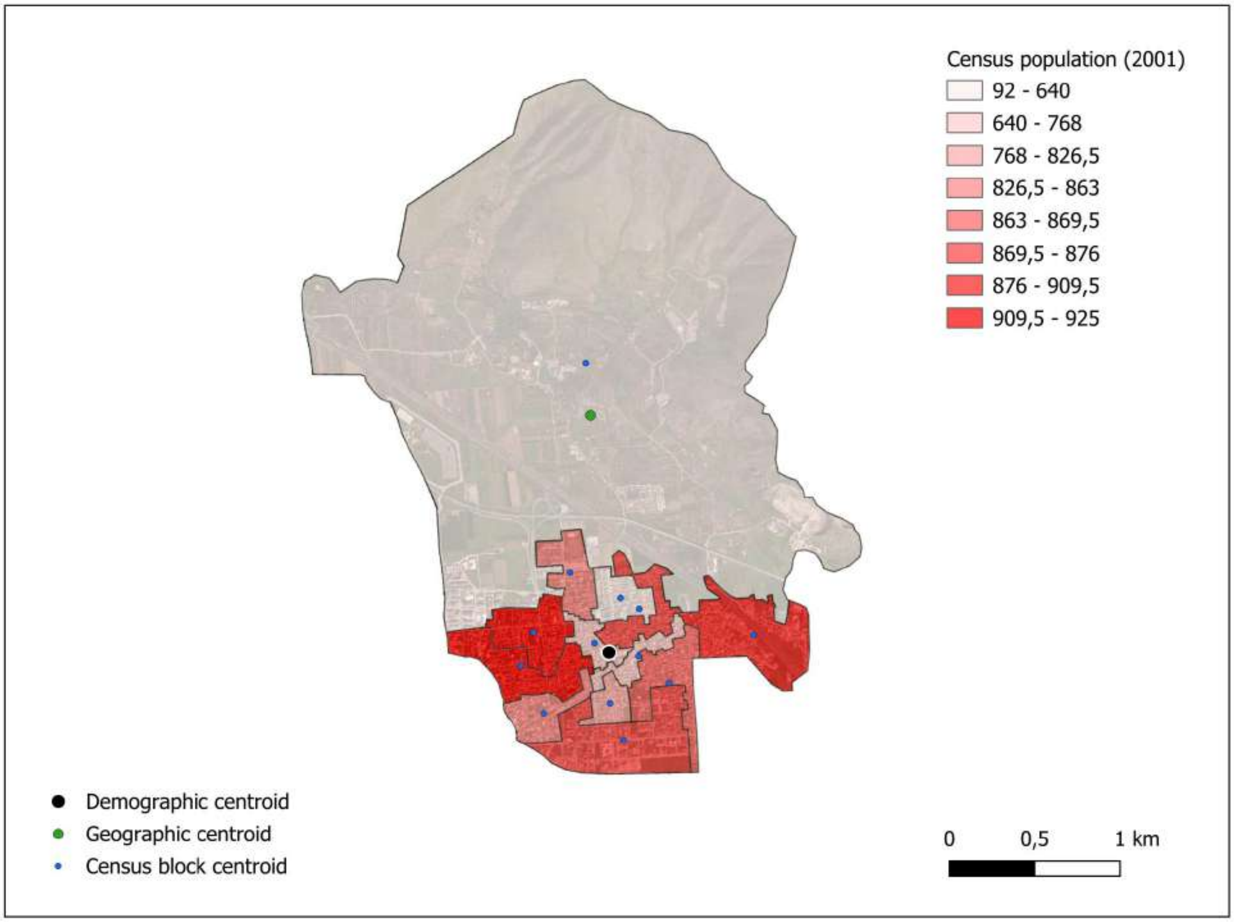

Notes: This figure displays the demographic and geographic centroids for the municipality of San Prisco (province of Caserta), which consists of 13 census blocks. Shaded polygons represent census blocks, with darker tones denoting higher 2001 census population. Blue dots mark the geographic centroids of each census block. The green dot is the municipality's geographic centroid, whereas the black dot is the demographic centroid. The latter is computed as the population–weighted average of census block centroids using 2001 census data. Since wind exposure is measured over 2001–2009, the 2001 census provides the closest snapshot of the spatial distribution of residents in this period. The underlying satellite image shows that the northern part of San Prisco is largely uninhabited, while residential areas are concentrated in the south. Consistently, the demographic centroid lies in the populated southern area rather than at the geometric center of the municipality, making it a more suitable proxy for individual exposure to pollution.

4.1 THE WIND MODEL: IDENTIFYING UPWIND PCS

To build our variable $WindExposed_m$, we need to identify PCS located upwind relative to the municipality's demographic centroid. We exploit historical wind direction data to classify upwind PCS. Our model is structured as follows. First, we assign one synthetic station to each of the 1,674 PCS. As prior knowledge, we have information on the 47 actual stations for 45 municipalities during the period 2001-2009. To approximate wind direction at synthetic stations, we implement a spatial matching technique inspired by the K-Nearest-Neighbors (KNN) methodology. We consider as valid nearest neighbors the five nearest actual stations for which the Wind Influence indicator ($WI_{i,j}$) is equal to

1. We proceed in two steps. First, for each synthetic station i we compute the angle (θ) between the wind direction vector at the $j-th$ actual station in municipality m on day t ($WINDDIR^{act}_{j,m,t}$) and the connection vector linking the synthetic station i to the j-th actual station, following **?**. Second, we define the binary indicator $WI_{i,j}$ as equal to 1 if θ falls within the range $[0°, 90°]$. We denote the subset of all actual stations j such that $WI_{i,j} = 1$ as $\mathbf{J^i}$. This subset represents the acceptable region within municipality's borders: it is the half-space delimited by a line orthogonal to the wind direction vector and passing through the synthetic station i (see Figure B1). Then, for each actual station j in $\mathbf{J^i}$, we compute weights $\alpha_{i,j}$, as the inverse of the distance between the synthetic station i and the actual station j.[9] Subsequently, we select the five smallest $\alpha_{i,j}$.[10] The wind direction in synthetic station i in municipality m on day t ($WINDDIR^{syn}_{i,m,t}$) is then computed as the weighted average of wind directions observed at these selected actual stations:

$$WINDDIR^{syn}_{i,m,t} = \sum_{j=1}^{5} \alpha_{i,j} WINDDIR^{act}_{j,m,t}$$

Finally, we compute the average wind direction at PCS level ($\overline{WINDDIR^{syn}_{PCS}}$) over the entire period 2001-2009. In this way, we retrieve the historical wind direction for all the 1,674 synthetic stations and we are able to assign upwind PCS.

[9] In this way, closer actual stations receive higher weights.

[10] Appendix B provides further details on the computation of θ and $\alpha_{i,j}$.

FIGURE 4: Historical average wind direction at synthetic PCS stations

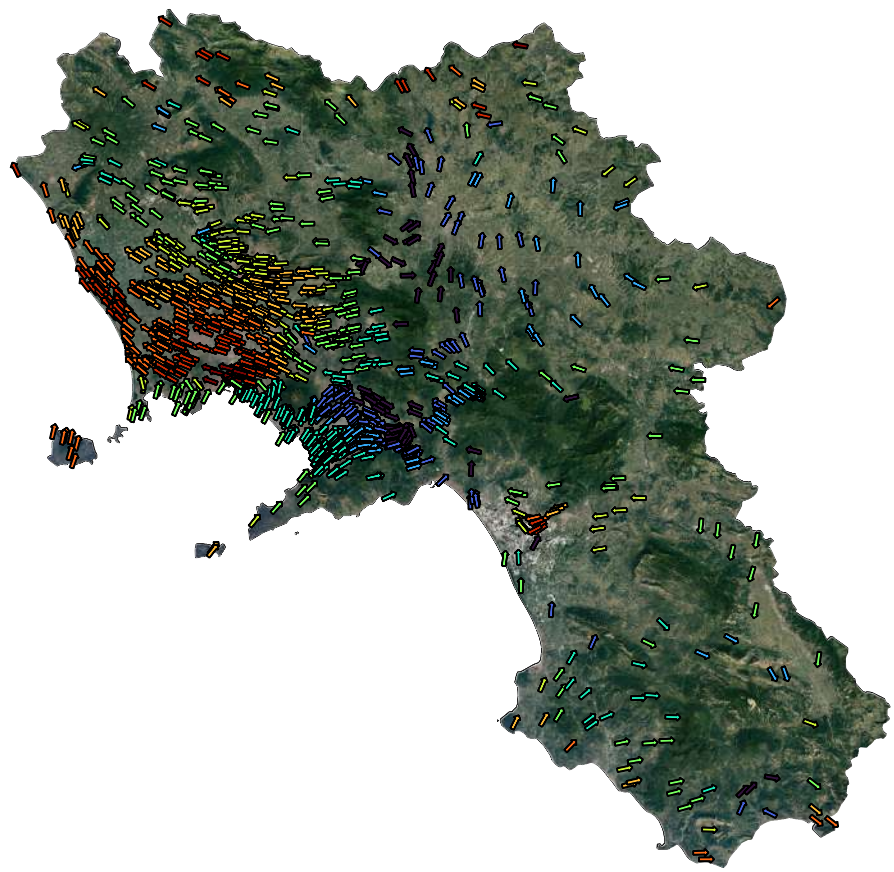

Notes: This figure displays the interpolated historical average wind direction (2001-2009) at all the 1,674 synthetic stations, each placed at the coordinates of a PCS. Color intensity denotes wind speed (darker red arrows correspond to higher average wind speeds).

4.2 EMPIRICAL STRATEGY

To estimate the causal effect of pollutant exposure on voter turnout, we implement a difference-in-differences (DiD) design with an instrumented treatment, included within a two-way fixed effects (TWFE) model:

$$Turnout_{m,t} = \alpha_m + \lambda_t + \gamma WindExposed_m + PCS_m^{sqkm} + \sum_{k \in [1972,2022]} \xi_k \boldsymbol{X_{m,t-1}} \times \mathbf{1}(Year_t = k) + \epsilon_{m,t} \quad (1)$$

where α_m denotes municipality fixed effects, capturing time-invariant unobserved heterogeneity across municipalities, and λ_t represents time fixed effects, absorbing common shocks across time. The treatment variable, $WindExposed_m$, is a binary indicator equal to 1 if municipality m has a number of upwind exposed PCS greater than zero (extensive margin). Upwind exposure is determined by computing a 3 km buffer around each PCS and evaluating whether the municipality's demographic centroid falls within the acceptable region (see Figure 5 and Figure 6).

FIGURE 5: Upwind PCS classification

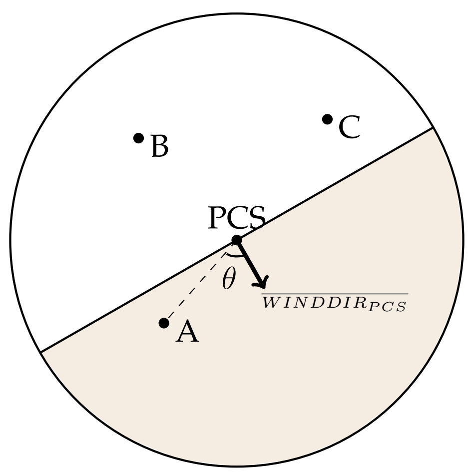

(a) $WindExposed_m$

Notes: This figure illustrates how a Potentially Contaminated Site (PCS) is classified as upwind relative to the municipality's demographic centroid (centroid A). This occurs when the angle (θ) between the connection vector (dashed line from the demographic centroid to the PCS) and the historical average wind direction ($\overline{WINDDIR_{PCS}}$) falls within the range $[0°, 90°]$. Centroids B and C show the opposite case, where a PCS is not upwind exposed relative to the demographic centroid, as θ is greater than 90 degrees. The circle represents a 3 km buffer radius centered on the PCS. The acceptable region for upwind classification (shaded area) is defined by the half-space created by a line orthogonal to the wind direction and passing through the demographic centroid, ensuring that a PCS is counted in the $WindExposed_m$ variable only when a municipality's demographic centroid is located in that area. This classification allows us to isolate the subset of PCS_m that are likely to transmit pollutants towards the municipality's demographic centroid, which serves as a proxy for the municipality's electorate.

The post-treatment period is identified by the indicator variable $Post$, which equals 1 for all election years after 2001 (i.e. the release of the first official map in 2005), and 0 otherwise. This model also controls for a set of year dummies interacted with a set of control variables ($\boldsymbol{X_{m,t-1}}$) which include the total number of PCS per square kilometer, municipality surface, historical weather variables at municipality level (average wind direction, wind speed, humidity, maximum temperature, and rainfall over 2001-2009), predetermined socio-demographic variables (share of men, share of higher educated individuals, employment rate in the health sector, share of daily commuters, share of foreign residents, historical average taxable income per capita over 2000-2012), and geographical characteristics (maximum altitude and radon levels in 2007). The model is weighted by electorate size at the municipality level in 2001.

To examine the causal effect of toxic winds on mainstream reaction after the news shock, we implement the following DiD with instrumented treatment:

$$\begin{aligned} MentionsShare^{D}_{m,t} = \alpha_m + \lambda_t + \gamma WindExposed_m + PCS^{sqkm}_{m} \\ + \sum_{k\in[1994,2022]} \xi_k \boldsymbol{X_{m,t-1}} \times \mathbf{1}(Year_t = k) + \epsilon_{m,t} \end{aligned} \tag{2}$$

where $MentionsShare^{D}_{m,t}$ is the ratio of all dominant (mainstream) D speeches that mention a Campania municipality. α_m denotes municipality fixed effects, and λ_t represents time fixed effects. The treatment variable, $WindExposed_m$, is a binary indicator equal to 1 if municipality m has a number of upwind exposed PCS greater than zero (extensive margin). The post-treatment period is identified by the indicator variable $Post$, which equals 1 for all parliamentary speeches held after year 2004, and 0 otherwise. This model also controls for a set of year dummies interacted with the set of control variables ($\boldsymbol{X_{m,t-1}}$) described in Equation 1. The model is weighted by electorate size at the municipality level in 2001.

Third, to study the effect of toxic winds on parties vote share, we estimate a Weighted Least Square (WLS) with weights equal to municipality electorate size:

$$VoteShare^{i}_{m,t} = \alpha + \beta WindExposed_m + PCS^{sqkm}_{m} + X_{m,t-1} + \gamma_p + \lambda_t + \epsilon_{m,t} \tag{3}$$

where $VoteShare^{i}_{m,t}$ is the vote share for party i in municipality m at time t (national elections) and $WindExposed_m$, the key regressor of interest, is a binary indicator equal to 1 if municipality m has a number of upwind exposed PCS greater than zero (extensive margin). PCS_m^{sqkm} is the total number of PCS per sqkm in municipality m. $X_{m,t-1}$ is a vector of predetermined controls, including socio-demographic, geographical, electoral and historical weather variables at the municipality level. The full set of controls used in the most stringent specification is detailed in Table 6. The model also includes province fixed effects (γ_p) and year fixed effects (λ_t). Standard errors are clustered at municipality level. The error term is denoted by $\epsilon_{m,t}$.

FIGURE 6: Buffer 3 km

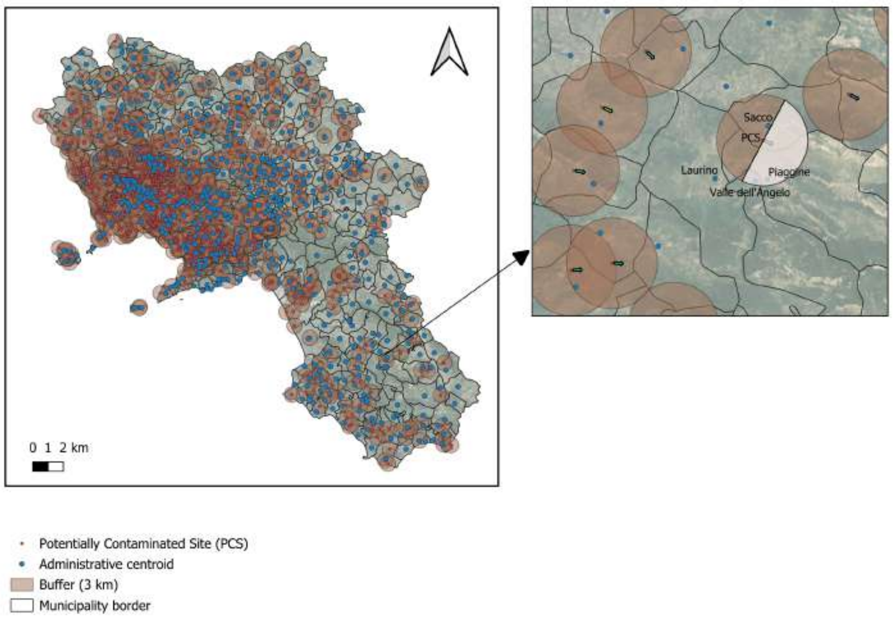

Notes: This figure displays the spatial buffer used to identify upwind exposed PCS. Each circle represents a 3 km radius centered on each Potentially Contaminated Site (PCS), marked by red dots. Blue dots represent the demographic centroids of municipalities. A municipality is classified as affected by the buffer if any part of its demographic centroid intersects the 3 km buffer circle. To define upwind exposure, this buffer-based classification is combined with the historical average wind direction at each PCS, denoted by $\overline{WINDDIR_{PCS}}$. The top-right panel provides a zoomed-in view where a single PCS intersects multiple municipalities (Sacco, Piaggine, and Valle dell'Angelo). Based on $\overline{WINDDIR_{PCS}}$, Piaggine and Valle dell'Angelo fall within the acceptable upwind region (shaded area), and are thus considered exposed.

In Figure 7 we report a series of balancing checks by regressing the entire set of controls (historical weather variables at municipality level, socio-demographic variables, geographical characteristics, electoral outcomes in 2001) on our key regressor $WindExposed_m$. This specification controls also for province and year fixed effects. Most covariates appear well balanced between treated and control municipalities. Meteorological variables, as well as the total number of PCS, are plausibly mechanically correlated with the treatment by construction.

FIGURE 7: Balance test (upwind PCS exposure)

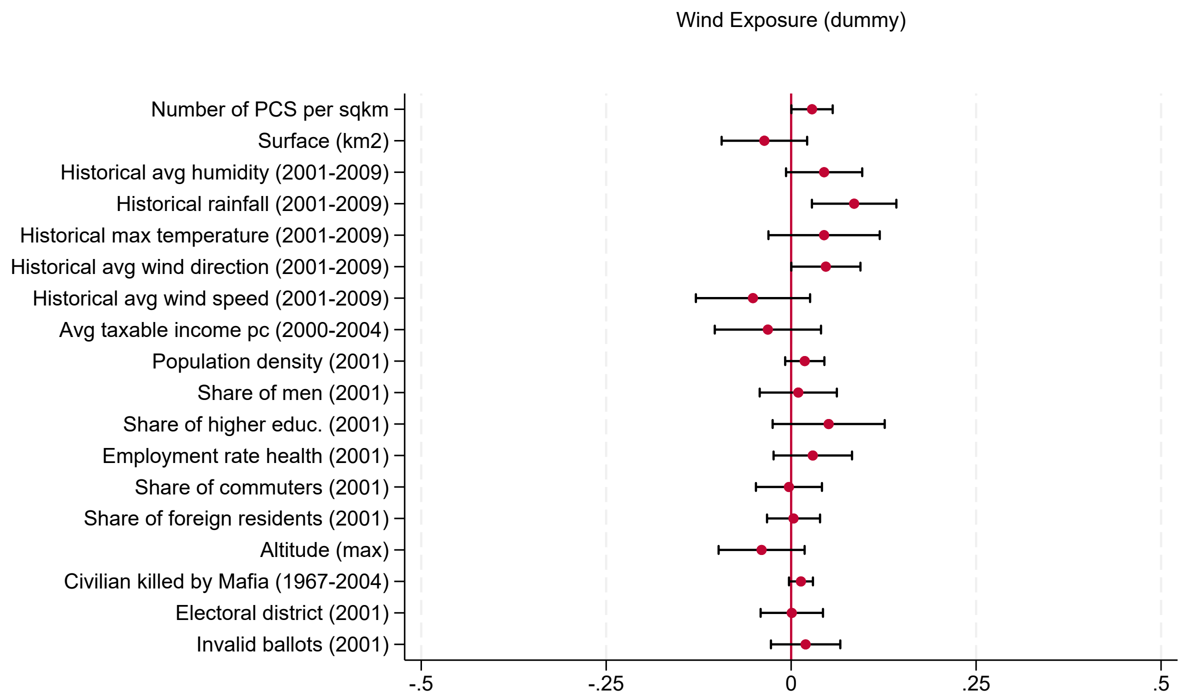

Notes: This figure reports WLS estimates of the variable $WindExposed_m$ on the entire set of control variables, together with 95% confidence intervals. All covariates have been standardized to have mean zero and unit standard deviation. This specification controls for province and year fixed effects. Standard errors are clustered at the municipality level.

5 UPWIND EXPOSURE AND MAINSTREAM INERTIA

Following the political entrepreneurship framework proposed by **?**, we define dominant (or mainstream) parties as those currently in government or with recent experience in governing. Given our focus on the Italian Second Republic (i.e., from 1996 onward), we classify as dominant parties both the left-wing coalition and the right-wing coalition, the latter led by post-fascist *Alleanza Nazionale* ("National Alliance") and *Forza Italia*, the party founded by Silvio Berlusconi. We also include *Il Popolo della Libertà* ("People of Freedom"), founded in 2007 through the merger of *Forza Italia* and *Alleanza Nazionale*. Additionally, we classify *Fratelli d'Italia* ("Brothers of Italy") as a dominant party, since it is the direct successor of *Alleanza Nazionale*. By contrast, we exclude the "League", which is widely recognized as a far-right populist party (**?**). We also define as challenger parties those that have never held national executive office during the period under analysis (e.g. "Five Star Movement"). Hence, we study the effect of upwind exposure after the news shock on mainstream behaviour by estimating Equation 2 while using as outcome variable the ratio of total mentions of Campania municipalities by deputies from dominant parties D to the total number of deputies from dominant parties. Table 1 reports WLS difference-in-differences estimates. In the post-period, we estimate a higher number of mentions per deputy for dominant parties. However, the magnitude is negligible, suggesting no meaningful change in parliamentary attention after the shock. Results are stable as progressively richer controls are added.

Figure 8 plots dynamic difference-in-differences estimates from Table 1. First, we notice the absence of pre-trends between treatment and control municipalities before the news shock (95% confidence intervals), as coefficients are small and statistically indistinguishable from zero. Following the news shock (dashed vertical line), we observe a rise in mentions per deputy by dominant parties. However, the magnitude suggests inertia among mainstream parties. A clear shift emerges after M5S parliamentary entry in 2013 (solid red vertical line), as mentions per deputy among dominant parties decline significantly and persistently in the following years. This could suggest that mainstream parties tend to reallocate their programmatic supply on other topics.

TABLE 1: Effect of wind exposure to PCS on parliamentary activity (all years)

	Weighted Least Squares (WLS)			
Buffer radius: 3 km	(1) Mentions ratio	(2) Mentions ratio	(3) Mentions ratio	(4) Mentions ratio
Wind Exposure (dummy) × $Post$	0.000379**	0.000236**	0.000154*	0.000144*
	(0.000147)	(0.0000934)	(0.0000797)	(0.0000744)
Municipality FE	✓	✓	✓	✓
Year FE	✓	✓	✓	✓
PCS number per sqkm	✓	✓	✓	✓
Year × Surface	✓	✓	✓	✓
Year × Historical weather variables		✓	✓	✓
Year × Socio-demographic controls			✓	✓
Year × Geographical characteristics				✓
Observations	14904	14904	14904	14904
R-squared	0.851	0.891	0.902	0.904
F-stat	94.32	.	.	.

Notes: This table shows WLS difference-in-differences estimates of the effect of wind exposure to PCS after the news shock on the annual number of mentions of Campania municipalities per deputy for dominant parties in the Italian Chamber of Deputies from 1996 to 2022. Each column refers to a 3 km buffer radius from the PCS center (see Figure 6). The treatment is instrumented by $WindExposed_m$, defined as a binary indicator equal to 1 if municipality m has a number of upwind exposed PCS greater than zero (extensive margin). The post-treatment period begins in 2005, following the release of the official contamination map. Column (1) presents a baseline model with municipality and year fixed effects to account for time-invariant unobserved heterogeneity at the local level and common time shocks. It also includes the total number of PCS per sqkm and municipality surface (interacted with year dummies). Columns (2)-(4) progressively introduce controls fully interacted with year dummies. Column (2) adds historical weather variables at municipality level (average wind direction, wind speed, humidity, and rainfall over 2001-2009). Column (3) includes socio-demographic controls: share of men, share of higher-educated individuals, employment rate in the health sector, share of foreign residents, share of daily commuters. Column (4) further adds geographical characteristics (maximum altitude and radon levels in year 2007). All regressions are weighted by electorate size at the municipality level in the year 2001. Heteroscedasticity and cluster-robust standard errors at the municipality level are in parentheses. Stars indicate significance levels (* $p < 0.1$, ** $p < 0.05$, *** $p < 0.01$).

FIGURE 8: Effect of wind exposure on parliamentary activity: dynamic specification

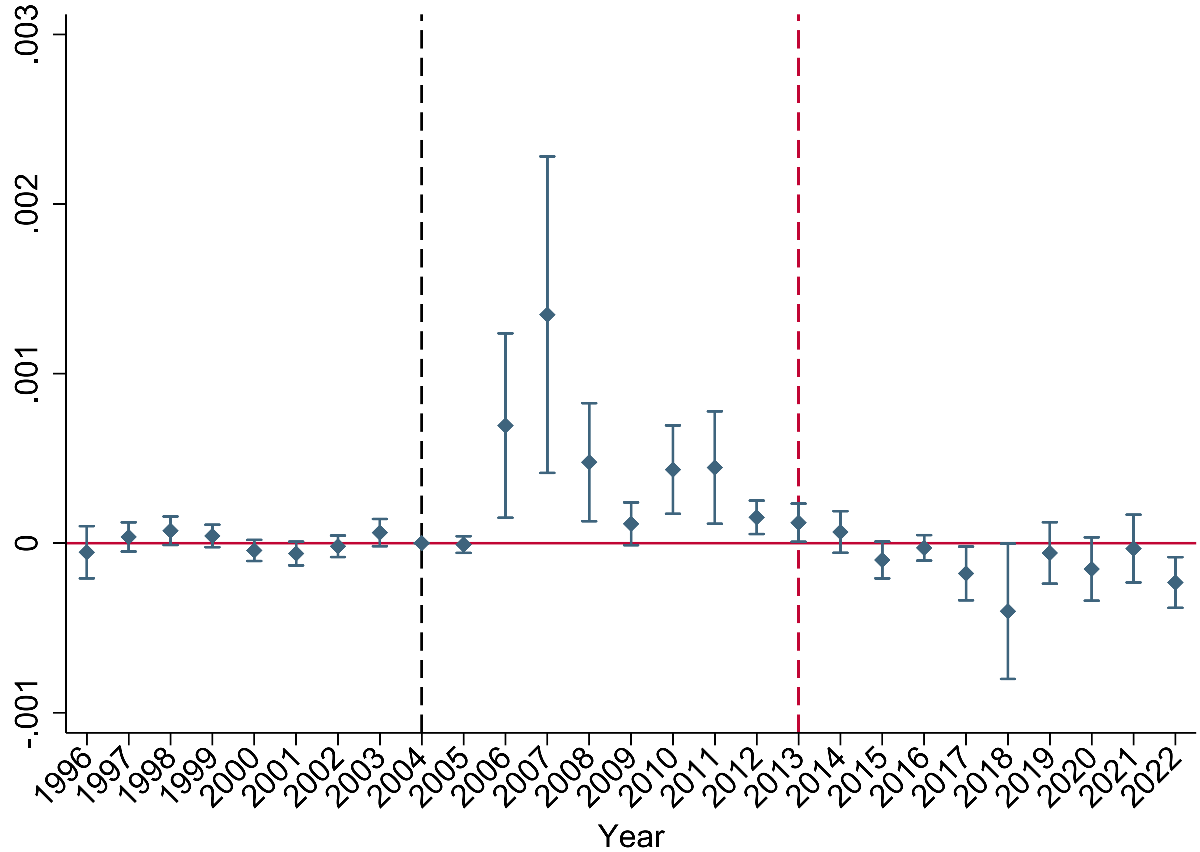

Notes: This figure plots coefficients from a dynamic specification estimating the interaction between the treatment variable $WindExposed_m$ and year indicators, with 2004 omitted as the reference year. Each point shows the estimated effect of wind exposure on the number of annual mentions of Campania municipalities per deputy for dominant parties in the Italian Chamber of Deputies, relative to 2004. The solid red vertical line marks the entry of the Five Star Movement into the Italian parliament. This model controls for the most stringent specification reported in Table 1 and it is weighted by electorate size at the municipality level in year 2001, with 95% confidence intervals. Standard errors are clustered at the municipality level.

To fully understand the mechanism underlying mainstream inertia, we run a text analysis of parliamentary speeches. Table 2 shows how wind exposure is associated with the tone of parliamentary speeches that mention Campania municipalities. Polarity ranges from -1 (entirely negative) to 1 (entirely positive), while subjectivity ranges from 0 (fully objective) to 1 (fully subjective). The Five Star Movement (M5S) stands out in this comparison. Although its estimated polarity is not significant, the negative coefficient suggests a more critical tone when discussing upwind-exposed municipalities. For subjectivity, it exhibits the largest decline (i.e. a more objective tone). By contrast, the Democratic Party exhibits a more positive tone and less objective (0.09), suggesting a reframing strategy aimed at portraying these municipalities as more than merely depressed areas. Far left/green parties adopt a critical tone (-0.15), though their subjectivity estimates are not significant and the limited number of mentions in this group warrants caution in interpretation.

TABLE 2: Exposure and sentiment for main political parties (2005-2022)

Party ↓ Sentiment →	Polarity	Subjectivity
Five Star Movement	-0.05311	-0.30237**
	(0.04586)	(0.14388)
Democratic party	0.05012	0.11344**
	(0.05795)	(0.04422)
Forza Italia	-0.12633**	-0.03724
	(0.05270)	(0.09607)
League	0.07089	-0.04024
	(0.06739)	(0.06703)
Brothers of Italy	0.12393**	-0.13270
	(0.05702)	(0.10842)
Far Left/Green	0.00469	-0.03229
	(0.05526)	(0.12202)

Notes: This table reports the effect of wind exposure to Potentially Contaminated Sites (PCS) on sentiment scores of Italian Chamber of Deputies speeches (columns) for the main Italian political parties (rows). Each entry shows the effect of wind exposure based on the specification reported in Table 6, which includes controls for PCS number per sqkm, municipality surface, historical weather variables at municipality level (average humidity, maximum temperature, rainfall, wind direction, and wind speed over 2001-2009), as well as province and year fixed effects, socio-demographic controls (population density, share of men, share of higher-educated individuals, employment rate in the health sector, share of daily commuters, share of foreign residents, number of civilians killed by Mafia, historical average taxable income per capita over 2000-2004), geographical characteristics (maximum altitude), and electoral outcomes (electoral districts in year 2001 and invalid ballots in 2001). All regressions are weighted by electorate size at the municipality level in year 2001. Sentiment scores are computed for every complete speech that contains at least one mention of a Campania municipality. Heteroscedasticity and cluster-robust standard errors at the municipality level are in parentheses. Stars indicate significance levels (* $p < 0.1$, ** $p < 0.05$, *** $p < 0.01$).

We also check whether mainstream inertia in parliamentary attention is mirrored by a lack of financial commitment to environmental remediation. To that end, we study per capita EU cohesion funding over the period 2001-2022, restricting our focus to cohesion fund allocations explicitly related to health and environment (e.g. soil protection, waste management, environmental protection, public health). Table 3 reports WLS difference-in-differences estimates of the effect of upwind exposure on cohesion funding transfers after the news shock. Across all specifications, upwind exposed municipalities receive significantly less funding in the post-period.

TABLE 3: Effect of wind exposure on EU cohesion fund (2001-2022)

	Weighted Least Squares (WLS)			
Buffer radius: 3 km	(1) Public funding p.c.	(2) Public funding p.c.	(3) Public funding p.c.	(4) Public funding p.c.
Wind Exposure (dummy) × $Post$	-56.87***	-47.72***	-42.27**	-45.07**
	(20.46)	(16.30)	(18.10)	(18.63)
Municipality FE	✓	✓	✓	✓
Year FE	✓	✓	✓	✓
PCS number per sqkm	✓	✓	✓	✓
Year × Surface	✓	✓	✓	✓
Year × Historical weather variables		✓	✓	✓
Year × Socio-demographic controls			✓	✓
Year × Geographical characteristics				✓
Observations	12144	12144	12144	12144
R-squared	0.110	0.152	0.162	0.172
F-stat	38.02	50.78	172.4	299.0

Notes: This table shows WLS difference-in-differences estimates of the effect of wind exposure to PCS after the news shock on EU cohesion fund from 2001 to 2022. Each column refers to a 3 km buffer radius from the PCS center (see Figure 6). The treatment is instrumented by $WindExposed_m$, defined as a binary indicator equal to 1 if municipality m has a number of upwind exposed PCS greater than zero (extensive margin). The post-treatment period begins in 2005, following the release of the official contamination map. Column (1) presents a baseline model with municipality and year fixed effects to account for time-invariant unobserved heterogeneity at the local level and common time shocks. It also includes the total number of PCS per sqkm and municipality surface (interacted with year dummies). Columns (2)-(4) progressively introduce controls fully interacted with year dummies. Column (2) adds historical weather variables at municipality level (average wind direction, wind speed, humidity, and rainfall over 2001-2009). Column (3) includes socio-demographic controls: share of men, share of higher-educated individuals, employment rate in the health sector, share of foreign residents, share of daily commuters. Column (4) further adds geographical characteristics (maximum altitude and radon levels in year 2007). All regressions are weighted by electorate size at the municipality level in the year 2001. Heteroscedasticity and cluster-robust standard errors at the municipality level are in parentheses. Stars indicate significance levels (* $p < 0.1$, ** $p < 0.05$, *** $p < 0.01$).

Figure 9 plots dynamic difference-in-differences estimates from Table 3. We do not detect any differential trend between treated and control municipalities in the pre-period, as coefficients are small and statistically indistinguishable from zero (95% confidence intervals). After the news shock (dashed vertical line), coefficients remain close to zero and statistically indistinguishable from zero in most years. This indicates that exposed municipalities did not experience a systematic increase in cohesion funding in the post-period.

FIGURE 9: Effect of wind exposure on EU cohesion fund: dynamic specification

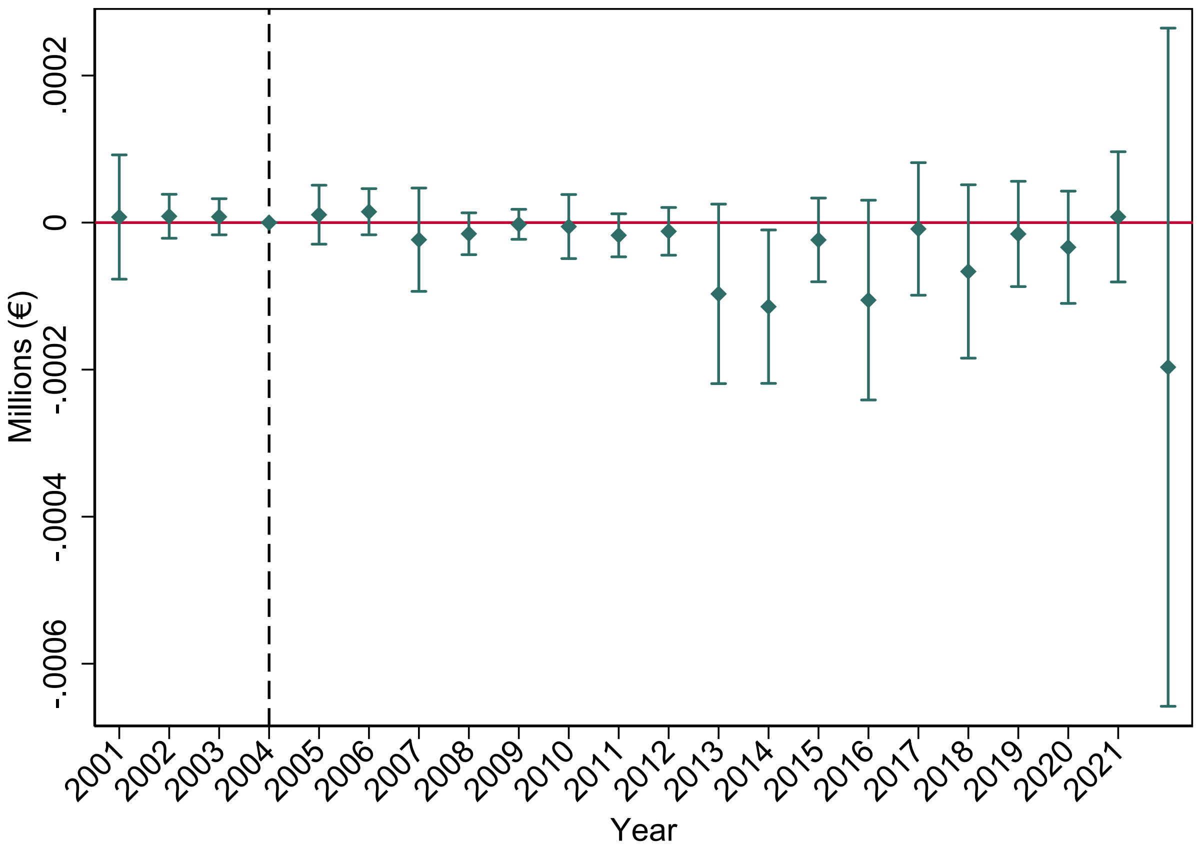

Notes: This figure plots coefficients from a dynamic specification estimating the interaction between the treatment variable $WindExposed_m$ and year indicators, with 2004 omitted as the reference year. Each point shows the estimated effect of wind exposure on EU cohesion funding, relative to 2004. This model controls for the most stringent specification reported in Table 3 and it is weighted by electorate size at the municipality level in year 2001, with 95% confidence intervals. Standard errors are clustered at the municipality level.

6 Main results

6.1 The effect of toxic winds on voter turnout

We study the effect of upwind exposure on voter turnout by estimating Equation 1 using as outcome the ratio of actual voters to registered electors. Difference-in-differences estimates are reported in Table 4, where each column corresponds to a different set of controls, as shown in the notes. After the news shock, municipalities with at least one upwind exposed PCS experience a reduction in turnout of approximately 5.8 percentage points relative to not exposed municipalities, conditional on the full set of control group reported in column 4. The intensive margin coefficient without upwind exposure (total number of PCS per sqkm) is also negative but smaller in magnitude, indicating that the 2005 information shock depresses turnout where PCS are more concentrated, while the upwind measure captures an additional decrease associated with plausibly greater toxic exposure.

TABLE 4: Effect of wind exposure to PCS on turnout (all years)

	Weighted Least Squares (WLS)			
	(1)	(2)	(3)	(4)
Buffer radius: 3 km	Turnout	Turnout	Turnout	Turnout
Wind Exposure (dummy) $\times$ *Post*	-0.0771***	-0.0700***	-0.0658***	-0.0576***
	(0.00803)	(0.00775)	(0.00763)	(0.00739)
Total number of PCS per sqkm $\times$ *Post*	-0.00737***	-0.00472***	-0.00527***	-0.00283**
	(0.00151)	(0.00157)	(0.00148)	(0.00136)
Municipality FE	✓	✓	✓	✓
Year FE	✓	✓	✓	✓
PCS number per sqkm	✓	✓	✓	✓
Year $\times$ Surface	✓	✓	✓	✓
Year $\times$ Historical weather variables		✓	✓	✓
Year $\times$ Socio-demographic controls			✓	✓
Year $\times$ Geographical characteristics				✓
Observations	7692	7692	7692	7692
R-squared	0.900	0.915	0.920	0.924
F-stat	2168.6	1731.6	3036.3	3667.5

Notes: This table shows WLS difference-in-differences estimates of the effect of wind exposure to PCS after the news shock on voter turnout in national elections from 1972 to 2022. Each column refers to a 3 km buffer radius from the PCS center (see Figure 6). The treatment is instrumented by $WindExposed_m$, defined as a binary indicator equal to 1 if municipality m has a number of upwind exposed PCS greater than zero (extensive margin). The post-treatment period is identified by the indicator variable $Post$, which equals 1 for all election years after 2001, and 0 otherwise. Column (1) presents a baseline model with municipality and year fixed effects to account for time-invariant unobserved heterogeneity at the local level and common time shocks. It also includes the total number of PCS per sqkm and municipality surface (interacted with year dummies). Columns (2)-(4) progressively introduce controls fully interacted with year dummies. Column (2) adds historical weather variables at municipality level (average wind direction, wind speed, humidity, and rainfall over 2001-2009). Column (3) includes socio-demographic controls: share of men, share of higher-educated individuals, employment rate in the health sector, share of foreign residents, share of daily commuters. Column (4) further adds geographical characteristics (maximum altitude and radon levels in year 2007). All regressions are weighted by electorate size at the municipality level in the year 2001. Heteroscedasticity and cluster-robust standard errors at the municipality level are in parentheses. Stars indicate significance levels (* $p < 0.1$, ** $p < 0.05$, *** $p < 0.01$).

Figure 10 plots the dynamic specification of Equation 1. First, we notice the absence of pre-trends between treatment and control municipalities before the news shock (95% confidence intervals). Second, after the news shock, estimates turn negative, reaching a persistent magnitude greater than 5 percentage points relative to 2001.

Figure 11 repeats the exercise using as key regressor the PCS density per square kilometer (without wind exposure) interacted with year dummies. The pre-period again shows no systematic differences relative to 2001. After 2005, coefficients become negative and statistically distinguishable from zero but smaller in absolute value than in the upwind specification. Together, these dynamics reinforces the parallel trends assumption and align with difference-in-differences estimates reported in Table 4, showing a bigger and persistent post shock decline in turnout in municipalities affected by toxic winds.

FIGURE 10: Effect of wind exposure to PCS on turnout: dynamic specification

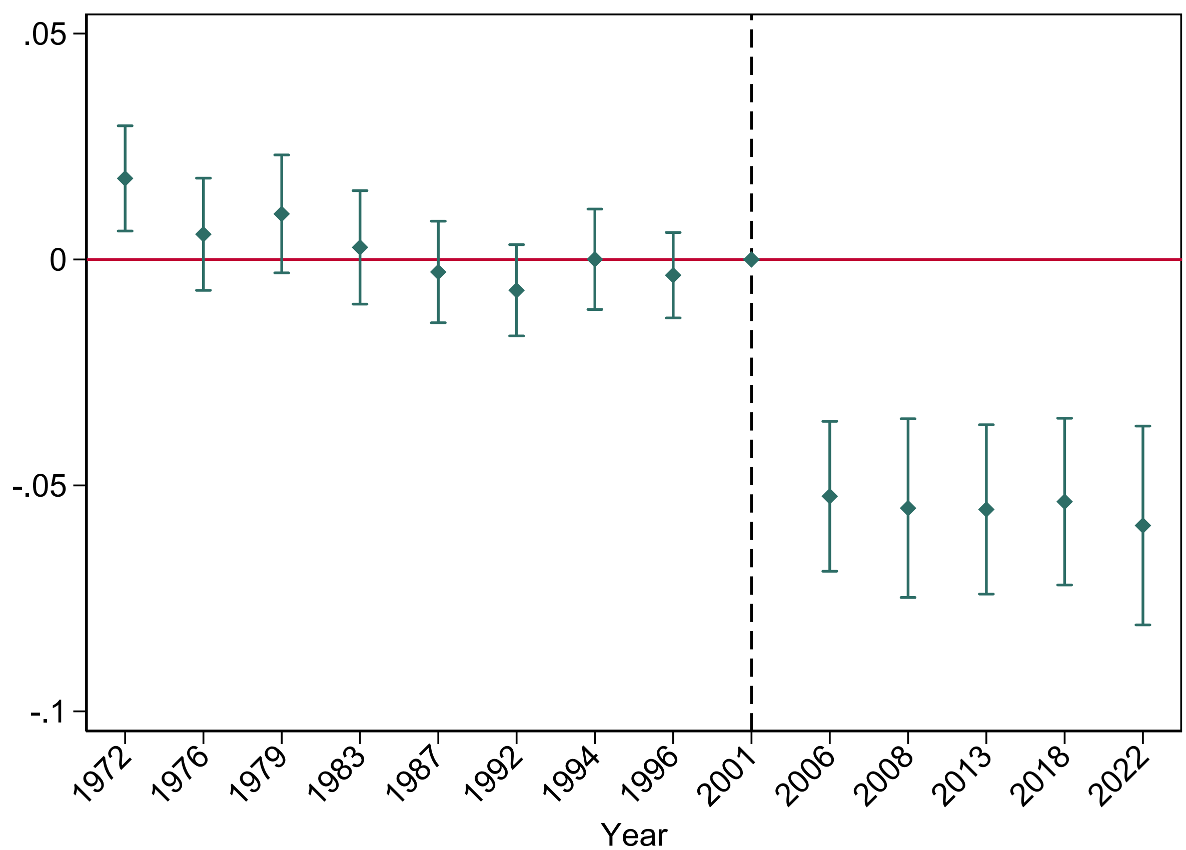

Notes: This figure reports coefficients from a dynamic specification estimating the interaction between the treatment variable $WindExposed_m$ and year indicators, with 2001 omitted as the reference year. Each point represents the estimated effect of wind exposure on turnout in a given year, relative to 2001. Turnout is defined as the ratio of actual voters to registered electors. This model controls for the most stringent specification reported in Table 4 and it is weighted by electorate size at the municipality level in year 2001, with 95% confidence intervals. Standard errors are clustered at the municipality level.

FIGURE 11: Effect of the total number of PCS on turnout: dynamic specification

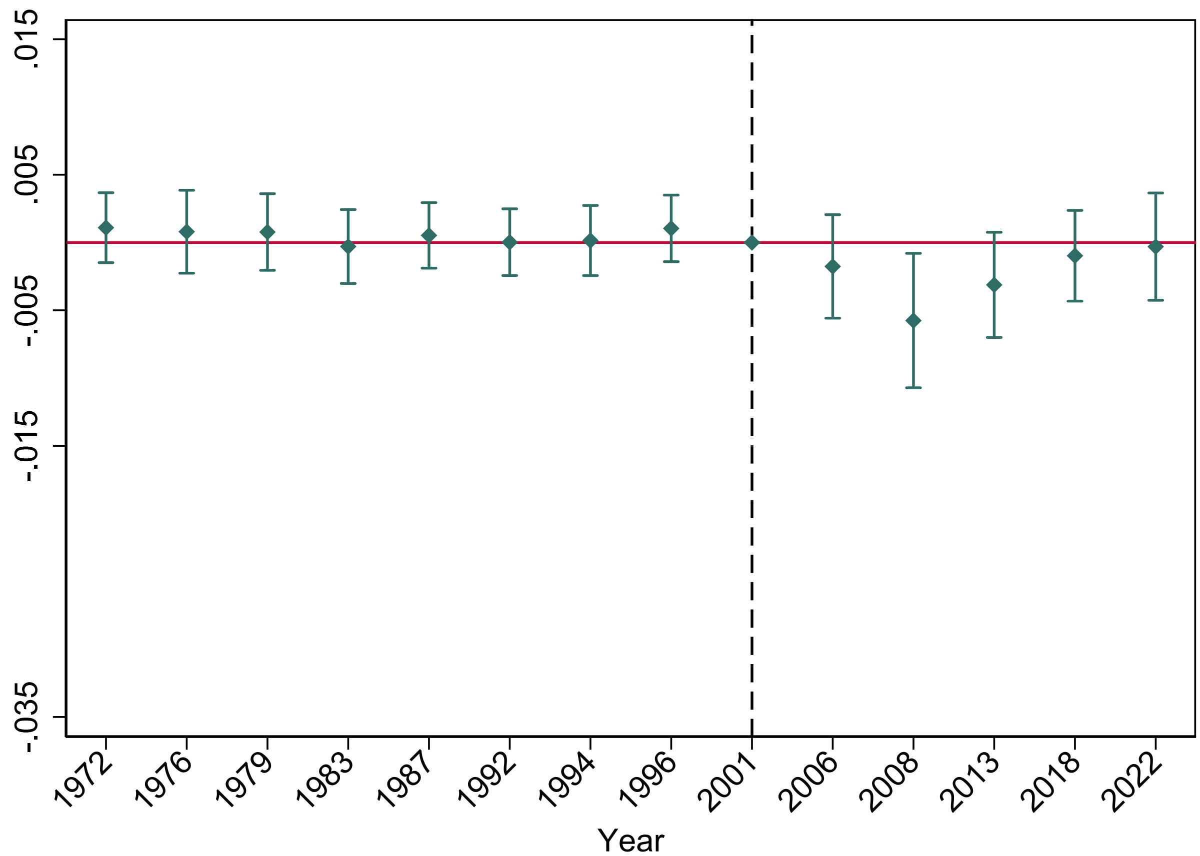

Notes: This figure reports coefficients from a dynamic specification estimating the interaction between the total number of PCS per sqkm and year indicators, with 2001 omitted as the reference year. Each point represents the estimated effect of the news shock related to the presence of potentially contaminated sites on turnout in a given year, relative to 2001. Turnout is defined as the ratio of actual voters to registered electors. This model controls for the most stringent specification reported in Table 4 and it is weighted by electorate size at the municipality level in year 2001, with 95% confidence intervals. Standard errors are clustered at the municipality level.

6.2 POLITICAL DISSATISFACTION

To investigate mechanisms behind effects on turnout, we build two salience indexes using the Italian National Election Study (ITANES) database. It accompanies every general election since 1972, with pre and post-election surveys based on a nationally representative sample of roughly 2,000-3,000 respondents per wave. Since our questions of interest are available from 2001, we focus on the post-treatment period, examining surveys conducted between 2006 and 2022. These surveys record (self-reported) vote choice and rich sociodemographics information, including questions on trust about parties and Parliament. Each wave is a repeated cross-section, built on a new nationally representative sample for each election. To capture municipal-level variation in distrust salience, we compute a normalized index for each municipality m and year t, defined as the vote-share-weighted average of voter preferences for each question on distrust. We use party-level mean preferences on distrust from ITANES computed on the national sample, excluding Campania. We then weight these party-level means by the party's municipal vote share in the corresponding national election, considering only the subset $S_{m,t}$ of parties present in both the electoral dataset and the ITANES dataset for year t. Hence, the Party Distrust Index measures the salience of distrust toward parties in municipality m at year t, combining party-level mean voter distrust ($PartyDistrust_{p,t}$) with their electoral vote share in each municipality.

First we compute the Z-score for each party p:

$$ZPartyDist^w_{p,t} = \frac{(Vote\ Share_{p,t} \times \overline{PreferencesforPartyDistrust_{p,t}}) - \mu^w_t}{\sigma^w_t}$$

where μ^w_t is the mean of $Vote\ Share_{p,t} \times \overline{PreferencesforPartyDistrust_{p,t}}$ and σ^w_t is the standard deviation of $Vote\ Share_{p,t} \times \overline{PreferencesforPartyDistrust_{p,t}}$.

Then, we compute the Party Distrust Index:

$$Party\ Distrust\ Index_{m,t} = \frac{\sum_{p_t \in S_t} Vote\ Share_{p,t} \times ZPartyDist^w_{p,t}}{\sum_{p_t \in S_t} Vote\ Share_{p,t}} \tag{4}$$

Analogously, the Parliament Distrust Index is computed as

$$Parliament\ Distrust\ Index_{m,t} = \frac{\sum_{p_t \in S_t} Vote\ Share_{p,t} \times ZParlDist^w_{p,t}}{\sum_{p_t \in S_t} Vote\ Share_{p,t}} \tag{5}$$

Table 5 shows the effects of upwind exposure on both the party and parliament distrust indexes. The $WindExposed_m$ coefficient is positive and statistically significant for both indexes across all specifications. Taken together, this empirical evidence is consistent with upwind exposure heightening party and parliamentary distrust, providing a plausible mechanism for the turnout declines documented in Table 4 and Figure 10.

TABLE 5: Effect of wind exposure on municipal institutional preferences (2006-2022)

	Weighted Least Squares (WLS)			
Buffer radius: 3 km	(1) Party Distrust Index	(2) Party Distrust Index	(3) Parliament Distrust Index	(4) Parliament Distrust Index
Wind Exposure (dummy)	0.0157** (0.00767)	0.0150** (0.00749)	0.0126* (0.00717)	0.0119* (0.00697)
PCS number per sqkm	✓	✓	✓	✓
Municipality surface	✓	✓	✓	✓
Historical weather variables	✓	✓	✓	✓
Province FE	✓	✓	✓	✓
Year FE	✓	✓	✓	✓
Socio-demographic controls	✓	✓	✓	✓
Geographical characteristics	✓	✓	✓	✓
Electoral outcomes (2001)		✓		✓
Observations	2753	2751	2753	2751
R-squared	0.697	0.698	0.649	0.650
F-stat	335.5	311.6	256.6	237.2

Notes: This table shows WLS estimates of the effect of exposure to PCS on both the Party Distrust Index and the Parliament Distrust Index, considering national elections from 2006 to 2022. Each column refers to a 3 km buffer radius from the PCS center (see Figure 6). All models include PCS number per sqkm, municipality surface, historical weather variables at municipality level (average humidity, maximum temperature, rainfall, wind direction, and wind speed over 2001-2009), province and year fixed effects, socio-demographic controls (population density, share of men, share of higher-educated individuals, employment rate in the health sector, share of daily commuters, share of foreign residents, number of civilians killed by Mafia, and the historical average taxable income per capita at municipality level over 2000-2004), as well as geographical characteristics (maximum altitude). Column (2) and (4) additionally control for electoral outcomes in year 2001 (electoral districts and invalid ballots), respectively. All regressions are weighted by electorate size at the municipality level in year 2001. Heteroscedasticity and cluster-robust standard errors at the municipality level are in parentheses. Stars indicate significance levels (* $p < 0.1$, ** $p < 0.05$, *** $p < 0.01$).

6.3 Environmental challengers in the Land of Fires

6.3.1 Media salience and political context

In summer 2013, the Five Star Movement (M5S) conducted a campaign tour across Campania municipalities using a slogan that revived the expression "Land of Fires" from the final chapter of Gomorrah's book. The expression "In movement through the Land of Fires" also echoed party's name. The campaign aligned with the party's platform: M5S is a widely recognized anti-establishment party that has prioritized environmental issues since its inception. In fact, one of its five stars denotes ecological protection. In winter 2013, the party presented a motion in the national parliament and organized protests, further amplifying visibility of this neglected issue. Figure 12 shows a sharp increase of "Land of Fires" reports on national public broadcasting (RAI) around 2013, coincident with M5S's entry into national politics. Since RAI radio transmits also parliamentary proceedings, radio mentions proxy parliamentary salience.

FIGURE 12: "Land of Fires" media exposure

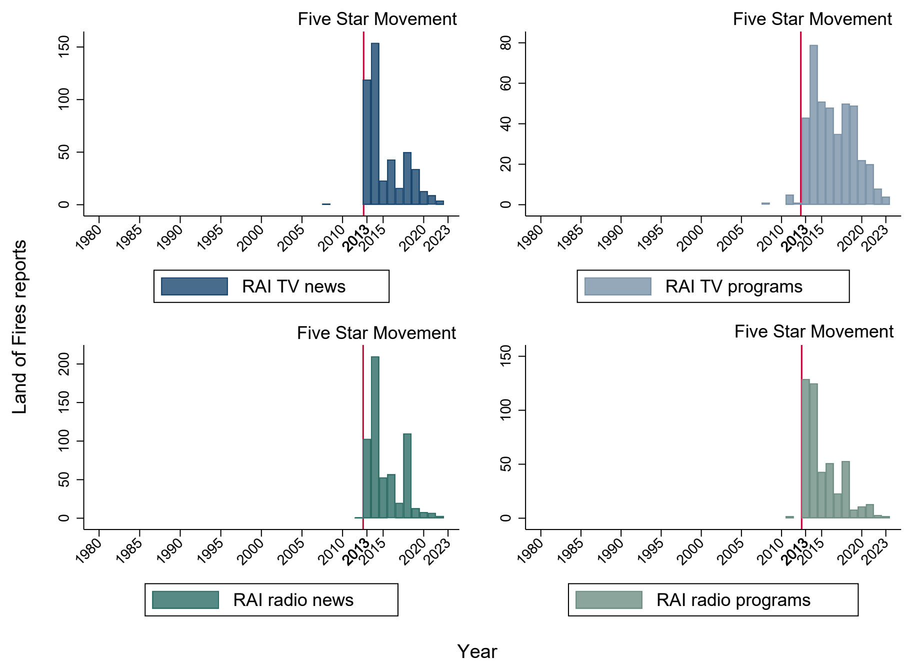

Notes: The panels depict the frequency of reports from 1980 to 2023 featuring the expression "Land of Fires" in national public broadcasting (RAI), across both television and radio, for news and programs. In each case, a sharp increase is observed in 2013, coinciding with the entry of the Five Star Movement into the national political arena. Radio broadcasts are included since RAI transmits parliamentary sessions, making radio data a useful proxy for parliamentary discussions. Data are sourced from RAI teche archives.

Figure 13 compares M5S vote shares in national elections (2013–2018–2022) with the spatial density of PCS over the period 2005–2013. Municipalities with higher PCS density broadly overlap areas of stronger M5S support. These descriptive patterns motivate our empirical analysis of turnout, institutional distrust, mainstream behaviour and environmental challengers.

FIGURE 13: Five Star Movement and pollution exposure

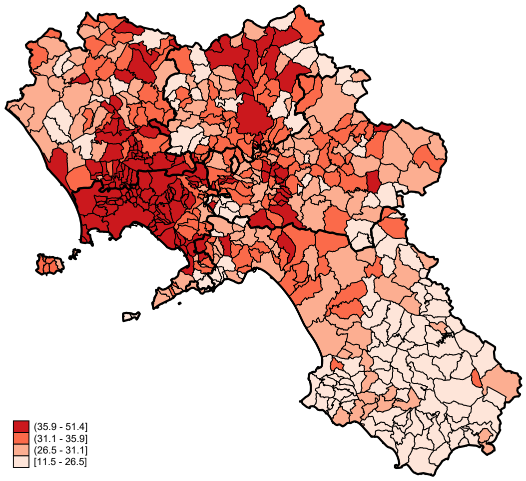

(a) National election Five Star Movement vote share (2013-2018-2022)

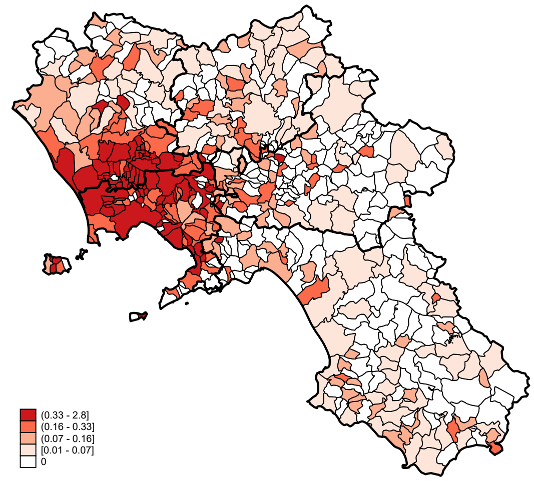

(b) Density of PCS^{LoF} per square kilometer at the municipality level (2005-2013)

6.3.2 CHALLENGER SUCCESS

We examine the effect on parties vote share by estimating Equation 3. WLS estimates are reported in Table 6, where each column corresponds to a different set of controls, as shown in the notes. Estimates show that municipalities with at least one upwind exposed PCS systematically give the M5S a larger vote share. Hence, upwind exposed municipalities deliver about 3.4 percentage points more votes to M5S than control group in the same year, province and electoral district, conditional on municipal-level controls: PCS number per sqkm, surface, historical weather variables, socio-demographic variables, as well as geographical characteristics and electoral outcomes.

Table 6: Effect of wind exposure to PCS on M5S vote share (all years)

	Weighted Least Squares (WLS)			
Buffer radius: 3 km	(1) M5S vote share	(2) M5S vote share	(3) M5S vote share	(4) M5S vote share
Wind Exposure (dummy)	0.0391***	0.0367***	0.0344***	0.0342***
	(0.00751)	(0.00738)	(0.00728)	(0.00713)
PCS number per sqkm	✓	✓	✓	✓
Municipality surface	✓	✓	✓	✓
Historical weather variables	✓	✓	✓	✓
Province FE	✓	✓	✓	✓
Year FE	✓	✓	✓	✓
Socio-demographic controls		✓	✓	✓
Geographical characteristics			✓	✓
Electoral outcomes (2001)				✓
Observations	1651	1651	1651	1651
R-squared	0.802	0.821	0.825	0.828
F-stat	345.2	283.3	267.3	255.6

Notes: This table shows WLS estimates of the effect of wind exposure to PCS on M5S vote share at national elections (all years). Each column refers to a 3 km buffer radius from the PCS center (see Figure 6). All models include PCS number per sqkm, municipality surface, historical weather variables at municipality level (average humidity, maximum temperature, rainfall, wind direction, and wind speed over 2001-2009), province and year fixed effects. Column (2) includes socio-demographic controls: population density, share of men, share of higher-educated individuals, employment rate in the health sector, share of daily commuters, share of foreign residents, number of civilians killed by Mafia, and the historical average taxable income per capita (2000-2004). Column (3) adds geographical characteristics (maximum altitude). Column (4) additionally controls for pre-determined electoral outcomes (electoral districts in year 2001 and invalid ballots in 2001). All regressions are weighted by electorate size at the municipality level in year 2001. Heteroscedasticity and cluster-robust standard errors at the municipality level are in parentheses. Stars indicate significance levels (* $p < 0.1$, ** $p < 0.05$, *** $p < 0.01$).

Table 7 reports election-specific effects of upwind exposure on party vote shares after M5S's entry. As expected, there is no electoral gain for M5S in 2013. The estimate is negative because its "Land of Fires" campaign began in summer 2013, whereas the election was held in February. By contrast, having at least one upwind-exposed PCS is associated with a higher M5S vote share of about 4.4 percentage points in 2018 and about 8.7 percentage points in 2022. For mainstream parties, effects are generally negative and statistically significant. The Democratic Party shows a small negative coefficient in 2013 that becomes statistically significant and greater in magnitude thereafter, indicating no systematic gains in exposed areas. On the right-wing side, Forza Italia and the League lose vote share in both 2018 and 2022. Brothers of Italy's small positive coefficients in 2013–2018 reverse to a sizable negative in 2022. Far-left/green lists do not display statistically significant effects. Finally, turnout is lower in exposed municipalities in every election, consistent with the difference-in-differences results reported earlier.

TABLE 7: Exposure and voting for main political parties (2013-2022)

Party ↓ Election →	2013	2018	2022
Five Star Movement	-0.02771***	0.04389***	0.08651***
	(0.00871)	(0.00970)	(0.01061)
Democratic party	-0.00897	-0.02875***	-0.03441***
	(0.00627)	(0.00764)	(0.00803)
Forza Italia	0.01628**	-0.02553***	-0.01814***
	(0.00771)	(0.00629)	(0.00684)
League	0.00744***	-0.02404***	-0.01943***
	(0.00169)	(0.00248)	(0.00482)
Brothers of Italy	0.00957*	0.01673***	-0.04674***
	(0.00514)	(0.00473)	(0.00721)
Far Left/Green	-0.00111	-0.00309	0.00097
	(0.00221)	(0.00323)	(0.00143)
Other parties	-0.01513**	0.00118	0.01166**
	(0.00676)	(0.00347)	(0.00513)
Invalid ballots	0.00457	-0.02442***	–0.03745***
	(0.00436)	(0.00605)	(0.01227)
Turnout	-0.04869***	-0.04279***	-0.03943***
	(0.00814)	(0.00794)	(0.00717)

Notes: This table reports the effect of wind exposure to Potentially Contaminated Sites (PCS) on the vote share of the main Italian political parties (rows) across the three national elections held between 2013 and 2022 (columns). Each entry shows the estimated average marginal effect of wind exposure to PCS, based on the most stringent specification reported in Table 6. All regressions are weighted by electorate size at the municipality level in year 2001. Standard errors, obtained via the delta method and clustered at the municipality level, are reported in parentheses. Stars indicate significance levels (* $p < 0.1$, ** $p < 0.05$, *** $p < 0.01$).

7 MECHANISMS

7.1 THE HEALTH AND ECONOMIC CONSEQUENCES OF TOXIC WINDS

In this section, we investigate potential mechanisms underlying our main findings. Anecdotal evidence suggests a negative impact of the Land of Fires crisis on health and economic outcomes. Table 8 estimates the effect of upwind exposure on the raw relative risk (RR) of death from malignant tumors (2006–2014). The coefficient on $WindExposed_m$ is positive and statistically significant in all specifications, ranging from 0.0751 (column 1) to 0.0618 (column 4). These results are consistent with the spatial patterns descriptively shown in **??**. To our knowledge, no previous work shows evidence of the role of winds on the risk of deaths for malignant cancers in the Land of Fires.

TABLE 8: Effect of wind exposure to PCS on the RR of death for malignant tumors

	Ordinary Least Squares (OLS)			
Buffer radius: 3 km	(1) RR death malignant tumors	(2) RR death malignant tumors	(3) RR death malignant tumors	(4) RR death malignant tumors
Wind Exposure (dummy)	0.0751^{***} (0.00869)	0.0663^{***} (0.00838)	0.0629^{***} (0.00811)	0.0618^{***} (0.00806)
PCS number per sqkm	✓	✓	✓	✓
Municipality surface	✓	✓	✓	✓
Historical weather variables	✓	✓	✓	✓
Province FE	✓	✓	✓	✓
Socio-demographic controls		✓	✓	✓
Geographical characteristics			✓	✓
Electoral outcomes (2001)				✓
Observations	552	552	552	551
R-squared	0.794	0.836	0.844	0.855
F-stat	215.4	204.8	199.0	193.0

Notes: This table shows OLS estimates of the effect of wind exposure to PCS on the raw relative risk of death for all malignant tumors over the period 2006-2014. Each column refers to a 3 km buffer radius from the PCS center (see Figure 6). All models include PCS number per sqkm, municipality surface, historical weather variables at municipality level (average humidity, maximum temperature, rainfall, wind direction, and wind speed over 2001-2009), and province fixed effects. Column (2) includes socio-demographic controls: population density, share of men, share of higher-educated individuals, employment rate in the health sector, share of daily commuters, share of foreign residents, number of civilians killed by Mafia, and the historical average taxable income per capita (2000-2004). Column (3) adds geographical characteristics (maximum altitude). Column (4) additionally controls for pre-determined electoral outcomes (electoral districts in year 2001 and invalid ballots in 2001). Heteroscedasticity and cluster-robust standard errors at the municipality level are in parentheses. Stars indicate significance levels (* $p < 0.1$, ** $p < 0.05$, *** $p < 0.01$). Data on the raw relative risk of death are sourced from the *"Mortality atlas of the Campania region (all-cause and cause-specific mortality at municipal level, 2006-2014)"*.

Last, we explore the impact of upwind exposure on local tourism using ISTAT municipal data for 2014-2023. Since no pre-2005 data are available, we estimate the post-period (2014-2023) using the main WLS specification reported in Equation 3, including the full set of controls shown in Table 6. Hence, Table 9 shows the effects of upwind exposure on the number of hotel arrivals. The coefficient on $WindExposed_m$ is negative and becomes larger (in absolute value) as controls are added. Thus, municipalities with at least one upwind-exposed PCS receive approximately 79 fewer hotel arrivals per year compared to similar non-exposed municipalities. The magnitude is not negligible when compared to the average number of tourist arrivals (see Table A1). These estimates highlight a tourism penalty associated with toxic winds exposure, consistent with anecdotal evidence on a reputational or risk-perception channel.

TABLE 9: Effect of wind exposure to PCS on tourism (2014-2023)

	Weighted Least Squares (WLS)			
Buffer radius: 3 km	(1) Hotel arrivals	(2) Hotel arrivals	(3) Hotel arrivals	(4) Hotel arrivals
Wind Exposure (dummy)	7.852 (64.35)	-67.80** (32.24)	-71.55** (32.17)	-79.31** (32.32)
PCS number per sqkm	✓	✓	✓	✓
Municipality surface	✓	✓	✓	✓
Historical weather variables	✓	✓	✓	✓
Province FE	✓	✓	✓	✓
Year FE	✓	✓	✓	✓
Socio-demographic controls		✓	✓	✓
Geographical characteristics			✓	✓
Electoral outcomes (2001)				✓
Observations	704	704	704	704
R-squared	0.712	0.826	0.828	0.830
F-stat	122.5	1998.4	1775.8	2096.5

Notes: This table shows WLS estimates of the effect of wind exposure to PCS on tourism (hotel arrivals) over the period 2014-2023. Each column refers to a 3 km buffer radius from the PCS center (see Figure 6). All models include PCS number per sqkm, municipality surface, historical weather variables at municipality level (average humidity, maximum temperature, rainfall, wind direction, and wind speed over 2001-2009), province and year fixed effects. Column (2) includes socio-demographic controls: population density, share of men, share of higher-educated individuals, employment rate in the health sector, share of daily commuters, share of foreign residents, number of civilians killed by Mafia, and the historical average taxable income per capita (2000-2004). Column (3) adds geographical characteristics (maximum altitude). Column (4) additionally controls for pre-determined electoral outcomes (electoral districts in year 2001 and invalid ballots in 2001). All regressions are weighted by electorate size at the municipality level in year 2001. Heteroscedasticity and cluster-robust standard errors at the municipality level are in parentheses. Stars indicate significance levels (* $p < 0.1$, ** $p < 0.05$, *** $p < 0.01$).

7.2 CHANNELS OF ENVIRONMENTAL CHALLENGERS SUCCESS

In this section, we investigate channels behind M5S's electoral success in the Land of Fires. First, we start showing the positive residualized relationship between M5S vote share and wind exposure to PCS (Figure 14). We then estimate year-specific effects using a fully interacted model and report the average marginal effects (AME). The coefficient is negative in 2013, when M5S's "Land of Fires" campaign post-dated the February election, but turns positive thereafter (statistically significant in 2018 and largest in 2022), consistent with the party converting this neglected issue by mainstream parties into electoral support (see also Table 7).

FIGURE 14: Wind exposure and M5S vote share: residualized correlation

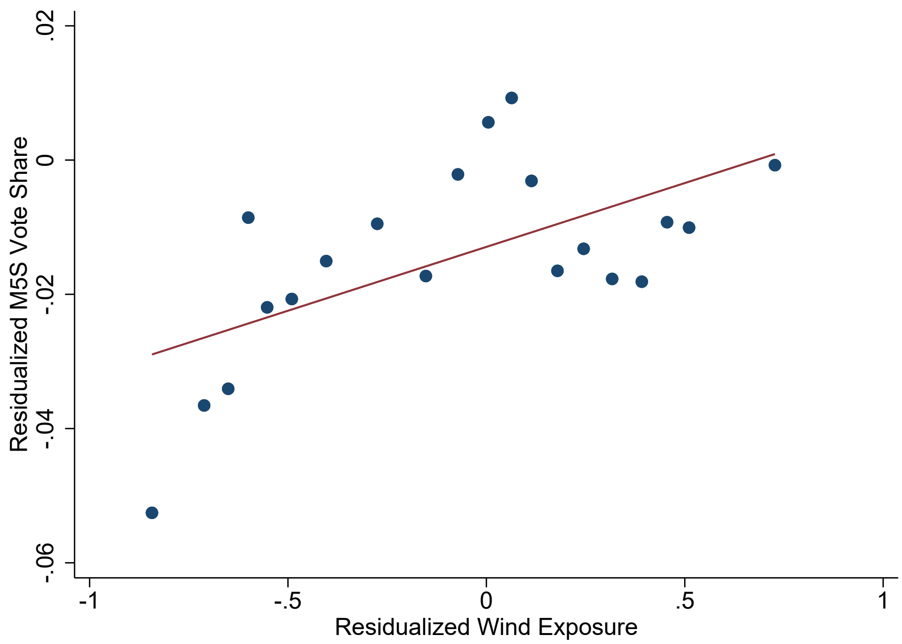

Notes: This figure displays the residualized relationship between M5S vote share and wind exposure to Potentially Contaminated Sites (PCS). Both variables are residualized from the full set of controls used in the main specification (column (4) of Table 6), including PCS number per sqkm, municipality surface, historical weather variables, province and year fixed effects, socio-demographic controls, geographical characteristics, and pre-determined electoral outcomes. The residuals are computed using Weighted Least Squares (WLS), with weights equal to municipality electorate size in year 2001. The line represents the best linear fit across the 20 quantile bins. The upward slope indicates a positive partial correlation between wind exposure and M5S support, net of covariates.

FIGURE 15: Average marginal effect (AME) of wind exposure on M5S support by year

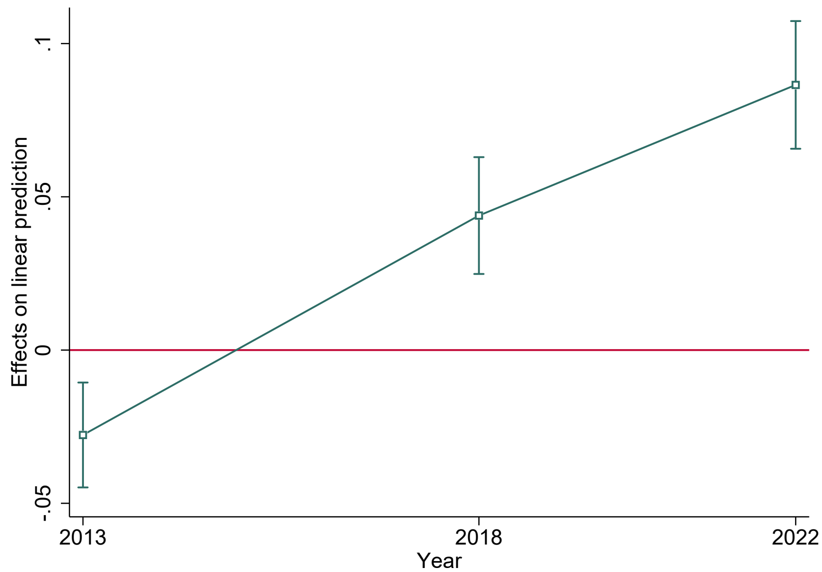

Notes: This figure displays the average marginal effect of wind exposure to PCS on M5S vote share in national elections, separately by year. Estimates are derived from a fully interacted model with year-by-treatment interactions, using the most stringent specification detailed in column (4) of Table 6. Estimates are weighted by municipality electorate size in year 2001 and standard errors are clustered at the municipality level (95% confidence intervals).

To reinforce this interpretation, we present descriptive evidence on coverage of this issue by Italy's public broadcaster (RAI), both television and radio. Figure 16 zooms in on 2013 and plots monthly mentions of "Land of Fires" on the national public broadcaster (RAI), separately for TV news, TV programs, radio news, and radio programs. Coverage is negligible through the first half of the year and around the February election (vertical line). Mentions begin to rise in July and then surge in the last quarter (October–December) across all four series. The timing aligns with M5S's adoption of the "Land of Fires" frame in July and its subsequent parliamentary motion and street mobilizations in winter. Because RAI radio also carries parliamentary proceedings, the parallel increase in radio counts is consistent with heightened legislative salience. While descriptive, this pattern is consistent with our interpretation of M5S's electoral dynamics (negative in 2013 and positive by 2018).

FIGURE 16: National election (2013) and "Land of Fires" media exposure

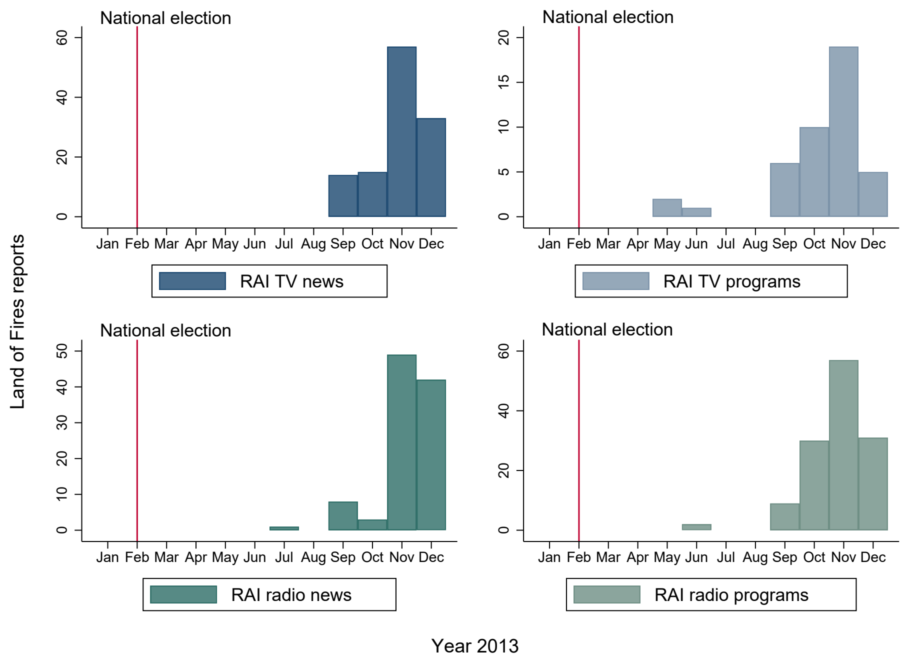

Notes: This figure provides a zoomed-in version of Figure 12, displaying the monthly frequency of media reports referencing the expression "Land of Fires" on national public broadcasting (RAI) during 2013, across both television and radio, including news and programs. The sharp increase observed in Figure 12 for the year 2013 actually follows the entry of the Five Star Movement (M5S) into the national political scene in February 2013. In July 2013, M5S recovered the expression "Land of Fires" from the final chapter of the book "Gomorrah" ("*In Movement through the Land of Fires*") for their campaign, where the word "movement" also recalled party's name. That winter, they presented a motion in the national parliament and organized public demonstrations. This political mobilization coincides with the surge in "Land of Fires" media coverage recorded in the last quarter of 2013. Data are sourced from *RAI teche* archives.

Since M5S was born as an internet-driven movement, we complement the broadcast descriptive evidence with Google search data. Figure 17 plots Google Trends for the query "Land of Fires". Panel (a) shows that search intensity is modest until 2012 and then rises sharply in 2013. Panel (b) focuses on 2013 and reveals virtually no interest around the February election, followed by a steep acceleration from October through December. The fourth-quarter spike coincides with M5S's mid-year adoption of the "Land of Fires" frame and its subsequent mobilization, and mirrors the surge in RAI coverage in Figure 16. While descriptive, these patterns indicate a broad salience shock that materialized only after the 2013 election, consistent with M5S's later electoral success.

FIGURE 17: Online salience of "Land of Fires" in Google searches

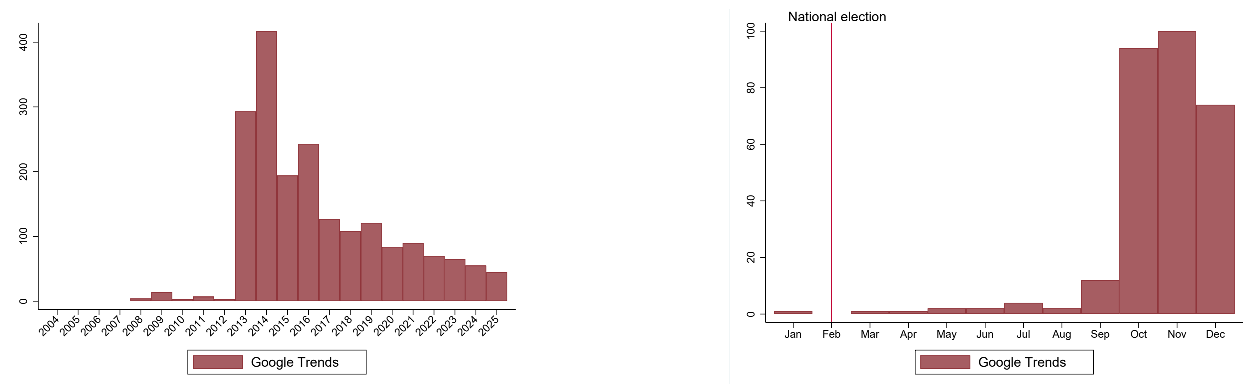

(a) Google Trends aggregated by year

(b) Google Trends (2013)

Notes: This figure presents Google Trends data on the search term "Land of Fires" in Italy. Panel (a) reports yearly aggregates for the period 2004–2025, where monthly search intensity values (ranging from 1 to 100) are summed within each year. Panel (b) focuses on the year 2013 and displays the monthly distribution of search interest, revealing a sharp increase in the final quarter. This pattern aligns with the surge in media attention documented in Figure 16. Since M5S emerged as an internet-driven political movement, Google search data serve as a proxy for shifts in public attention.

A plausible channel behind M5S's national success is their radicalized presence in local elections. We test this directly using an outcome that equals one when M5S lists a candidate in municipal elections (2010-2022). Table 10 shows the effect on upwind exposure on M5S running at municipal elections. $WindExposed_m$ is positive and statistically significant in each specification. This result supports a "local presence" channel: M5S was more likely to run locally where the Land of Fires issue was salient, building the groundwork for their success in national elections.

TABLE 10: Effect of wind exposure to PCS on M5S running (municipal elections)

	Weighted Least Squares (WLS)			
Buffer radius: 3 km	(1) M5S running	(2) M5S running	(3) M5S running	(4) M5S running
Wind Exposure (dummy)	0.316***	0.223***	0.209***	0.206***
	(0.0576)	(0.0375)	(0.0351)	(0.0340)
PCS number per sqkm	✓	✓	✓	✓
Municipality surface	✓	✓	✓	✓
Historical weather variables	✓	✓	✓	✓
Province FE	✓	✓	✓	✓
Year FE	✓	✓	✓	✓
Socio-demographic controls		✓	✓	✓
Geographical characteristics			✓	✓
Electoral outcomes (2001)				✓
Observations	1734	1734	1734	1734
R-squared	0.390	0.489	0.499	0.515
F-stat	67.93	144.3	163.1	176.0

Notes: This table shows WLS estimates of the effect of wind exposure to PCS on M5S running at municipal elections (2010-2022). Each column refers to a 3 km buffer radius from the PCS center (see Figure 6). All models include PCS number per sqkm, municipality surface, historical weather variables at municipality level (average humidity, maximum temperature, rainfall, wind direction, and wind speed over 2001-2009), province and year fixed effects. Column (2) includes socio-demographic controls: population density, share of men, share of higher-educated individuals, employment rate in the health sector, share of daily commuters, share of foreign residents, number of civilians killed by Mafia, and the historical average taxable income per capita (2000-2004). Column (3) adds geographical characteristics (maximum altitude). Column (4) additionally controls for pre-determined electoral outcomes (electoral districts in year 2001 and invalid ballots in 2001). All regressions are weighted by electorate size (municipal elections) at the municipality level. Heteroscedasticity and cluster-robust standard errors at the municipality level are in parentheses. Stars indicate significance levels (* $p < 0.1$, ** $p < 0.05$, *** $p < 0.01$).

Table 11 examines whether the association between upwind exposure and M5S support is amplified when the party's candidate is born in the municipality where they are running (national elections). The interaction term $WindExposed_m \times OriginsM5S$ is negative and statistically significant, meaning that the positive effect of upwind exposure on M5S support disappears when the candidate is local. This suggests that M5S's electoral advantage in polluted areas is not driven by local candidates in national elections.

TABLE 11: Heterogeneous effect on M5S vote share by candidate origin (2018-2022)

	Weighted Least Squares (WLS)			
Buffer radius: 3 km	(1) M5S vote share	(2) M5S vote share	(3) M5S vote share	(4) M5S vote share
Wind Exposure (dummy) $\times$ $OriginsM5S$	-0.120***	-0.115***	-0.0906***	-0.0767***
	(0.0189)	(0.0268)	(0.0278)	(0.0283)
Wind Exposure (dummy)	0.0550***	0.0534***	0.0498***	0.0487***
	(0.00939)	(0.00803)	(0.00815)	(0.00822)
PCS number per sqkm	✓	✓	✓	✓
Municipality surface	✓	✓	✓	✓
Historical weather variables	✓	✓	✓	✓
Province FE	✓	✓	✓	✓
Year FE	✓	✓	✓	✓
Socio-demographic controls		✓	✓	✓
Geographical characteristics			✓	✓
Electoral outcomes (2001)				✓
Observations	1100	1100	1100	1100
R-squared	0.746	0.788	0.793	0.800
F-stat	.	.	.	.

Notes: This table reports WLS estimates assessing how the impact of wind exposure on M5S vote share varies if prior to 2013 the municipality was dissolved due to mafia infiltration, capturing possible mechanism of M5S success. Each column refers to a 3 km buffer radius from the PCS center (see Figure 6). All models include PCS number per sqkm, municipality surface, historical weather variables at municipality level (average humidity, maximum temperature, rainfall, wind direction, and wind speed over 2001-2009), province and year fixed effects. Column (2) includes socio-demographic controls: population density, share of men, share of higher-educated individuals, employment rate in the health sector, share of daily commuters, share of foreign residents, number of civilians killed by Mafia, and the historical average taxable income per capita (2000-2004). Column (3) adds geographical characteristics (maximum altitude). Column (4) additionally controls for pre-determined electoral outcomes (electoral districts in year 2001 and invalid ballots in 2001). All regressions are weighted by electorate size at the municipality level in year 2001. Heteroscedasticity and cluster-robust standard errors at the municipality level are in parentheses. Stars indicate significance levels (* $p < 0.1$, ** $p < 0.05$, *** $p < 0.01$).

Table 12 tests whether the relationship between upwind exposure and M5S vote share is stronger in municipalities that were dissolved for mafia infiltration before 2013. Overall, M5S support is particularly strong where environmental exposure coincides with a recent history of institutional breakdown, consistent with a channel of protest against corruption.

TABLE 12: Heterogeneous effect of wind exposure on M5S vote share

	Weighted Least Squares (WLS)			
Buffer radius: 3 km	(1) M5S vote share	(2) M5S vote share	(3) M5S vote share	(4) M5S vote share
Wind Exposure (dummy) × Dissolved	0.0687***	0.0782***	0.0709***	0.0803***
	(0.0145)	(0.0135)	(0.0135)	(0.0141)
Wind Exposure (dummy)	0.0389***	0.0363***	0.0345***	0.0342***
	(0.00763)	(0.00755)	(0.00746)	(0.00736)
PCS number per sqkm	✓	✓	✓	✓
Municipality surface	✓	✓	✓	✓
Historical weather variables	✓	✓	✓	✓
Province FE	✓	✓	✓	✓
Year FE	✓	✓	✓	✓
Socio-demographic controls		✓	✓	✓
Geographical characteristics			✓	✓
Electoral outcomes (2001)				✓
Observations	1651	1651	1651	1651
R-squared	0.803	0.822	0.825	0.829
F-stat	.	.	.	.

Notes: This table reports WLS estimates assessing how the impact of wind exposure on M5S vote share varies if prior to 2013 the municipality was dissolved due to mafia infiltration, capturing possible mechanism of M5S success. Each column refers to a 3 km buffer radius from the PCS center (see Figure 6). All models include PCS number per sqkm, municipality surface, historical weather variables at municipality level (average humidity, maximum temperature, rainfall, wind direction, and wind speed over 2001-2009), province and year fixed effects. Column (2) includes socio-demographic controls: population density, share of men, share of higher-educated individuals, employment rate in the health sector, share of daily commuters, share of foreign residents, number of civilians killed by Mafia, and the historical average taxable income per capita (2000-2004). Column (3) adds geographical characteristics (maximum altitude). Column (4) additionally controls for pre-determined electoral outcomes (electoral districts in year 2001 and invalid ballots in 2001). All regressions are weighted by electorate size at the municipality level in year 2001. Heteroscedasticity and cluster-robust standard errors at the municipality level are in parentheses. Stars indicate significance levels (* $p < 0.1$, ** $p < 0.05$, *** $p < 0.01$).

8 ROBUSTNESS CHECKS

In this section, we present different sets of results to corroborate the robustness of our empirical findings. Appendix Table C1 shows significant results when varying the treatment as a binary indicator equal to 1 if the number of upwind exposed PCS exceeds the median value, as a quartile distribution, as a binary indicator equal to 1 if the number of upwind exposed PCS exceeds the average value, or as the logarithm transformation of upwind exposed PCS (number). Appendix Figure C5 reports the corresponding event study coefficients (2001 omitted), which show no pre-trends and a persistent post-period decline. Appendix Table C2 varies the buffer radius around each PCS (5, 10, and 20 km).

Appendix Figure C6 plots the dynamic specification for each different buffer radius. We find a robust and negative effect up to 10 km with no evidence of pre-trends. At 20 km, pre-trends emerge and the coefficient is not informative. Appendix Table C3 varies both the computation of historical average wind direction at each PCS and the definition of the key regressor $WindExposed_m$. In particular, $WI_{i,j}$ equals 1 as the angle (θ) between the connection vector (line from the actual station j to the synthetic station i) and the wind direction vector falls within $[0, 45°]$. Appendix Figure C7 plots the dynamic specification for turnout when $\theta = 45°$. Appendix Table C4 varies electorate weight size at the municipality level from election year 2001 to 1996 and Figure C8 exhibits the dynamic specification. Appendix Figure C9 tests for spatial correlation in standard errors. Appendix Table C5 restricts the sample to municipalities that existed in 1972 and are observed in every election year, excluding the seven municipalities created later and the merged municipality of Montoro, as well as Montoro Inferiore and Montoro Superiore. Figure C10 plots the dynamic specification. Appendix Table C6 tests alternative definitions for Five Star Movement vote share. Appendix Table C7 varies the buffer radius around each PCS and Figure C11 reports year-specific estimated average marginal effects when varying the buffer radius. The positive association between upwind exposure and M5S support is detectable up to a 20 km radius, reinforcing the main results. Appendix Table C8 varies both the computation of $\overline{WINDDIR}_{PCS}$ and θ as in Table C3. Last, Appendix Table C9 varies electorate weight size from election year 2001 to 1996.

9 Conclusions

This paper examines the impact of an environmental information shock on turnout and challenger parties. Our findings show that challengers can act as political entrepreneurs, placing ignored issues back on the political agenda. Using a novel municipality-level dataset on PCS, we construct a measure of toxic winds exposure at municipality level by combining wind direction with 3 km buffers centered on each PCS. Leveraging plausibly exogenous variation in wind direction, we identify upwind PCS relative to municipal centroids. First, we study mainstream inertia. Parliamentary speeches show that, after the 2005 news shock, dominant parties devote little attention to this issue. Party level sentiment evidence provides a plausible mechanism for mainstream inertia: M5S combines a more critical tone with the largest movement toward objective language, whereas mainstream parties either soften polarity or exhibit modest changes in subjectivity. We also find that mainstream parties do not allocate public funding to exposed areas. Then, we show that upwind exposure significantly and persistently reduces voter turnout by about 5.8 percentage points relative to non-exposed municipalities. Increases in distrust toward parties and Parliament, together with adverse local conditions (higher risk of death by malignant cancers and weaker tourism), provide plausible explanations for this decline. We also examine the electoral consequences. Upwind exposure is associated with a 3.4 percentage point increase in M5S vote share in national elections. Local participation can represent a channel for Five Star Movement electoral success at national level, since M5S is more likely to run in municipal elections in exposed municipalities.

Taken together, our findings are consistent with political entrepreneurship theories (**?**): challenger parties gain votes from both left and right mainstream coalitions, acting as disruptive political entrepreneurs who elevate new or previously ignored policy issues and attack old parties by employing anti-establishment rhetoric.

References

Acconcia, Antonio, Giancarlo Corsetti, and Saverio Simonelli, "Mafia and Public Spending: Evidence on the Fiscal Multiplier from a Quasi-experiment," *American Economic Review*, 2014, *104* (7), 2185–2209.

Algan, Yann, Sergei Guriev, Elias Papaiannou, and Evgenia Passari, "The European Trust Crisis and the Rise of Populism," *Brookings Papers on Economic Activity*, 2017, *47* (2), 309—-382.

Barro, Robert, "The Control of Politicians: An Economic Model," *Public Choice*, 1973, *14* (1), 19–42.

Bellodi, Luca, Massimo Morelli, and Matia Vannoni, "A Costly Commitment: Populism, Economic Performance, and the Quality of Bureaucracy," *American Journal of Political Science*, 2024, *68* (1), 193–209.

Besley, Timothy, "Principled Agents?: The Political Economy of Good Government," *Oxford University Press*, 2006.

Bordignon, Massimo and Tommaso Colussi, "Dancing with the Populist. New Parties, Electoral Rules and Italian Municipal Elections," *IZA Discussion Papers*, 2020, (13775).

_ , Federico Franzoni, and Matteo Gamalerio, "Is Populism Reversible? Evidence from Italian Local Elections during the Pandemic," *European Journal of Political Economy*, 2024, *81*, 102480.

Borgschulte, Mark, David Molitor, and Eric Yongchen Zou, "Air Pollution and Labour Market: Evidence from Wildfire Smoke," *The Review of Economics and Statistics*, 2024, *106* (6), 1558–1575.

Buonanno, Paolo, Irene Ferrari, and Alessandro Saia, "All is Not Lost: Organized Crime and Social Capital Formation," *Journal of Public Economics*, 2024, *240*, 105257.

Cantoni, Enrico, Vincent Pons, and Jerome Schafer, "Voting Rules, Turnout, and Economic Policies," *Annual Review of Economics*, 2025, *17*, 217–239.

Cavalcanti, Francisco, Gianmarco Daniele, and Sergio Galletta, "Popularity Shocks and Political Selection," *Journal of Public Economics*, 2018, *165*, 201–216.

Cipullo, Davide and Barton E. Lee, "Legislative Effectiveness, Trade Shocks, and Electoral Accountability," *Working Paper*, 2025.

_ , Massimiliano G. Onorato, and Gianmario Pelleschi, "Organized Crime, Hidden Pollution, and Long-Run Health Costs," *Working Paper*, 2026.

Colantone, Italo and Piero Stanig, "The Trade Origins of Economic Nationalism: Import Competition and Voting Behavior in Western Europe," *American Journal of Political Science*, 2018, *62* (4), 936–953.

_ , Livio Di Lonardo, Yotam Margalit, and Marco Percoco, "The Political Consequences of Green Policies: Evidence from Italy," *American Political Science Review*, 2023, *118* (1), 108–126.

Cova, Joshua, "A New Database for Italian Parliamentary Speeches: Introducing the ItaParlCorpus Dataset.," *Italian Political Science Review*, 2025, *55* (1), 77—-86.

Cremaschi, Simone, Nicola Bariletto, and Catherine E. De Vries, "Without Roots: The Political Consequences of Collective Economic Shocks," *American Political Science Review*, 2025, *119* (4), 1963–1982.

Dal Bò, Ernesto, Frederico Finan, Olle Folke, Torsten Persson, and Johanna Rickne, "Economic and Social Outsiders but Political Insiders: Sweden's Populist Radical Right," *Review of Economic Studies*, 2023, *90* (2), 675—-706.

D'Alisa, Giacomo, Pasquale Marcello Falcone, Anna Rita Germani, Cesare Imbriani, Piergiuseppe Morone, and Filippo Reganati, "Victims in the "Land of Fires": A Case Study on the Consequences of Buried and Burnt Waste in Campania, Italy," *EFFACE project, University of Rome La Sapienza*, 2015.

Daniele, Gianmarco and Benny Geys, "Organised Crime, Institutions and Political Quality: Empirical Evidence from Italian Municipalities," *The Economic Journal*, 2015, *125* (586), F233–F55.

De Vries, Catherine E. and Sara B. Hobolt, "Political Entrepreneurs: The Rise of Challenger Parties in Europe," *Princeton University Press*, 2020.

Deryugina, Tatyana, Garth Heutel, Nolan H. Miller, David Molitor, and Julian Reif, "The Mortality and Medical Costs of Air Pollution: Evidence from Changes in Wind Direction," *American Economic Review*, 2019, *109* (12), 4178–4219.

Di Cataldo, Marco and Nicola Mastrorocco, "Organized Crime, Captured Politicians, and the Allocation of Public Resources," *The Journal of Law, Economics, and Organization*, 2022, *38* (3), 774–839.

Fearon, James D., "Electoral Accountability and the Control of Politicians: Selecting Good Types Versus Sanctioning Poor Performance," in Adam Przeworski, Susan C. Stokes, and Bernard Manin, eds., *Democracy, Accountability, and Representation*, Cambridge University Press, 1999, pp. 55–97.

Fenizia, Alessandra and Raffaele Saggio, "Organized Crime and Economic Growth: Evidence from Municipalities Infiltrated by the Mafia," *American Economic Review*, 2024, *114* (7), 2171–2200.

Ferraz, Claudio and Frederico Finan, "Exposing Corrupt Politicians: the Effects of Brazil's Publicly Released Audits on Electoral Outcomes," *The Quarterly Journal of Economics*, 2008, *123*, 703–745.

Fetzer, Thiemo, "Did Austerity Cause Brexit?," *American Economic Review*, 2019, *109* (11), 3489–3886.

Funke, Manuel, Moritz Schularick, and Christoph Trebesch, "Going to Extremes: Politics after Financial Crises, 1870-2014," *European Economic Review*, 2016, *88*, 227–260.

_ , _ , and _ , "Populist Leaders and the Economy," *American Economic Review*, 2023, *113* (12), 3249–3288.

Gagliarducci, Stefano, M. Daniele Paserman, and Eleonora Patacchini, "Hurricanes, Climate Change Policies and Electoral Accountability," *American Economic Journal: Economic Policy*, forthcoming.

Graff Zivin, Joshua, Matthew Neidell, Nicholas J. Sanders, and Gregor Singer, "When Externalities Collide: Influenza and Pollution," *American Economic Journal: Applied Economics*, 2023, *15* (2), 320–351.

Guiso, Luigi, Helios Herrera, Massimo Morelli, and Tommaso Sonno, "Global Crises and Populism: the role of Eurozone Institutions," *Economic Policy*, 2019, *34* (97), 95–139.

Guriev, Sergei and Elias Papaioannou, "The Political Economy of Populism," *Journal of Economic Literature*, 2022, *60* (3), 753–832.

Hazlett, Chad and Matto Mildenberger, "Wildfire Exposure Increases Pro-environment Voting within Democratic but not Republican Areas," *American Political Science Review*, 2020, *114* (4), 1359–1365.

Hoffmann, Roman, Raya Muttarak, Jonas Peisker, and Piero Stanig, "Climate Change Experiences Raise Environmental Concerns and Promote Green Voting," *Nature Climate Change*, 2022, *12*, 148–155.

Jones, Daniel, Neil Silveus, and Carly Urban, "Partisan Gerrymandering and Turnout," *The Journal of Law and Economics*, 2023, *66* (3), 557–579.

Kaplan, Ethan, Jörg L. Spenkuch, and Haishan Yuan, "Pandering in the Shadows: How Natural Disasters Affect Special Interest Politics," *American Economic Journal: Economic Policy*, 2025, *17* (3), 441–470.

Kim, Seo-Young Silvia, "Automatic Voter Reregistration as a Housewarming Gift: Quantifying Causal Effects on Turnout Using Movers," *American Political Science Review*, 2023, *117* (3), 1137–1144.

Manacorda, Marco, Edward Miguel, and Andrea Vigorito, "Government Transfers and Political Support," *American Economic Journal: Applied Economics*, 2011, *3* (3), 1–28.

Masiero, Giuliano and Michael Santarossa, "Natural Disasters and Electoral Outcomes," *European Journal of Political Economy*, 2021, *67*, 101983.

Mehic, Adrian, "The Electoral Consequences of Environmental Accidents: Evidence from Chernobyl," *Journal of Public Economics*, 2023, *225*, 104964.

Qiu, Yun, Yunning Liu, Wei Shi, and Maigeng Zhou, "The Impact of Ozone Pollution on Mortality: Evidence from China," *Journal of Environmental Economics and Management*, 2024, *125*, 102980.

Rodrik, Dani, "Why Does Globalization Fuel Populism? Economics, Culture, and the Rise of Right-Wing Populism," *Annual Review of Economics*, 2021, *13*, 133–170.

Senior, Kathryn and Alfredo Mazza, "Italian "Triangle of death" Linked to Waste Crisis," *The Lancet Oncology*, 2004, *5* (9), 525—-527.

References

Autor, David, David Dorn, Gordon Hanson, and Kaveh Majlesi. 2020. "Importing Political Polarization? The Electoral Consequences of Rising Trade Exposure." *American Economic Review*, **110(10)**: 3139-3183.

Bonomi, Giampaolo, Nicola Gennaioli, and Guido Tabellini. 2021. "Identity, Beliefs, and Political Conflict." *Quarterly Journal of Economics*, **136(4)**: 2371–2411.

Gagliarducci, Stefano, Tomasso Nannicini and Paolo Naticchioni 2011. "Electoral rules and politicians' behavior: a micro test." *American Economic Journal: Economic Policy*, **3**: 144-174.

Gennaioli, Nicola, and Guido Tabellini. 2023. "Identity Politics." *Working Papers 693, IGIER, Bocconi University*.

Gethin, Amory, Clara Martínez-Toledano, and Thomas Piketty. 2022. "Brahmin Left versus Merchant Right: Changing Political Cleavages in 21 Western Democracies, 1948-2020." *Quarterly Journal of Economics*, **137(1)**: 1-48.

Guiso, Luigi, Helios Herrera, Massimo Morelli, and Tommaso Sonno. 2024. "Economic Insecurity and the Demand for Populism in Europe." *Economica*, **91(362)**: 588-620.

Herrnstadt, Evan, and Erich Muehlegger. 2014. "Weather, Salience of Climate Change and Congressional Voting." *Journal of Environmental Economics and Management*, **68(3)**: 435-448.

Saviano, Roberto. 2006. "Gomorrah: A Personal Journey into the Violent International Empire of Naples' Organized Crime System." *Mondadori*, 2006.

Slaybaugh, Jason A. 2017. "Garbage Day: Will Italy Finally Take out Its Trash in the Land of Fires?" *Washington International Law Journal*, **26(1)**: 179-208.

Tabellini, Marco. 2020. "Gifts of the Immigrants, Woes of the Natives: Lessons from the Age of Mass Migration." *Review of Economic Studies*, **87(1)**: 454–486.

Turvani Margherita, Aline Chiabai, Anna Alberini and Stefania Tonin. 2006. "Public Support for Policies Addressing Contaminated Sites: Evidence from a Survey of the Italian Public." *Working paper*.

Appendix

A Additional Tables and Figures

Figure A1: Identification of Illegal Disposal Sites (2005-2022)

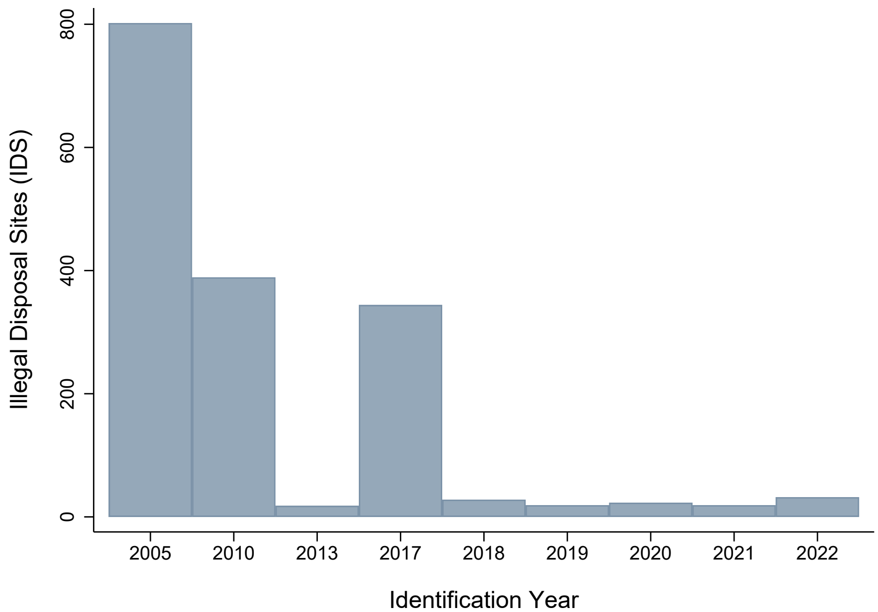

Notes: This figure plots the number of Illegal Disposal Sites (IDS) by identification year according to the ARPAC inventory. We classify a site as an IDS when the description indicates illegal disposal or burning of waste, and we drop observations associated with legal activities such as production facilities, petrol/fuel suppliers, and authorized landfills/dumps.

FIGURE A2: Illegal Disposal Sites (2005-2022)

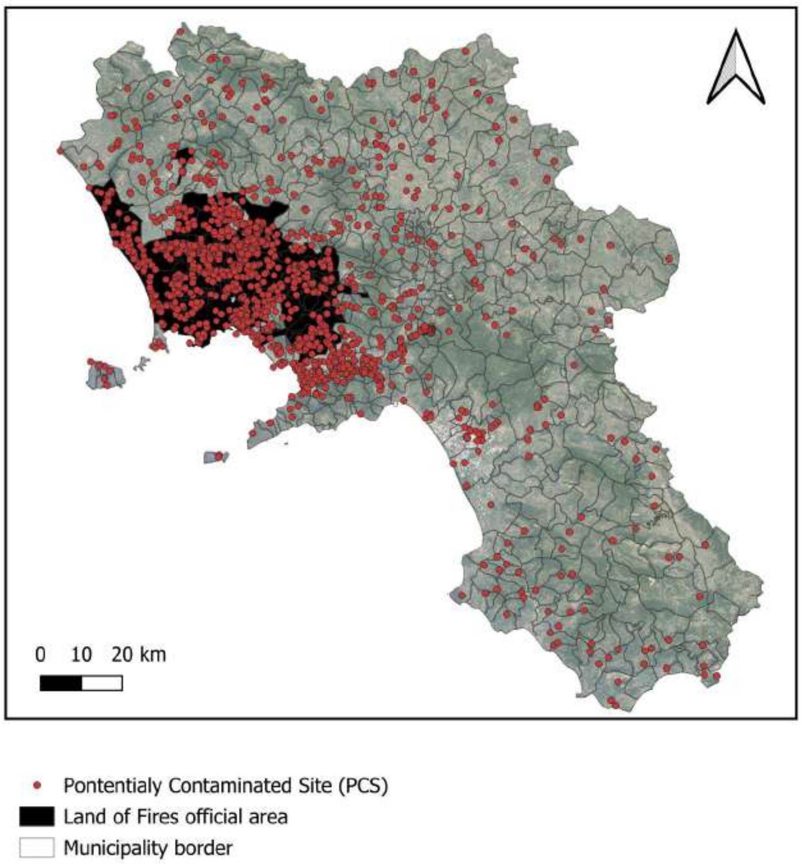

Notes: This map plots all Illegal Disposal Sites (IDS) recorded by the Campania Regional Environmental Protection Agency (ARPAC) from 2005 to 2022 (red dots). The black area marks the perimeter of the "Land of Fires", i.e., the 90 municipalities officially designated by the Italian government in 2013–2015.

FIGURE A3: Potentially Contaminated Sites (PCS)

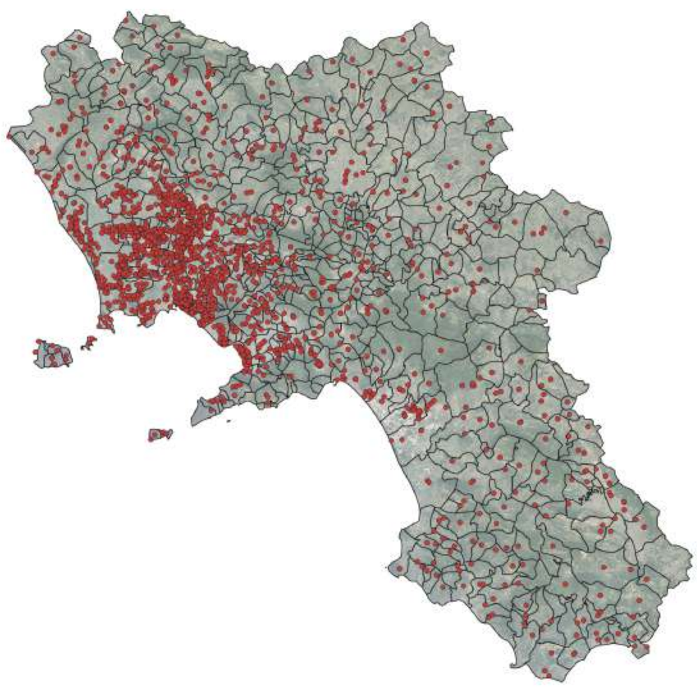

Notes: This figure shows the first official map of Potentially Contaminated Sites (PCS) released by the Regional Agency for the Protection of the Environment Campania (ARPAC) in 2005. PCS are defined as areas where there is a possibility that soil, subsoil, surface water, or groundwater contains pollutants at concentrations high enough to pose a risk to public health or the natural environment.

FIGURE A4: Official Land of Fires and PCS^{LoF} density

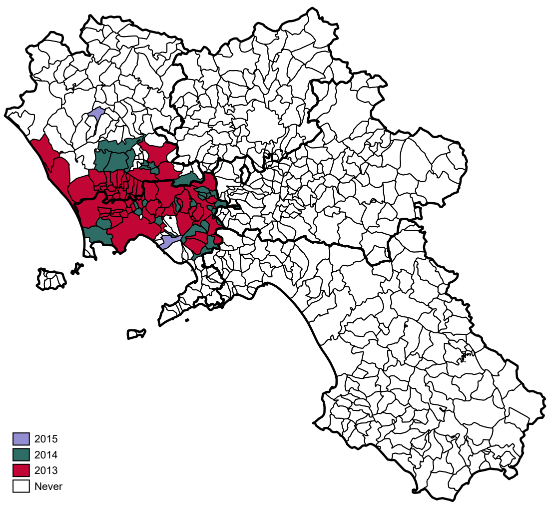

(a) Map of the 90 municipalities officially recognized by the Italian government

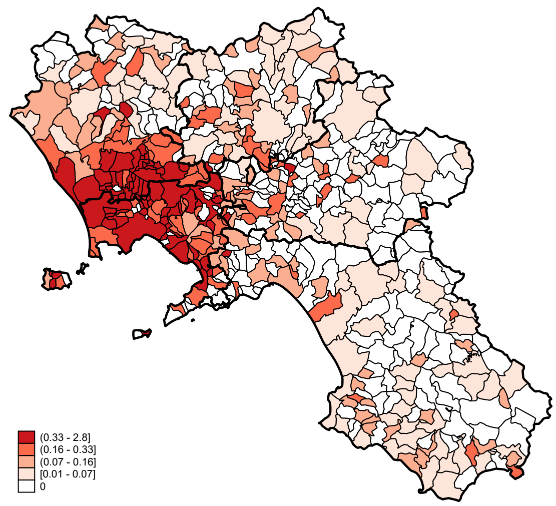

(b) Density of PCS per square kilometer at the municipality level (2005-2013)

Notes: Panel (a) maps the 90 municipalities officially recognized by the Italian government as part of the Land of Fires in 2013, 2014 and 2015. Panel (b) reports the density of PCS per square kilometer using ARPAC inventories for 2005–2013. PCS density is computed as the number of PCS divided by municipality surface. For the empirical analysis, we rely on the PCS data since site coordinates are available, which allows us to build a measure of wind exposure. The official government list is provided only at the municipality level (no site coordinates) and is therefore used only descriptively.

FIGURE A5: Conceptual framework

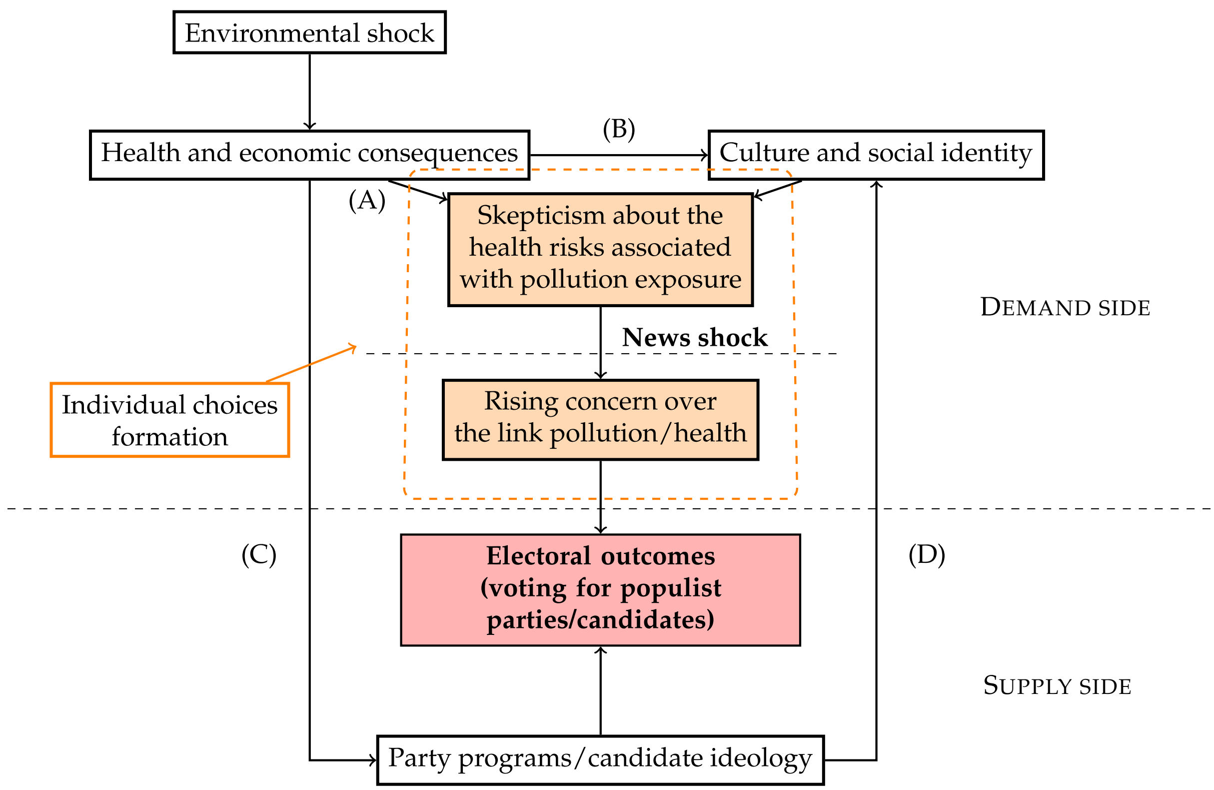

Notes: Adapted version of Rodrik (2021) model. The assumption of initial skepticism about the relationship between health and pollution exposure is supported by survey evidence. In May 2005, just right after the release of the first official map of potentially contaminated sites in Campania, Turvani et al., (2006) conducted a survey among residents of four Italian major cities (Venice, Milan, Bari, and Naples). The questionnaire asked respondents about their awareness of health risks associated with exposure to contaminated sites. The results showed that 90% of the respondents had previously heard about contaminated sites, and 77% of this "informed" group had obtained their information from media sources such as newspapers and television. Notably, the study found that the probability of higher health risk perception was significantly greater when respondents were aware of contaminated sites being close to their home or workplace. This finding aligns with our conceptual framework, as, prior to the news shock, the issue was predominantly neglected and perceived only as a localized problem.

FIGURE A6: Mortality time series

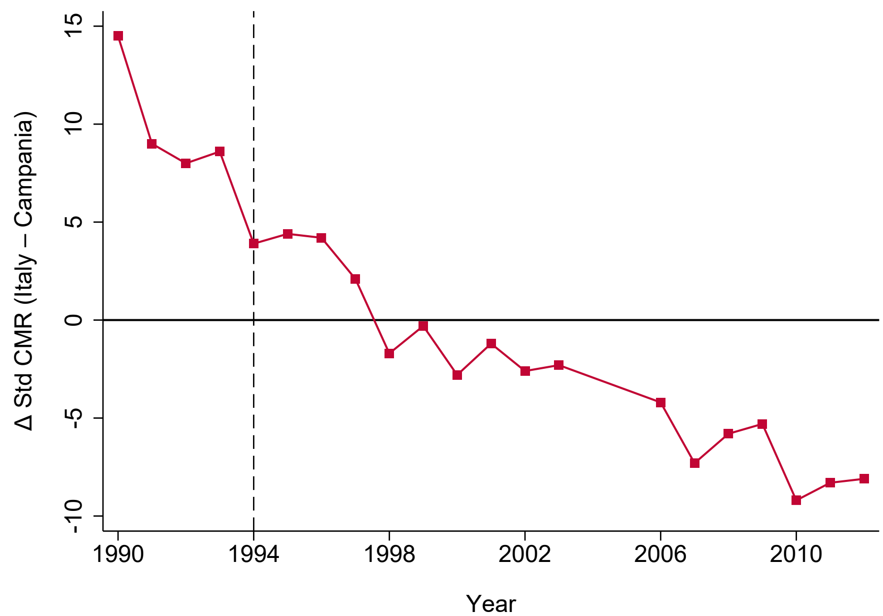

Notes: This figure illustrates the evolution of the difference in standardized Cancer Mortality Rate (CMR) between Italy and Campania from 1990 to 2012. During the 1990s, Campania's CMR was lower than the national average despite a lower healthcare quality, limited preventive healthcare, and reduced access to medical services. After a 10 p.p. increase in the Std CMR in Campania with respect to the national average within just four years, the region declared a national emergency in 1994.

FIGURE A7: Quartile distribution of RR of death from cancer (I)

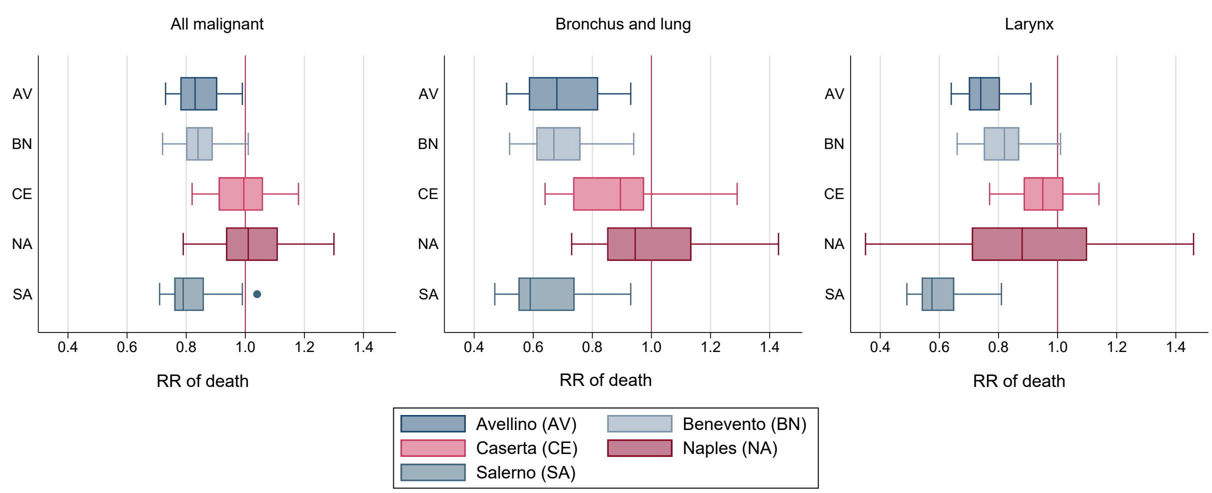

(a) Air pollution

Notes: This panel displays the quartile distribution of the Relative Risk (RR) of death from various types of cancer (all malignant, bronchus and lung, larynx) across all municipalities, grouped by province, for the period 2006–2014. The provinces of Caserta and Naples, which have the highest PCS density, exhibit a higher RR of death for all malignant, lung and laryngeal cancers, likely linked to dioxins and air pollution from the illegal burning of toxic waste.

FIGURE A8: Quartile distribution of RR of death from cancer (II)

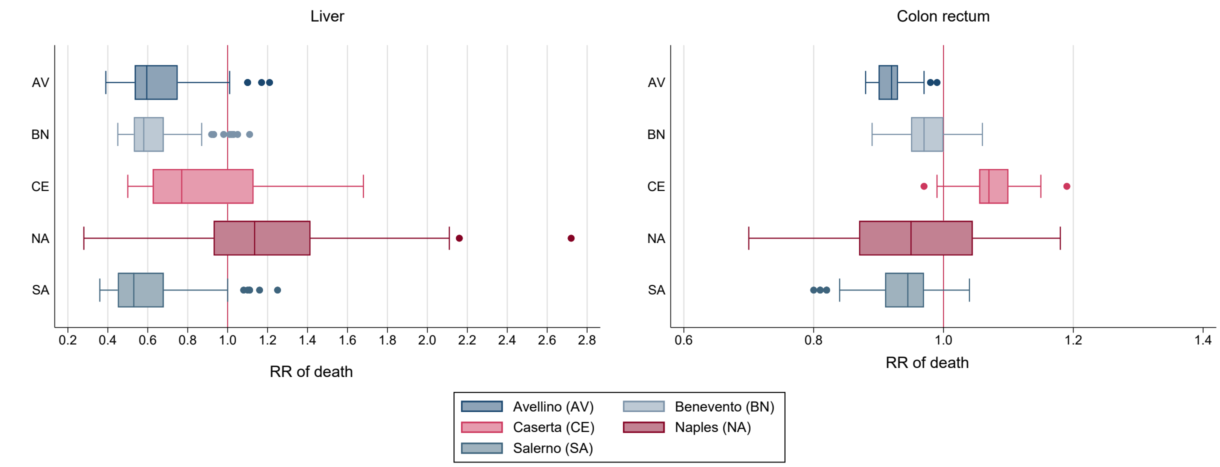

(a) Soil and water pollution

Notes: This panel displays the quartile distribution of the Relative Risk (RR) of death from cancers potentially associated with soil and water contamination across all municipalities, grouped by province, for the period 2006-2014. Naples, followed by Caserta, exhibits the highest risk, whereas Benevento and Avellino show lower risk levels. This heterogeneity aligns with the distribution of PCS density.

FIGURE A9: National public broadcasting TV exposure

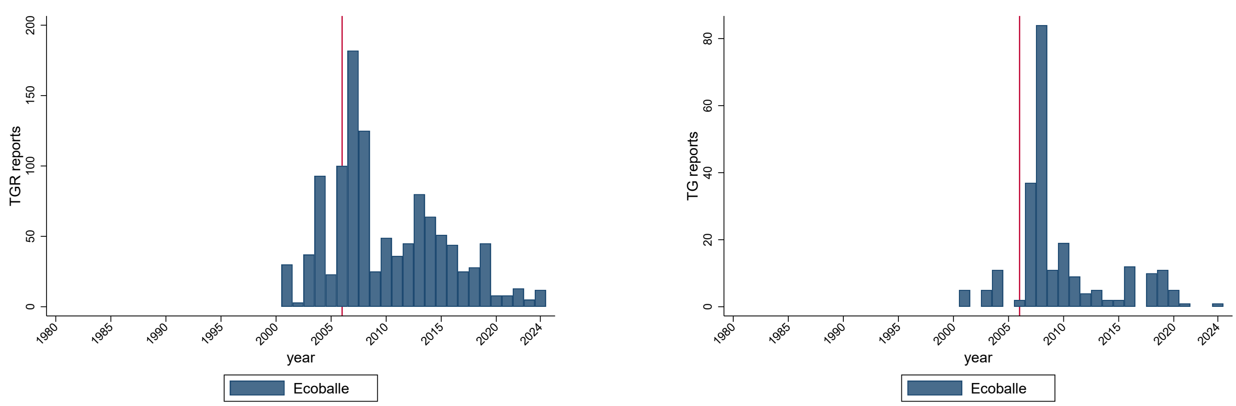

(a) Regional TV news reports

(b) National TV news reports

Notes: Panel (a) displays the frequency of TV news reports from the national public broadcaster, RAI (*Radio Audizioni Italiane*) at the regional level in Campania (TGR - Telegiornale Regionale) that mention the keyword "Ecoballe" (large waste disposal units). Panel (b) presents the frequency of TV news reports from RAI at the national level for the same keyword. The red line indicates the release of the book *Gomorrah*. Data are sourced from RAI teche archives.

FIGURE A10: Historical national elections cumulative vote shares by coalitions

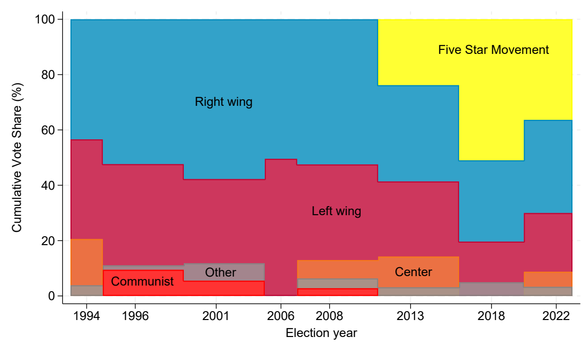

(a) Campania region

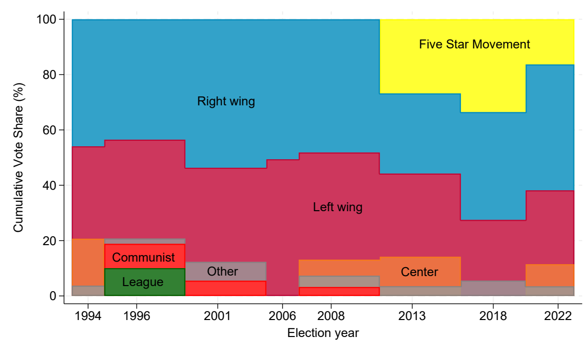

(b) Italy

Notes: This figure illustrates the cumulative vote share received by coalitions in national elections between 1994 and 2022. Panel (a) presents election results for the Campania region, while Panel (b) displays results for Italy. In 2018 and 2022, the Five Star Movement's vote share in Campania was considerably higher than the corresponding national outcome.

Table A1: Descriptive statistics

	(1) Mean	(2) St. Dev.	(3) Min	(4) Max	(5) Obs.
Panel A) Sociodemographic census data (2001)					
Share of men	0.489	0.010	0.453	0.532	552
Share of higher educ.	0.049	0.020	0.010	0.156	552
Employment rate health	0.049	0.021	0.009	0.192	552
Share of commuters	0.182	0.060	0.036	0.392	552
Share of foreign residents	0.006	0.006	0	0.049	552
Avg taxable income pc (2000-2004)	4936.911	984.874	2589.708	10089.355	552
Population density (2001)	787.461	1621.697	11.022	13914.62	552
Panel B) Geographical characteristics					
Municipality surface (km^2)	24.825	23.757	0.105	186.875	552
PCS (number)	5.634	9.041	0.000	55.000	552
PCS (number per sqkm)	0.775	1.740	0.000	11.667	552
Wind exposure (dummy)	0.572	0.495	0.000	1.000	552
Maximum altitude (km)	0.793	0.479	0.010	1.912	552
Radon 2007 (bq/m^3)	238.132	137.685	10.000	1360.200	552
Panel C) Meteorological variables (2001-2009)					
Historical avg humidity (%)	74.029	1.580	67.752	78.350	552
Historical rainfall (mm)	2.644	0.236	1.885	3.120	552
Historical max temperature (°C)	21.322	0.963	18.093	23.014	552
Historical avg wind direction (°)	214.369	115.026	0.179	359.789	552
Historical avg wind speed (m/s)	0.476	0.234	0.011	1.528	552
Panel D) National elections (1972–2022)					
Electorate	7781.345	36625.268	207.000	892867.000	7692
Turnout	0.767	0.110	0.051	1.187	7692
Invalid ballots	0.077	0.060	0.000	0.581	7691
M5S vote share	0.314	0.132	0.056	0.696	1651
PD vote share	0.246	0.107	0.047	0.694	2753
FI vote share	0.233	0.111	0.016	0.814	3304
League vote share	0.029	0.044	0.000	0.655	2753
FDI vote share	0.103	0.103	0.000	0.525	1651
Far left/green vote share	0.020	0.020	0.000	0.269	2753
Invalid ballots (2001)	0.156	0.059	0.063	0.443	552
Candidate origins M5S (2018-2022)	0.005	0.074	0	1	1100
Panel E) Parliamentary speeches (1996-2022)					
Mentions ratio (mainstream parties)	0.00014	0.0017	0	0.10472	14904
Panel F) Health, economic, institutional outcomes					
Avg relative risk of death (2006-2014)	0.892	0.117	0.710	1.300	552
Hotel arrivals	56.517	125.961	1.013	967	704
Civilian killed by Mafia (1967-2004)	0.292	2.147	0	47	552
Party Distrust Index (2006-2022)	0.966	0.230	-0.113	1.656	2753
Parliament Distrust Index (2006-2022)	0.954	0.215	-0.135	1.642	2753
Panel G) Municipal elections (1992-2024)					
Electorate	8967.248	36349.419	327.000	879237.000	3989
Turnout	0.732	0.116	0.119	0.950	3989
M5S running	0.054	0.227	0.000	1.000	3989

FIGURE A11: Distribution of PCS across municipalities

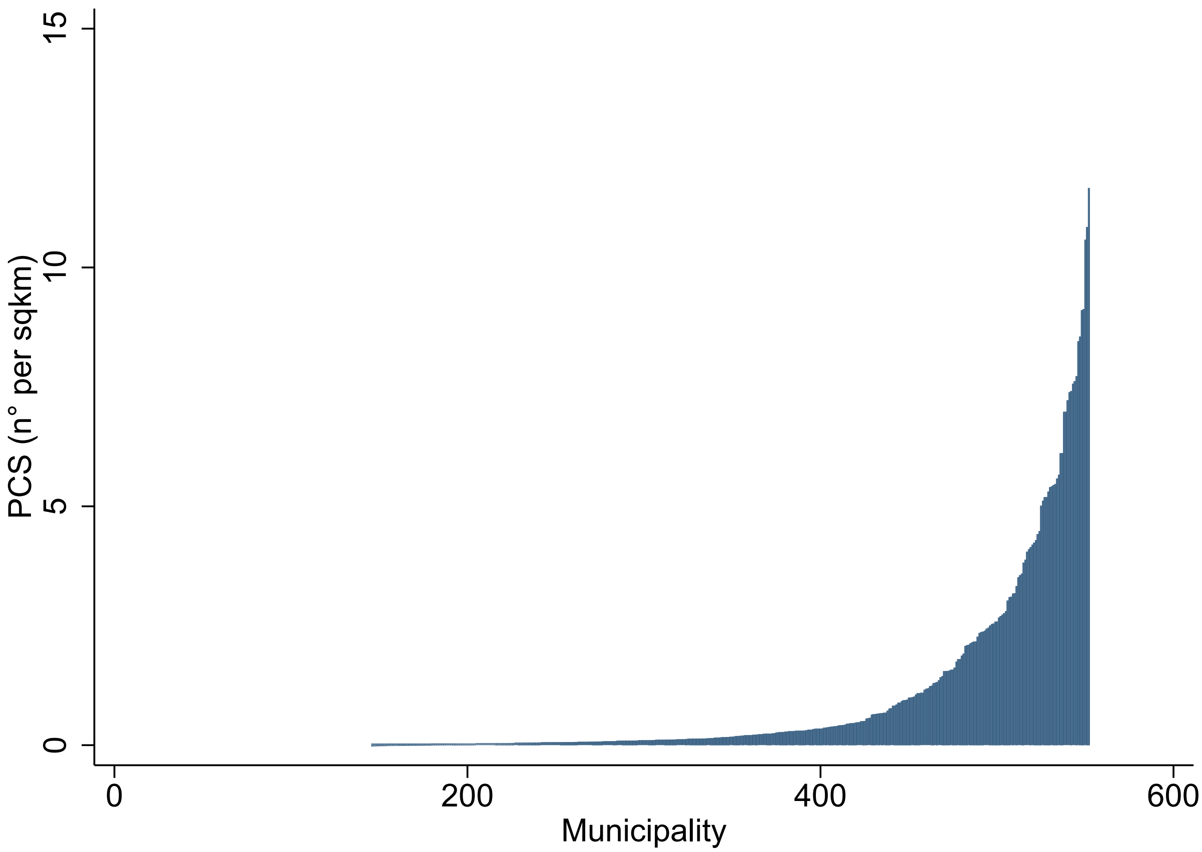

(a) Number of $PCS_{m,2005-2022}$ per sqkm

Notes: This figure displays the distribution of Potentially Contaminated Sites (PCS) per sqkm across the 552 municipalities in Campania. Municipalities on the x-axis are ordered from the lowest to the highest number of sites per sqkm, while the y-axis reports the corresponding site count per sqkm.

B THE WIND MODEL

This section details the procedures used to compute the key variables θ and $\alpha_{i,j}$ employed in the wind model. First, we define the inverse distance as

$$Dist_j^{inv} = \frac{1}{d_j} \quad \text{with} \quad j \quad \in \{1, 2, 3, 4, 5\}$$

where d_j represents the distance (in km) between the synthetic station i and the $j-th$ nearest actual station. Then, we compute the total inverse distance as $TotDist^{inv} = \sum_{j=1}^{5} Dist_j^{inv}$. Last, we define the inverse distance weight coefficients:

$$\alpha_{i,j} = \frac{Dist_j^{inv}}{TotDist^{inv}} \quad \text{with} \quad j \in 1, 2, 3, 4, 5 \quad \text{and} \quad \sum_{j=1}^{5} \alpha_{i,j} = 1$$

In this way, closer actual stations receive higher weights whereas farther actual stations receive lower weights. In order to estimate the Wind Influence dummy ($WI_{i,j}$), we first compute the connection vector $C_{i,j}$ between the synthetic station i and the actual station j.

$$C_{i,j} = (x_i - x_j, y_i - y_j) = (C_x, C_y)$$

C_x and C_y represent the wind vector components. The angle between the connection vector and wind direction is defined as θ. Unlike the cosine method (based on the $arccos$ of the dot product), which does not distinguish whether the angle is measured clockwise or counterclockwise, we rely on the bearing method in order to find θ, which provides a well defined clockwise angle from North. This ensures consistency with meteorological wind data, which are expressed as compass bearings.[11] Hence, we use the $atan2$ function in order to compute the raw bearing from North (clockwise) of the connection vector.

$$Bearing_c = arctan2(C_x, C_y) \times \frac{180}{\pi}$$

Values are normalized into the range $[0, 360)$, so that $0°$ corresponds to North, $90°$ to East, and so on. We therefore consider the reported wind direction, denoted as $WindFrom$, which also lies in $[0, 360)$, and compare it with $Bearing_c$. The angular difference between these two angles identifies θ:

$$\theta = min(|Bearing_c - WindFrom|), \in [0, 180]$$

[11]Meteorological convention defines wind direction as the bearing from which the wind blows.

Wind influence dummy:

$$WI_{i,j} = \begin{cases} 1 & if \quad 0 \leq \theta \leq 90 \\ 0 & if \quad \theta > 90 \end{cases}$$

where θ is the angle between the wind vector of actual station j and the connection vector.

FIGURE B1: Wind influence dummy ($WI_{i,j}$)

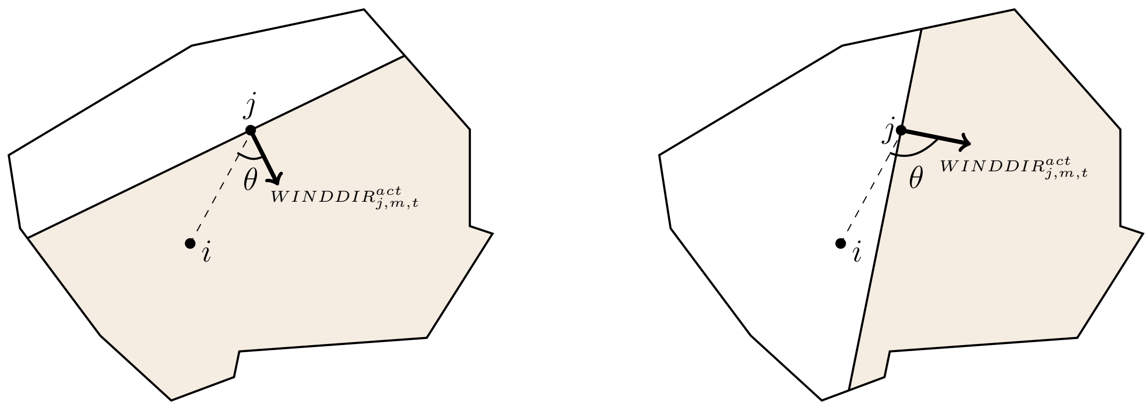

(a) $WI_{i,j} = 1$ **(b)** $WI_{i,j} = 0$

Notes: Panel (a) shows a case in which the Wind Influence binary indicator ($WI_{i,j}$) equals 1, as the angle (θ) between the connection vector (dashed line from the actual station j to the synthetic station i) and the wind direction vector falls within $[0°, 90°]$. Panel (b) shows the opposite case, where $WI_{i,j} = 0$, since $\theta > 90°$. The acceptable region for wind influence is defined by the half-space delimited by a line orthogonal to the wind direction vector and passing through the synthetic station i. This ensures that are take into account actual stations with wind potentially blowing toward i. Note that synthetic station i is located at the PCS coordinates. $WINDDIR^{act}_{j,m,t}$ denotes the wind direction at actual station j in municipality m on day t.

FIGURE B2: Actual stations

Notes: This figure displays the average wind direction recorded at the 47 actual monitoring stations across 45 municipalities in Campania during the period 2001–2009.

FIGURE B3: Historical average wind direction at municipality level

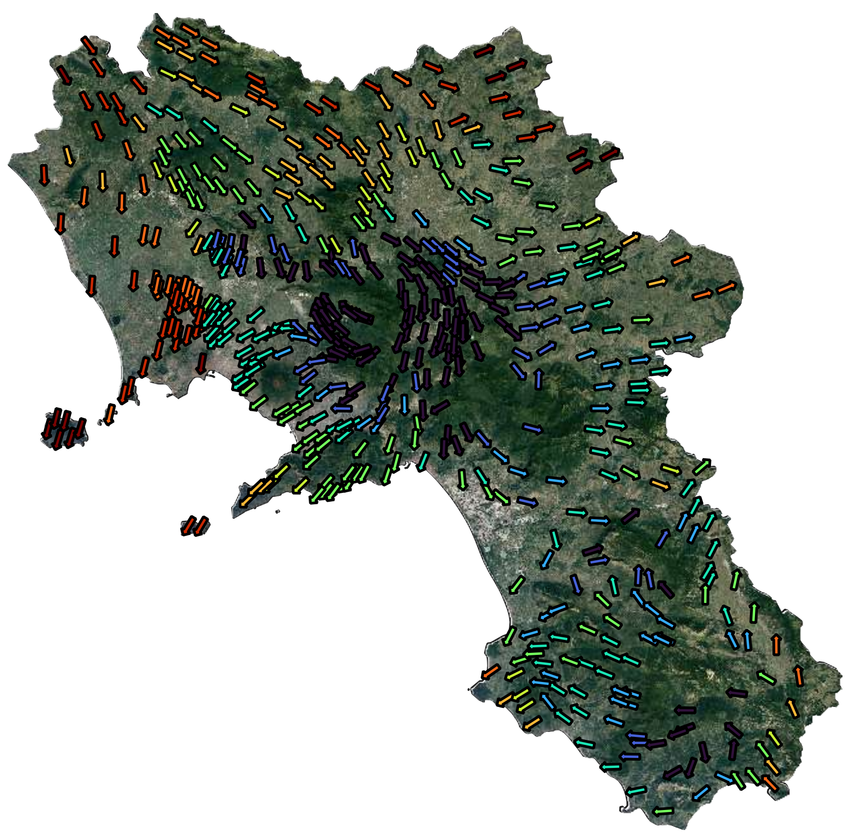

Notes: This figure shows the interpolated historical average wind direction (2001-2009) at the municipality level. Each station is located at the municipality demographic centroid. Color intensity indicates wind speed (darker red arrwos correspond to higher average wind speeds).

FIGURE B4: Salience of "Land of Fires" in Italy's parliament

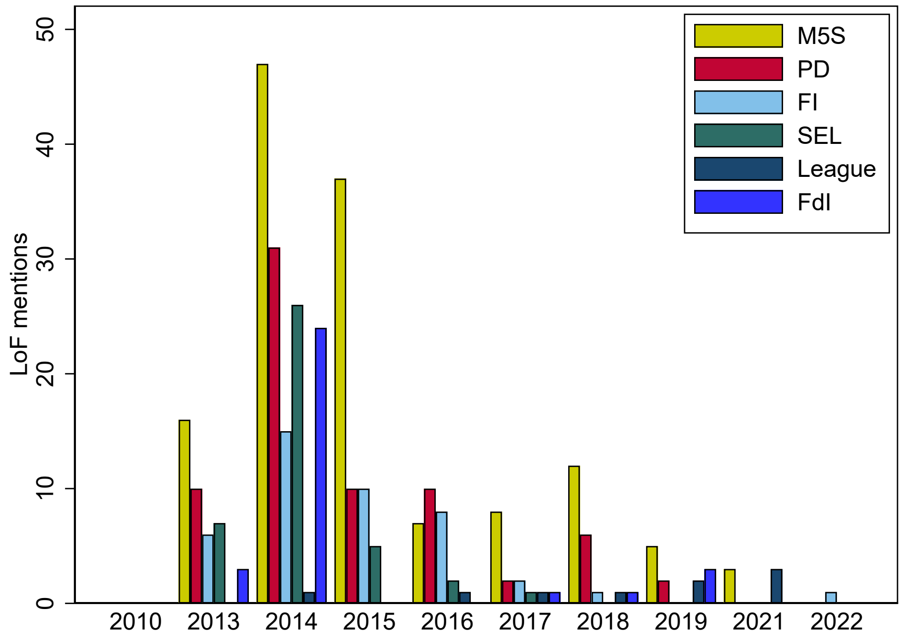

Notes: The figure reports annual raw counts (not normalized by the number of deputies) of lower house speeches that contain the expression "Land of Fires", disaggregated by party (M5S, PD, FI, SEL, League, FdI). The series spans 2010–2022; no occurrences appear before 2010 in the *ItaParlCorpus* dataset (1948–2022). Mentions surge in 2014 and 2015, driven primarily by M5S (with contributions by mainstream parties like PD and FI), and then decline with sporadic activity thereafter. Party labels reflect speaker's affiliation at the time of the speech. *Source*: *ItaParlCorpus*.

C Robustness checks

C.1 Turnout

Table C1: Robustness test I: alternative definitions of wind exposure

	Weighted Least Squares (WLS)			
Buffer radius: 3 km	(1) Turnout	(2) Turnout	(3) Turnout	(4) Turnout
Wind Exposure (above median) × $Post$	-0.0685***			
	(0.00654)			
Wind Exposure (quartile distribution) × $Post$		-0.0272***		
		(0.00246)		
Wind Exposure (above average) × $Post$			-0.0647***	
			(0.00696)	
ln[Wind Exposure (number) + 1] × $Post$				-0.0341***
				(0.00321)
Municipality FE	✓	✓	✓	✓
Year FE	✓	✓	✓	✓
PCS number per sqkm	✓	✓	✓	✓
Year × Surface	✓	✓	✓	✓
Year × Historical weather variables	✓	✓	✓	✓
Year × Socio-demographic controls	✓	✓	✓	✓
Year × Geographical characteristics	✓	✓	✓	✓
Observations	7692	7692	7692	7692
R-squared	0.929	0.928	0.927	0.927
F-stat	3769.4	3692.5	3780.9	3709.4

Notes: This table reports WLS difference-in-differences estimates of the effect of wind exposure to PCS on voter turnout in national elections from 1972 to 2022. Each column refers to a 3 km buffer radius from the PCS center (see Figure 6), while varying the definition of wind exposure. Column (1) defines the treatment as a binary indicator equal to 1 if the number of upwind exposed PCS exceeds the median value. Column (2) divides the number of upwind exposed PCS into a quartile distribution. Column (3) defines the key regressor of interest as a binary indicator equal to 1 if the number of upwind exposed PCS exceeds the average value, while column (4) applies an alternative functional form to the number of upwind exposed PCS (logarithm transformation). The post-treatment period is identified by the indicator variable $Post$, which equals 1 for all election years after 2001, and 0 otherwise. All regressions are weighted by electorate size at the municipality level. Heteroscedasticity and cluster-robust standard errors at the municipality level are in parentheses. Stars indicate significance levels (* $p < 0.1$, ** $p < 0.05$, *** $p < 0.01$).

FIGURE C5: Robustness test I: alternative definitions of exposure (dynamic specification)

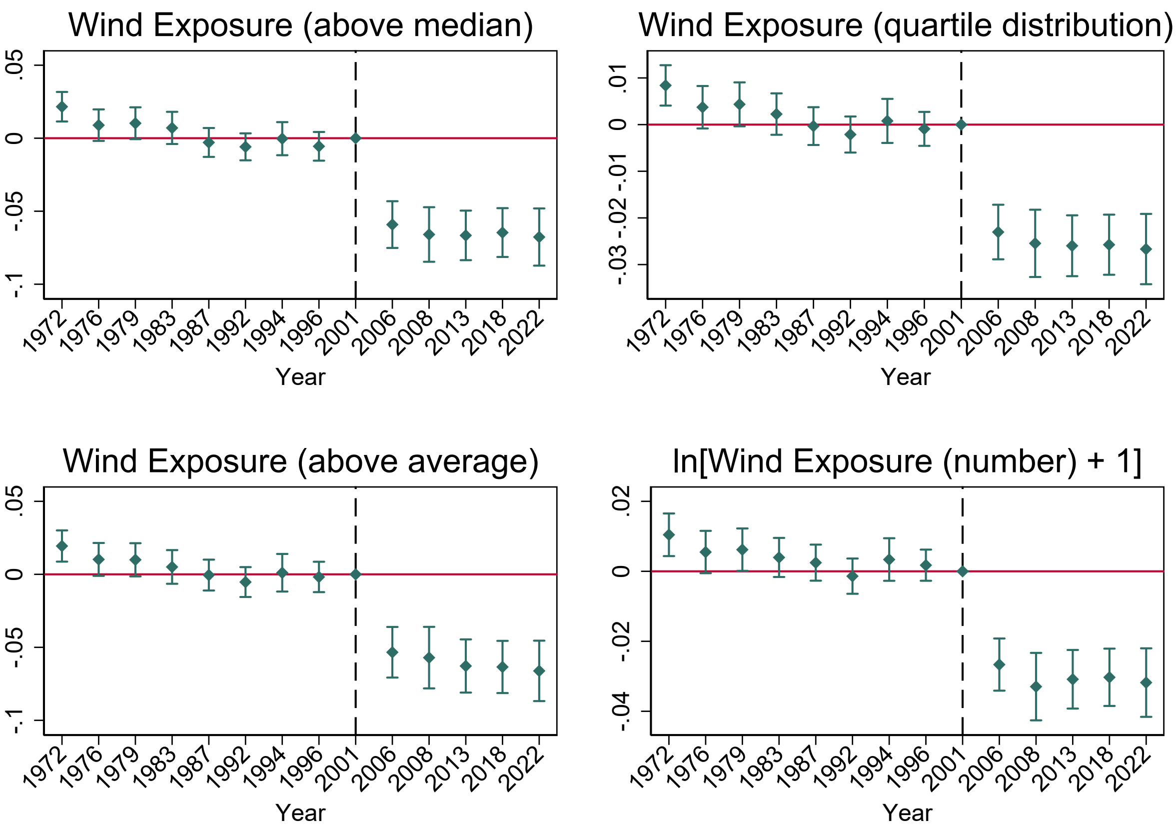

Notes: This figure reports coefficients from a dynamic specification estimating the interaction between the alternative definitions of wind exposure from Table C1 and year indicators, with 2001 omitted as the reference year. Each point represents the estimated effect of wind exposure on turnout in a given year, relative to 2001. Turnout is defined as the ratio of actual voters to registered electors. This model controls for the most stringent specification reported in Table 4, with 95% confidence intervals. Standard errors are clustered at the municipality level.

TABLE C2: Robustness test II: alternative buffers

	Weighted Least Squares (WLS)			
	Dep. variable: Turnout			
	(1)	(2)	(3)	(4)
Buffer radius	3 km	5 km	10 km	20km
Wind Exposure (dummy) $\times$ *Post*	-0.0576***	-0.0500***	-0.0390**	0.0226
	(0.00739)	(0.0100)	(0.0181)	(0.0160)
Total number of PCS per sqkm $\times$ *Post*	-0.00283**	-0.00121**	-0.000482***	-0.000179***
	(0.00136)	(0.000515)	(0.000161)	(0.0000619)
Municipality FE	✓	✓	✓	✓
Year FE	✓	✓	✓	✓
PCS number per sqkm	✓	✓	✓	✓
Surface	✓	✓	✓	✓
Historical weather variables	✓	✓	✓	✓
Socio-demographic controls	✓	✓	✓	✓
Geographical characteristics	✓	✓	✓	✓
Observations	7692	7692	7692	7692
R-squared	0.924	0.921	0.918	0.917
F-stat	3667.5	3554.0	3631.6	3661.9

Notes: This table shows WLS estimates of the effect of wind exposure to PCS on turnout at national elections (1972-2022). Each column refers to the most stringent specification reported in Table 4, while varying the buffer radius from the PCS center (see Figure 6). The post-treatment period is defined by the indicator variable $Post$, which equals 1 for all election years after 2001, and 0 otherwise. All regressions are weighted by electorate size at the municipality level. Heteroscedasticity and cluster-robust standard errors at the municipality level are in parentheses. Stars indicate significance levels (* $p < 0.1$, ** $p < 0.05$, *** $p < 0.01$).

FIGURE C6: Robustness test II: alternative buffers (dynamic specification)

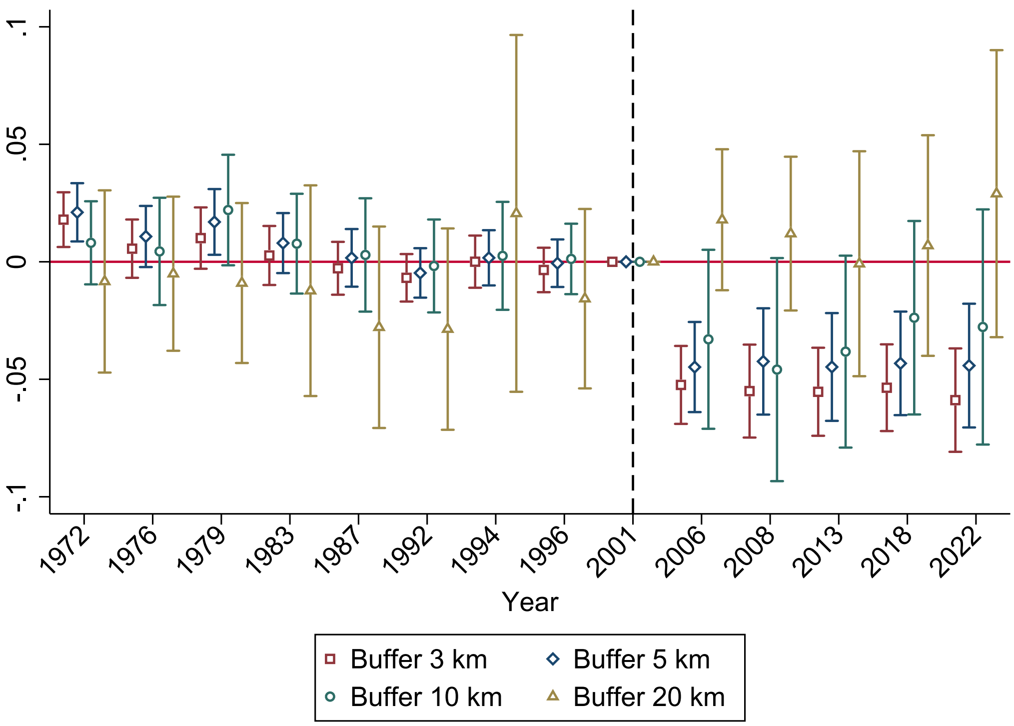

Notes: This figure reports coefficients from a dynamic specification estimating the interaction between the treatment variable $WindExposed_m$ and year indicators, with 2001 omitted as the reference year. Each point represents the estimated effect of wind exposure on turnout in a given year, relative to 2001. Turnout is defined as the ratio of actual voters to registered electors. Coefficients are shown separately by election year and buffer radius from the PCS center (3, 5, 10, and 20 km). Bars represent 95% confidence intervals, with standard errors clustered at the municipality level.

TABLE C3: Robustness test III: alternative definition of $WI_{i,j}$ and $WindExposed_m$ ($\theta = 45°$)

	Weighted Least Squares (WLS)			
	(1)	(2)	(3)	(4)
Buffer radius: 3 km	Turnout	Turnout	Turnout	Turnout
Wind Exposure (dummy) $\times$ $Post$	-0.0456***	-0.0564***	-0.0548***	-0.0500***
	(0.00936)	(0.00875)	(0.00807)	(0.00774)
Total number of PCS per sqkm $\times$ $Post$	-0.00895***	-0.00465***	-0.00516***	-0.00243*
	(0.00201)	(0.00170)	(0.00166)	(0.00146)
Municipality FE	✓	✓	✓	✓
Year FE	✓	✓	✓	✓
PCS number per sqkm		✓	✓	✓
Surface		✓	✓	✓
Historical weather variables		✓	✓	✓
Geographical characteristics			✓	✓
Number of electors (2001)				✓
Observations	7692	7692	7692	7692
R-squared	0.893	0.913	0.919	0.924
F-stat	2115.0	1811.1	3034.3	3646.0

Notes: This table shows WLS estimates of the effect of wind exposure to PCS on voter turnout at national elections (all years). Each column refers to a 3 km buffer radius from the PCS center, while varying both the computation of historical average wind direction at each PCS and $WindExposed_m$. $WI_{i,j}$ equals 1 as the angle (θ) between the connection vector (line from the actual station j to the synthetic station i) and the wind direction vector falls within $[0, 45°]$. A PCS is classified as upwind exposed relative to the municipality's demographic centroid if the angle (θ) between the connection vector (line from the demographic centroid to the PCS) and the historical average wind direction ($\overline{WINDDIR_{PCS}}$) falls within the range $[0, 45°]$. All regressions are weighted by electorate size at the municipality level (year 2001). Heteroscedasticity and cluster-robust standard errors at the municipality level are in parentheses. Stars indicate significance levels (* $p < 0.1$, ** $p < 0.05$, *** $p < 0.01$).

FIGURE C7: Robustness test III: dynamic specification ($\theta = 45°$)

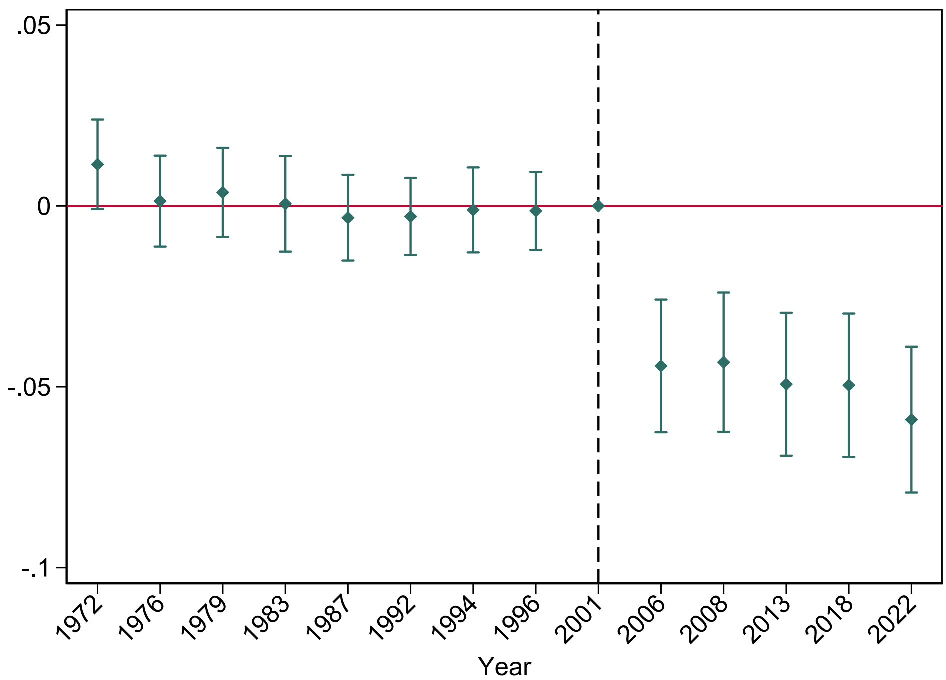

Notes: This figure reports coefficients from a dynamic specification estimating the interaction between the treatment variable $WindExposed_m$ and year indicators, with 2001 omitted as the reference year. This specification varies both the computation of historical average wind direction and $WindExposed_m$. $WI_{i,j}$ equals 1 as the angle (θ) between the connection vector (line from the actual station j to the synthetic station i) and the wind direction vector falls within $[0, 45°]$. A PCS is classified as upwind exposed relative to the municipality's demographic centroid if the angle (θ) between the connection vector (line from the demographic centroid to the PCS) and the historical average wind direction ($\overline{WINDDIR_{PCS}}$) falls within the range $[0, 45°]$. Each point represents the estimated effect of wind exposure on turnout in a given year, relative to 2001. Turnout is defined as the ratio of actual voters to registered electors. This specification is weighted by electorate size at the municipality level (year 2001), with 95% confidence intervals. Standard errors clustered at the municipality level.

Table C4: Robustness test IV: alternative electorate size weight

	Weighted Least Squares (WLS)			
Buffer radius: 3 km	(1) Turnout	(2) Turnout	(3) Turnout	(4) Turnout
Wind Exposure (dummy) $\times$ $Post$	-0.0775***	-0.0704***	-0.0659***	-0.0579***
	(0.00804)	(0.00778)	(0.00766)	(0.00744)
Total number of PCS per sqkm $\times$ $Post$	-0.00749***	-0.00484***	-0.00541***	-0.00291**
	(0.00154)	(0.00163)	(0.00152)	(0.00139)
Municipality FE	✓	✓	✓	✓
Year FE	✓	✓	✓	✓
PCS number per sqkm	✓	✓	✓	✓
Surface	✓	✓	✓	✓
Year $\times$ Historical weather variables		✓	✓	✓
Year $\times$ Socio-demographic controls			✓	✓
Year $\times$ Geographical characteristics				✓
Observations	7692	7692	7692	7692
R-squared	0.900	0.914	0.920	0.924
F-stat	2295.2	1841.9	3138.8	3801.4

Notes: This table shows WLS estimates of the effect of wind exposure to PCS on turnout at national elections (1972-2022). Each column refers to the specifications reported in in Table 4, while varying electorate weight size at the municipality level from election year 2001 to 1996. The post-treatment period is defined by the indicator variable $Post$, which equals 1 for all election years after 2001, and 0 otherwise. Heteroscedasticity and cluster-robust standard errors at the municipality level are in parentheses. Stars indicate significance levels (* $p < 0.1$, ** $p < 0.05$, *** $p < 0.01$).

FIGURE C8: Robustness test IV: alternative electorate size weight (dynamic specification)

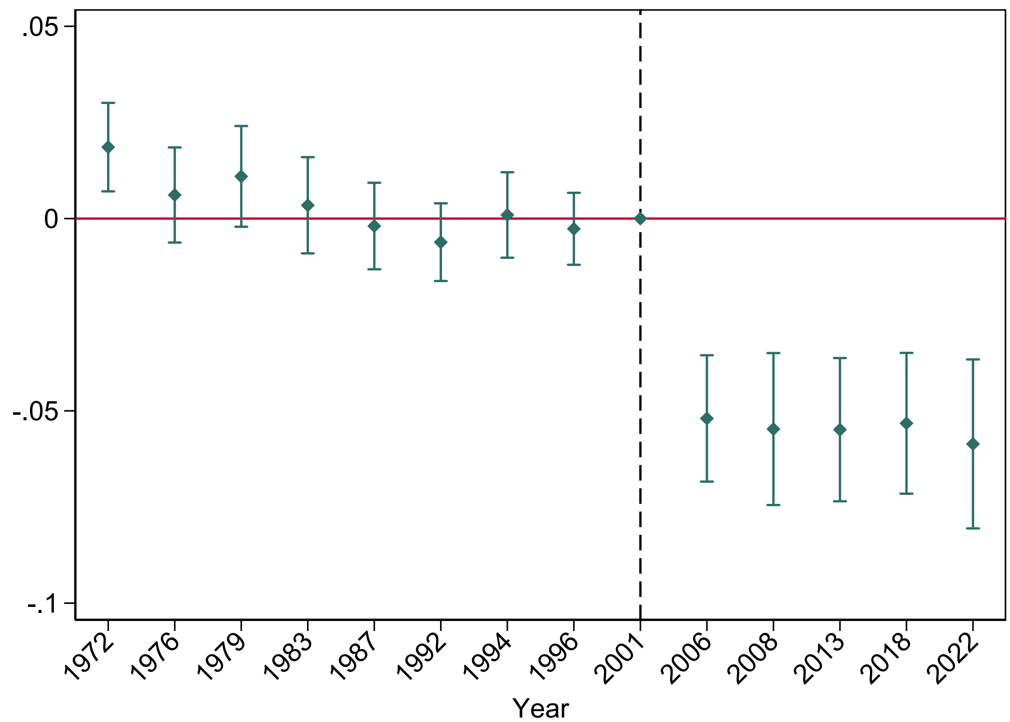

Notes: This figure reports coefficients from a dynamic specification estimating the interaction between the treatment variable $WindExposed_m$ and year indicators, with 2001 omitted as the reference year. Each point represents the estimated effect of wind exposure on turnout in a given year, relative to 2001. This specification is weighted by electorate size at the municipality level (year 1996), with 95% confidence intervals. Standard errors clustered at the municipality level.

FIGURE C9: Robustness test V: Conley HAC standard errors

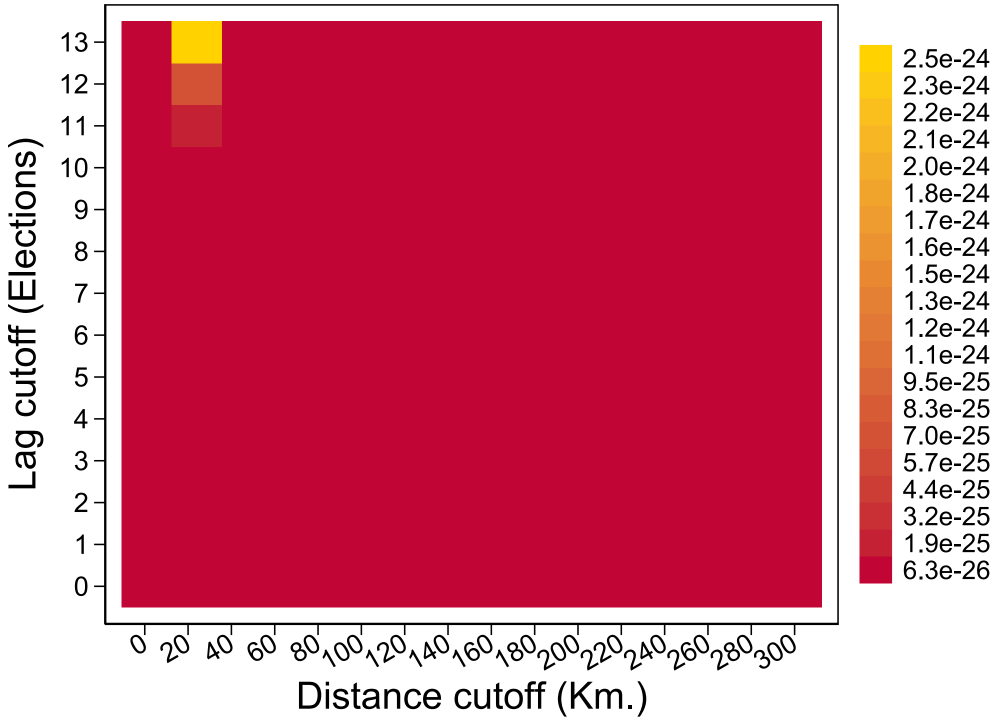

Notes: The figure displays p-values from estimating Table 4 across a series multiple regressions exploiting Conley HAC standard errors. Spatial and temporal cutoffs are sequentially expanded from their minimum to their maximum feasible values. Each iteration increases the spatial cutoff by 20 km or the temporal cutoff by one electoral cycle. Confidence intervals are based on standard errors that are robust to serial and spatial correlation and computed imposing maximum cutoff for both spatial and time lags.

TABLE C5: Robustness test VI: balanced-panel sample (fixed 1972 municipal boundaries)

	Weighted Least Squares (WLS)			
Buffer radius: 3 km	(1) Turnout	(2) Turnout	(3) Turnout	(4) Turnout
Wind Exposure (dummy) × $Post$	-0.0770***	-0.0700***	-0.0656***	-0.0574***
	(0.00806)	(0.00777)	(0.00765)	(0.00743)
Total number of PCS per sqkm × $Post$	-0.00769***	-0.00493***	-0.00553***	-0.00302**
	(0.00166)	(0.00173)	(0.00161)	(0.00146)
Municipality FE	✓	✓	✓	✓
Year FE	✓	✓	✓	✓
PCS number per sqkm	✓	✓	✓	✓
Surface	✓	✓	✓	✓
Year × Historical weather variables		✓	✓	✓
Year × Socio-demographic controls			✓	✓
Year × Geographical characteristics				✓
Observations	7588	7588	7588	7588
R-squared	0.900	0.914	0.920	0.924
F-stat	2157.6	1729.8	3062.1	3714.0

Notes: This table shows WLS difference-in-differences estimates of the effect of wind exposure to PCS after the news shock on voter turnout using a balanced-panel sample. We restrict the sample to municipalities that existed in 1972 and are observed in every election year, excluding the seven municipalities created later and the merged municipality of Montoro, as well as Montoro Inferiore and Montoro Superiore. Each column refers to a 3 km buffer radius from the PCS center (see Figure 6). The treatment is instrumented by $WindExposed_m$, defined as a binary indicator equal to 1 if municipality m has a number of upwind exposed PCS greater than zero (extensive margin). The post-treatment period is identified by the indicator variable $Post$, which equals 1 for all election years after 2001, and 0 otherwise. Column (1) presents a baseline model with municipality and year fixed effects to account for time-invariant unobserved heterogeneity at the local level and common time shocks. It also includes the total number of PCS per sqkm and municipality surface, both interacted with year dummies. Columns (2)-(4) progressively introduce controls fully interacted with year dummies. Column (2) adds historical weather variables at municipality level (average wind direction, wind speed, humidity, and rainfall over 2001-2009). Column (3) includes socio-demographic controls: share of men, share of higher-educated individuals, employment rate in the health sector, share of foreign residents, share of daily commuters. Column (4) further adds geographical characteristics (maximum altitude and radon levels in year 2007). All regressions are weighted by electorate size at the municipality level in the year 2001. Heteroscedasticity and cluster-robust standard errors at the municipality level are in parentheses. Stars indicate significance levels (* $p < 0.1$, ** $p < 0.05$, *** $p < 0.01$).

FIGURE C10: Robustness test VI: balanced-panel sample: dynamic specification

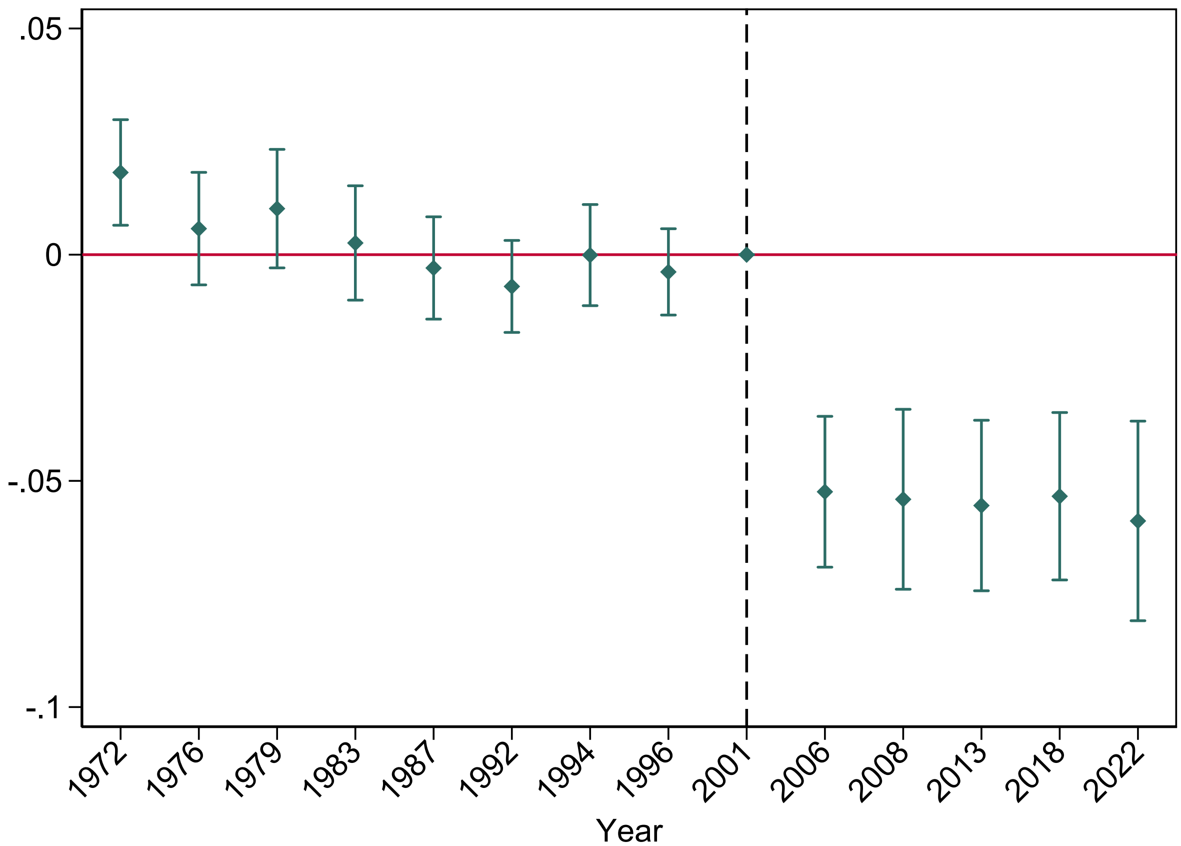

Notes: This figure reports coefficients from a dynamic specification estimating the interaction between the treatment variable $WindExposed_m$ and year indicators, with 2001 omitted as the reference year. Each point represents the estimated effect of wind exposure on turnout in a given year, relative to 2001. Turnout is defined as the ratio of actual voters to registered electors. This model controls for the most stringent specification reported in Table 4 and it is weighted by electorate size at the municipality level in year 2001, with 95% confidence intervals. Standard errors are clustered at the municipality level.

C.2 FIVE STAR MOVEMENT

TABLE C6: Robustness test I: alternative definitions of wind exposure

	Weighted Least Squares (WLS)			
	(1)	(2)	(3)	(4)
Buffer radius: 3 km	M5S vote share	M5S vote share	M5S vote share	M5S vote share
Wind Exposure (above median)	0.0381***			
	(0.00820)			
Wind Exposure (quartile distribution)		0.0166***		
		(0.00281)		
Wind Exposure (above average)			0.0308***	
			(0.00962)	
ln[Wind Exposure (number) + 1]				0.0231***
				(0.00366)
PCS number per sqkm	✓	✓	✓	✓
Municipality surface	✓	✓	✓	✓
Historical weather variables	✓	✓	✓	✓
Province FE	✓	✓	✓	✓
Year FE	✓	✓	✓	✓
Socio-demographic controls	✓	✓	✓	✓
Geographical characteristics	✓	✓	✓	✓
Electoral district (2001)	✓	✓	✓	✓
Observations	1651	1651	1651	1651
R-squared	0.829	0.830	0.827	0.831
F-stat	277.4	277.1	266.7	266.4

Notes: This table reports WLS estimates of the effect of wind exposure to PCS on M5S vote share at national elections. Each column refers to the most stringent specification reported in Table 6, while varying the definition of wind exposure. Column (1) defines the treatment as a binary indicator equal to 1 if the number of upwind exposed PCS exceeds the median value. Column (2) divides the number of upwind exposed PCS into a quartile distribution. Column (3) defines the key regressor of interest as a binary indicator equal to 1 if the number of upwind exposed PCS exceeds the average value, while column (4) applies an alternative functional form to the number of upwind exposed PCS (logarithm transformation). All regressions are weighted by electorate size at the municipality level (year 2001). Heteroscedasticity and cluster-robust standard errors at the municipality level are in parentheses. Stars indicate significance levels (* $p < 0.1$, ** $p < 0.05$, *** $p < 0.01$).

TABLE C7: Robustness test II: alternative buffers

	Weighted Least Squares (WLS)			
	Dep. variable: M5S vote share			
	(1)	(2)	(3)	(4)
Buffer radius	3 km	5 km	10 km	20km
Wind Exposure (dummy) × *Post*	0.0342***	0.0200**	0.0336***	0.0460**
	(0.00713)	(0.00875)	(0.0120)	(0.0225)
PCS number per sqkm	✓	✓	✓	✓
Municipality surface	✓	✓	✓	✓
Historical weather variables	✓	✓	✓	✓
Province FE	✓	✓	✓	✓
Year FE	✓	✓	✓	✓
Socio-demographic controls	✓	✓	✓	✓
Geographical characteristics	✓	✓	✓	✓
Electoral district (2001)	✓	✓	✓	✓
Observations	1651	1651	1651	1651
R-squared	0.828	0.824	0.823	0.823
F-stat	255.6	248.5	263.1	258.9

Notes: This table shows WLS estimates of the effect of wind exposure to PCS on M5S vote share at national elections (all years). Each column refers to the most stringent specification reported in Table 6, while varying the buffer radius from the PCS center (see Figure 6). All models include PCS number per sqkm, municipality surface, historical weather variables at municipality level (average humidity, rainfall, wind direction, and wind speed over 2001-2009), province and year fixed effects, socio-demographic controls (share of men, share of higher-educated individuals, employment rate in the health sector, share of daily commuters, share of foreign residents, and the historical average taxable income per capita over 2000-2012), geographical characteristics (maximum altitude and radon levels in year 2007), and electoral districts in year 2001. All regressions are weighted by electorate size at the municipality level (year 2001). Heteroscedasticity and cluster-robust standard errors at the municipality level are in parentheses. Stars indicate significance levels (* $p < 0.1$, ** $p < 0.05$, *** $p < 0.01$).

FIGURE C11: Robustness test II: alternative buffers (by year)

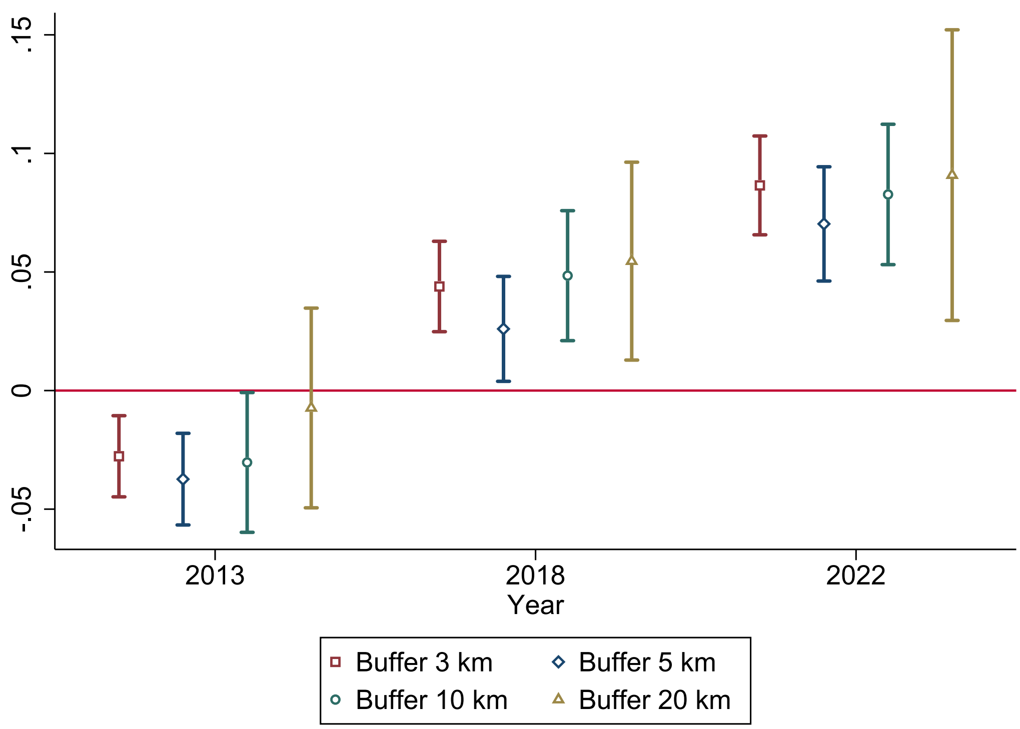

Notes: This figure shows the estimated average marginal effects of wind exposure to PCS on Five Star Movement (M5S) vote share at national elections, separately by year. Coefficients are shown separately by election year and buffer radius from the PCS center (3, 5, 10, and 20 km). Bars represent 95% confidence intervals. Each coefficient refers to the most stringent specification reported in Table 6. All regressions are weighted by electorate size at the municipality level (year 2001), and standard errors (obtained via the delta method) are clustered at the municipality level.

TABLE C8: Robustness test III: alternative definition of $WI_{i,j}$ and $WindExposed_m$ ($\theta = 45°$)

	Weighted Least Squares (WLS)			
	(1)	(2)	(3)	(4)
Buffer radius: 3 km	M5S vote share	M5S vote share	M5S vote share	M5S vote share
Wind Exposure (dummy)	0.0192**	0.0182**	0.0168**	0.0150*
	(0.00909)	(0.00813)	(0.00799)	(0.00818)
PCS number per sqkm	✓	✓	✓	✓
Municipality surface	✓	✓	✓	✓
Historical weather variables	✓	✓	✓	✓
Province FE	✓	✓	✓	✓
Year FE	✓	✓	✓	✓
Socio-demographic controls		✓	✓	✓
Geographical characteristics			✓	✓
Electoral district (2001)				✓
Observations	1651	1651	1651	1651
R-squared	0.797	0.817	0.821	0.824
F-stat	408.1	300.4	278.8	253.2

Notes: This table shows WLS estimates of the effect of wind exposure to PCS on M5S vote share at national elections (all years). Each column refers to a 3 km buffer radius from the PCS center, while varying both the computation of historical average wind direction at each PCS and $WindExposed_m$. $WI_{i,j}$ equals 1 as the angle (θ) between the connection vector (line from the actual station j to the synthetic station i) and the wind direction vector falls within $[0, 45°]$. A PCS is classified as upwind exposed relative to the municipality's demographic centroid if the angle (θ) between the connection vector (line from the demographic centroid to the PCS) and the historical average wind direction ($\overline{WINDDIR_{PCS}}$) falls within the range $[0, 45°]$. All regressions are weighted by electorate size at the municipality level (year 2001). Heteroscedasticity and cluster-robust standard errors at the municipality level are in parentheses. Stars indicate significance levels (* $p < 0.1$, ** $p < 0.05$, *** $p < 0.01$).

Table C9: Robustness test IV: alternative electorate size weight

	Weighted Least Squares (WLS)			
Buffer radius: 3 km	(1) M5S vote share	(2) M5S vote share	(3) M5S vote share	(4) M5S vote share
Wind Exposure (dummy)	0.0390***	0.0365***	0.0343***	0.0341***
	(0.00752)	(0.00741)	(0.00733)	(0.00719)
PCS number per sqkm	✓	✓	✓	✓
Municipality surface	✓	✓	✓	✓
Historical weather variables	✓	✓	✓	✓
Province FE	✓	✓	✓	✓
Year FE	✓	✓	✓	✓
Socio-demographic controls		✓	✓	✓
Geographical characteristics			✓	✓
Electoral district (2001)				✓
Observations	1651	1651	1651	1651
R-squared	0.802	0.821	0.824	0.828
F-stat	355.2	299.2	282.2	270.0

Notes: This table shows WLS estimates of the effect of wind exposure to PCS on M5S vote share at national elections (all years).Each column refers to the specifications reported in in Table 4, while varying electorate weight size at the municipality level from election year 2001 to 1996. Heteroscedasticity and cluster-robust standard errors at the municipality level are in parentheses. Stars indicate significance levels (* $p < 0.1$, ** $p < 0.05$, *** $p < 0.01$).